Convention on Long-range Transboundary Air Pollution

emep

Co-operative programme for monitoring and evaluation of the long-range transmission of air pollutants in Europe

STATUS REPORT
4/2011

Transboundary particulate matter in Europe

Status Report 4/2011

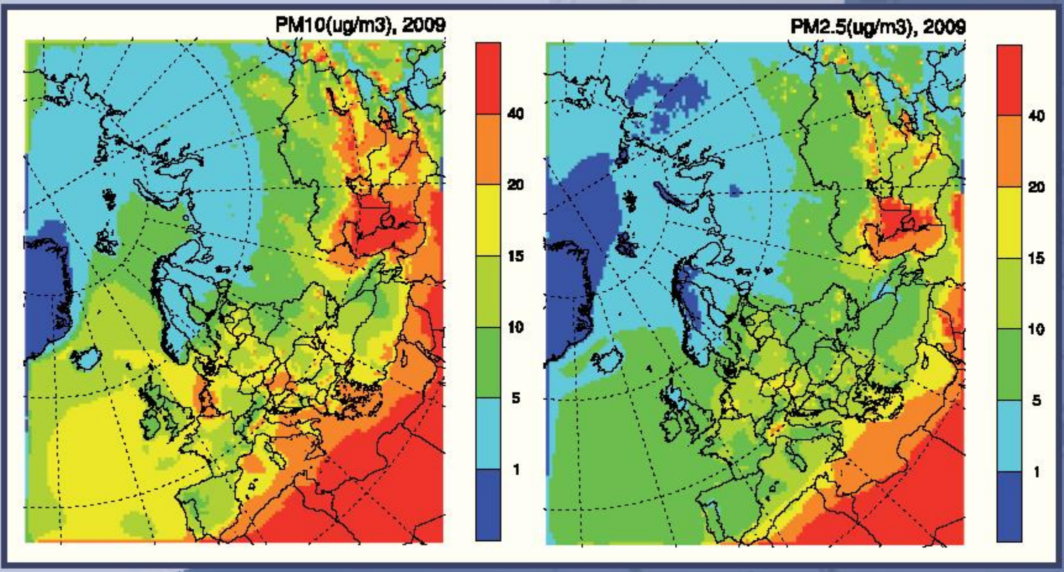

ccc & msc-w & ceip & ciam

NILU: EMEP Report 4/2011
REFERENCE: O-7726
DATE: AUGUST 2011
ISSN: 1504-6109 (print)
1504-6192 (online)

EMEP Co-operative Programme for Monitoring and Evaluation of the Long-Range Transmission of Air Pollutants in Europe

Transboundary particulate matter in Europe
Status report 2011

Joint
CCC, MSC-W, CEIP and CIAM
Report 2011

Norwegian Institute for Air Research
P.O. Box 100, NO-2027 Kjeller, Norway

Norwegian Meteorological Institute
P.O. Box 43 Blindern, NO-0313 Oslo, Norway

Umweltbundesamt GmbH
Spittelauer Lände 5, AT-1090 Vienna, Austria

IIASA – International Institute for Applied Systems Analysis
Schlossplatz 1, AT-2361 Laxenburg, Austria

List of Contributors

Karl Espen Yttri[1], Wenche Aas[1], Kjetil Tørseth[1], Markus Fiebig[1],
Ann Mari Fjæraa[1],
Svetlana Tsyro[2], David Simpson[2,5], Robert Bergström[6,7],
Katarína Marečková [3], Robert Wankmüller[3],
Zbigniew Klimont[4], Jens Borken-Kleefeld[4],
Fabrizia Cavalli[8], Jean-Philippe Putaud[8],
Martin Schultz[9],
Xavier Querol[10], Andrés Alastuey[10], Fulvio Amato[10], Michael Cusack[10], Cristina Reche[10], Angeliki Karanasiou[10], Mar Viana[10], Teresa Moreno[10], Jorge Pey[10],
Noemí Pérez[10],
Paolo Laj[11], Alfred Wiedensohler[12],

1) Norwegian Institute for Air Research, Kjeller, Norway
2) Norwegian Meteorological Institute, Oslo, Norway
3) Umweltbundesamt, Vienna, Austria
4) International Institute for Applied Systems Analysis, Laxenburg, Austria
5) Chalmers University of Technology, Gothenburg, Sweden
6) Swedish Meteorological and Hydrological Institute, Norrköping, Sweden
7) Department of Chemistry, University of Gothenburg, Sweden
8) European Commission, Joint Research Centre, Ispra, Italy
9) Forschungszentrum Jülich GmbH, Germany
10) Institute of Environmental Assessment and Water Research (IDÆA), Barcelona, Spain
11) Laboratoire de Glaciologie et Géophysique de l'Environnement (CNRS-LGGE), France
12) Leibniz Institute for Tropospheric Research (IfT) Leipzig, Germany

[1] EMEP Chemical Coordinating Centre
[2] EMEP Meteorological Synthesizing Centre – West
[3] EMEP Centre on Emission Inventories and Projections
[4] EMEP Centre on Integrated Assessment Modelling

Contents

Page

Executive Summary

The current report presents the status and progress of the emission reporting, observations and modelling activities undertaken under EMEP in relation to particulate matter in the European rural background environment. It also includes a special section related to mineral dust observation in Europe. Mineral dust may have a large impact on the PM level in Europe, but there are relatively few measurements to study and quantify this on a European scale. It is therefore recommended to have a focus on the mineral dust content in the next EMEP intensive measurement periods, which are scheduled for summer 2012 and winter 2013.

A small section is devoted to progress made for PM measurement in the EECCA (Eastern Europe, Caucasus and Central Asia) region. Further, the report gives an overview of the success of the recently finalized EU project EUSAAR by establishing standard operation procedure for measuring and reporting aerosol related data to EMEP and WMO/GAW.

As in 2006 (EMEP, 2006), this report has a chapter devoted to the main uncertainties in the assessment of transboundary PM. The aim is to repeat this evaluation every five year to document the progress of the EMEP Programme. Significant improvements have been made over the last five years. The measurement program has been extended with more parameters and better spatial resolution as well as more harmonized methodology across Europe. The emissions have improved by more complete reporting and better emission factors, though further progress on this field is still of vital importance. New and more advanced measurements are allowing improved testing of model parameterizations, especially concerning nitrate and secondary organic aerosols (SOA). Many of these improvements have benefited from cooperation with other European projects, including EUCAARI and EUSAAR. All this has increased the confidence in the assessment of transboundary PM. However, this field is especially challenging and considerable uncertainties remain. Continued developments in the basic scientific understanding are needed, as well as continued model development and evaluation against data are required in order to significantly improve the accuracy of transboundary PM estimates.

The main findings in the status for 2009 are described below.

Emission reporting

The number of Parties providing primary particulate matter emissions data increased by one from 2008 to 2009, and the total number of Parties was 35; out of 51 Parties to the Convention. Rather limited information is provided for the EECCA region, the Balkans, and Turkey.

The reported PM emissions trends vary quite considerably among the Parties. For most countries which have reported data since 2000, PM emissions have decreased, although with a few exceptions. PM_{10} emissions have increased for six Parties, whereas $PM_{2.5}$ emissions have increased for eight Parties. Improved (more complete) inventories reported for recent years could partly explain the increased PM emissions rather than an actual increase of emissions. However, there is still strong evidence indicating that of those countries that did report PM emission, not all Parties reported emissions from all sectors in which releases of PM are likely. Some of the sectors in which non-reporting appears common (e.g. agriculture or small combustion sources) may be significant sources with respect to national totals, therefore a general under-reporting of PM emissions to LRTAP from these sectors seems likely.

In the reporting period a major upgrade of the GAINS emission estimates from road transport sector (SNAP 7) has been conducted by implementation of the latest emission factors for road vehicles in European countries. Now the emissions factors refer to real world driving, and the emission factors for all vehicle categories and emission control stages are country specific, thus better reflecting the different developments of fleet mix. Most important change concerns NO_x emissions from diesel passenger cars which give higher emissions in real world driving than earlier anticipated.

Measurement and model assessment of particulate matter

For 2009, mass concentrations of PM are reported for 65 regional or global background sites (61 for PM_{10} and 40 for $PM_{2.5}$); two more than in 2008. The lowest measured concentrations of PM_{10} were observed in the northern and north-western parts of Europe, i.e. the Nordic countries, Northern Ireland and Scotland, and for high altitude sites (> 800 m asl) on the European mainland. The highest concentrations are found in the Netherlands, Hungary and Italy. Combined maps of EMEP model results and measurements show a pronounced north to south gradient, with the annual mean PM_{10} concentrations varying from 1-5 µg m^{-3} in Northern Europe to 10-25 µg m^{-3} in southern Europe. The average observed annual mean PM_{10} concentration for all sites was 15.0 µg/m^3, the lowest m^{-3}) site was recorded at the high altitude global site Jungfraujoch in Switzerland (2.7 µg/m^3) and the regional forest site Hyytiälä in Finland (4.5 µg/m^3), whereas the highest levels were recorded at the Italian site Montelibretti (29.9 µg/m^3) and Hungarian site K-puszta (27.9 µg/m^3). On average about 50% of the urban background concentration is likely to be attributed to the mean rural background concentration of PM_{10}.

The spatial pattern of annual mean $PM_{2.5}$ concentrations largely reflects that of PM_{10}. The combined map og model and measurements have a pronounced north to south gradient with the annual mean PM_{10} varying from 1-5 µg/m^3 in Northern Europe to 10-25 µg/m^3 in Southern Europe. The observed average annual mean concentration of $PM_{2.5}$ for all sites was 10.1 µg/m^3. The annual mean concentration of PM_1 was reported for six sites. The highest annual mean was observed at the Austrian site Illmitz (11.5 µg m^{-3}), which was more than three times higher than that observed at Hyytiälä in Finland (3.2 µg m^{-3}), reporting the lowest annual mean. No model calculated PM_1 concentrations are available.

The PM_{10} levels in 2009 and 2008 are quite comparable. On average there was a small decrease of 4%, which follows the decreasing trend from the previous years. However, there are large variations between sites). The general tendency seen using the model results is that PM_{10} and $PM_{2.5}$ concentration levels go up somewhat in the northern of the EMEP area (Fennoscandia and north-western

Russia), while they decrease in Central and Southern Europe in 2009 compared to 2008. In a longer time perspective, there is a relatively clear decrease in the PM_{10} mass concentration. Of the ten sites with significant reduction, out of seventeen sites having more than nine years of measurements, the average decease was 21%.

The combined model and observation maps show that the annual mean regional background PM_{10} concentration in 2009 was below the EU limit value of 40 $\mu g\ m^{-3}$ over all of Europe, with the exception of small areas in the EECCA countries. However, the annual mean PM_{10} concentrations calculated by the model exceed the WHO recommended AQG of 20 $\mu g/m^3$ in Benelux, Hungary and the Po Valley. As well as in the southern parts of the Mediterranean basin and in the Caucasus and the EECCA countries due to the influence of windblown dust from deserts and semi-arid soils. The regional background annual mean $PM_{2.5}$ concentrations were above the WHO recommended AQG value of 10 $\mu g/m^3$ in many parts of Central, Eastern and South-Eastern Europe.

Chemical composition data is essential to evaluate aerosol mass concentrations. The relative contributions of SIA and primary PM to PM_{10} and $PM_{2.5}$ vary during the year, and shows different geographical distribution in different months. Typically, SIA’s portion in PM is greatest in the cold season and during the periods of manure application in agriculture in spring. Geographically, the largest SIA contributions to PM_{10} mass are found in Central Europe and Central Russia most on the year.

Ten countries reported measurements of EC and OC for 2009, which are two more than for 2008. Seven of these sites apply the EUSAAR2 analytical protocol which is an important step towards harmonized and comparable data. A separate chapter is devoted to the EC/OC laboratory inter comparison which was conducted in 2010. Comparable data, in particular for OC, require that both the analytical and the sampling protocol are harmonized, which currently is not the case, though work is in progress for establishing a reference method.

The carbonaceous aerosol concentration was found to range by more than one order of magnitude within the European rural background environment. Elevated concentrations were observed in northern Italy and in Eastern Europe. Concentrations observed at sites in Scandinavia, the eastern Mediterranean and at high altitude sites in western/south-western Europe, were substantially lower.

The EMEP model for particulate carbonaceous matter (PCM) is an extension of the standard EMEP MSC-W photochemistry model, and includes the formation of secondary organic aerosol (SOA). Further developments and testing is presented in the present report. Summertime levels are quite well captured by some versions of the VBS scheme, it is hard however to know if the BVOC emissions which are the major summertime precursor to SOA are correct. There are problems matching wintertime OA levels with the model in general underestimating. When including the model results of carbonaceous matter in the standard EMEP model calculations, there is a clear improvement in modelled PM_{10} and $PM_{2.5}$ concentration levels and precision (RMSE), though the spatial correlation is slightly lower.

1 Status of emissions

1.1 PM emission reporting under LRTAP Convention, 2009

By Katarína Marečková, Robert Wankmüller

Parties to the LRTAP Convention submit air pollution emissions[1] and projections annually to the EMEP Centre on Emission Inventories and Projections (CEIP) and notify the LRTAP Convention secretariat thereof. Particulate matter (PM_{10} and $PM_{2.5}$) emissions should be reported for the years 2000 - 2009 as a minimum[2]. Gridded emissions and LPS data should be provided every five years.

1.1.1 Status of reporting

In 2011, 43 Parties (out of 51) to the LRTAP Convention submitted inventories for the year 2009 before 31 May. Of these, only 35 Parties[3] provided PM emissions. Rather limited information is provided for the EECCA region, the Balkans and Turkey. Data submitted by the Parties can be accessed via the CEIP homepage at http://www.ceip.at/submissions-under-clrtap/2011-submissions. Completeness, consistency, comparability and transparency of reported emissions are analyzed in an annual review process[4]. Feedback is provided to the Parties in form of individual country reports and summary findings are published in the EEA & CEIP technical report *Inventory Review 2011* (http://www.ceip.at/review-process/review-2011/review-results-2011).

1.1.2 PM emission trends

The PM emissions trends (as reported) vary quite considerably among the Parties to the CLRTAP. For most countries which have reported data since 2000, PM emissions have decreased. However, there are a few exceptions: PM_{10} emissions have increased for six Parties, whereas $PM_{2.5}$ emissions have risen for eight Parties. The biggest increase in $PM_{2.5}$ emissions is reported for Moldova (210%), Latvia (21%) and Slovakia (21%). From 2008 to 2009, $PM_{2.5}$ and PM_{10} emissions rose for five Parties, with the most substantial increase for Hungary (23% for $PM_{2.5}$ and 26% for PM_{10}) and Latvia (9% in $PM_{2.5}$) (see Table 1.1, Table 1.2). The higher PM emissions in these countries in the past few years might be based on more complete data rather than an actual increase of emissions.

---

[1] SO_x, NO_x, NMVOCs, NH_3, CO, HMs, POPs and PM

[2] Parties are requested to report emission inventory data using standard formats in accordance with the EMEP Reporting guidelines (UNECE, 2009).

[3] The Russian Federation submitted the 2009 inventory on 25 June 2011 and is therefore not included in this assessment.

[4] Methods and Procedures for the Technical Review of Air Pollutant Emission Inventories Reported under the Convention and its Protocols (EB.AIR/GE.1/2007/16)

Table 1.1: $PM_{2.5}$ emission trends (2000-2009) as reported by Parties.

Country / PM2.5 [Gg]	2000	2001	2002	2003	2004	2005	2006	2007	2008	2009	Change 2008 - 09	Change 2000 - 09
Albania	9	9	10	13	14	14	14	13	14			52%
Armenia								0				
Austria	23	23	22	22	22	23	21	21	21	20	-5%	-13%
Azerbaijan												
Belarus			NE	NE	36	25	28	27	28	27	-6%	
Belgium	33	30	30	29	28	26	25	21	20	16	-21%	-53%
Bosnia and Herzegovina												
Bulgaria		NE	NO	NE	NE	NE	NE	21	24	23	-3%	
Canada	NR	NR	NR	NR	NR	NR	NR	NR	NR	1 106		
Croatia	9	9	10	12	12	12	11	11	10	10	-5%	9%
Cyprus	4	4	4	4	3	3	3	3	3	2	-17%	-42%
Czech Republic		0	NE	38	35	21	22	21	21	20	-3%	
Denmark	22	22	22	23	23	25	26	29	27	24	-9%	12%
Estonia	21	22	23	21	22	20	15	20	20	19	-7%	-13%
European Union	1 596	1 583	1 510	1 493	1 474	1 432	1 389	1 354	1 332	1 273	-4%	-20%
Finland	37	38	39	38	38	34	35	34	38	38	-1%	4%
France	381	370	348	346	338	319	303	290	285	270	-5%	-29%
Georgia												
Germany	143	140	133	129	127	122	120	114	106	100	-6%	-30%
Greece												
Hungary	26	24	25	27	27	31	29	21	23	28	23%	8%
Iceland	NR	NR	NR	NR	NR	NR	NR	NR	NR			
Ireland	12	12	11	11	11	11	11	10	10	9	-9%	-22%
Italy	179	176	161	159	164	150	148	154	150	144	-4%	-19%
Kazakhstan												
Kyrgyzstan												
Latvia	23	26	25	26	28	27	27	26	26	28	9%	21%
Liechtenstein	0.03	0.03	0.03	0.03	0.03	0.03	0.03	0.03	0.03	0.03	5%	2%
Lithuania			NE	NE	9	9	9	10	10	10	-7%	
Luxembourg	NR	NR	NR	NR	NR	NR	NR	NR				
FYR of Macedonia				NE	NE	NE	NE	NE	NE	NE		
Malta	1	1	1	1	1	1	1	1	1			
Republic of Moldova	2	2	1	3	6	6	7		6	6	5%	210%
Monaco		NE	NE	NE	NE	NE	NE	NE	NE	NE		
Montenegro							5			4		
Netherlands	24	23	22	21	20	19	18	18	17	16	-8%	-34%
Norway	59	58	61	57	54	51	48	46	44	42	-2%	-28%
Poland	135	142	142	142	134	138	136	134	122	120	-2%	-12%
Portugal	87	86	79	78	82	81	78	79	77	76	-1%	-12%
Romania	NE	NE	NE	NE	NE	NE	NE	108	123	115	-7%	
Russian Federation			376	341	383	350	409	348	316			
Serbia						NE	NE	NE				
Slovakia	23	33	29	28	28	39	34	28	28	28	-1%	21%
Slovenia	14	14	14	14	14	14	14	14	13	13	-5%	-12%
Spain	100	99	99	99	98	97	94	96	87	77	-12%	-23%
Sweden	28	28	28	29	29	29	29	29	28	27	-2%	-3%
Switzerland	12	12	11	11	11	11	10	10	10	10	-3%	-19%
Turkey									0			
Ukraine		NO	0		15	125	NE	0	NA	NO		
United Kingdom	103	100	89	87	86	84	82	80	76	70	-8%	-32%
United States of America	6 061	6 154	5 059	5 048	5 036	5 029	4 981	4 944	4 091	4 134	1%	-32%

Notes: *Blank cell indicates that no data have been reported to EMEP*

NE: not estimated, NO: not occurring, NR: not relevant, NA: not applicable
Shaded cells (red) indicate increased emissions for the given period
Differences for Albania are between 2000 and 2008
Emissions in the row "Russian Federation" corresponds only to "Russian Federation in the former official EMEP domain"

Table 1.2: PM$_{10}$ emission trends (2000 - 2009) as reported by Parties.

Country / PM10 [Gg]	2000	2001	2002	2003	2004	2005	2006	2007	2008	2009	Change 2008 - 09	Change 2000 - 09
Albania	12	13	13	17	18	17	18	17	18			42%
Armenia								1				
Austria	39	39	38	38	38	39	37	36	37	35	-4%	-9%
Azerbaijan												
Belarus			NE	NE	48	36	40	39	41	39	-4%	
Belgium	45	45	44	44	42	35	34	29	28	22	-20%	-51%
Bosnia and Herzegovina												
Bulgaria		NE	NO	NE	NE	NE	NE	44	59	45	-24%	
Canada	NR	NR	NR	NR	NR	NR	NR	NR	NR	5 825		
Croatia	13	13	14	16	17	17	16	16	15	14	-6%	11%
Cyprus	6	6	5	5	5	4	4	4	4	4	-15%	-38%
Czech Republic		43	0	51	47	34	35	35	35	36	4%	
Denmark	29	29	29	30	30	32	33	36	33	31	-8%	7%
Estonia	37	37	33	30	30	27	20	29	25	23	-8%	-38%
European Union	2 274	2 268	2 123	2 125	2 136	2 111	2 059	2 088	2 052	1 965	-4%	-14%
Finland	47	54	55	55	57	51	55	48	53	52	-2%	10%
France	566	551	527	525	518	493	475	460	454	435	-4%	-23%
Georgia												
Germany	248	242	233	227	224	217	216	210	191	181	-5%	-27%
Greece												
Hungary	47	43	44	48	47	52	48	36	38	48	26%	2%
Iceland	NR	NR	NR	NR	NR	NR	NR	NR	NR			
Ireland	18	18	17	16	17	17	16	15	15	14	-10%	-24%
Italy	209	208	193	191	196	182	179	185	180	173	-4%	-18%
Kazakhstan												
Kyrgyzstan												
Latvia	27	29	29	30	39	33	32	33	32	33	2%	23%
Liechtenstein	0.04	0.04	0.04	0.04	0.04	0.04	0.04	0.04	0.04	0.04	4%	-2%
Lithuania		1	NE	NE	11	11	11	12	12	12	-1%	
Luxembourg	NR	NR	NR	NR	NR	NR	NR	NR				
FYR of Macedonia				NE	NE	NE	NE	NE	NE	NE		
Malta	1	2	2	2	2	2	2	2	2			
Republic of Moldova	5	3	5	6	11	8	8		10	10	-1%	118%
Monaco		NE	NE	NE	NE	NE	NE	NE	NE	NE		
Montenegro							9			7		
Netherlands	39	37	37	35	34	33	32	32	32	30	-6%	-23%
Norway	65	65	67	64	60	58	55	53	50	49	-2%	-25%
Poland	282	300	291	267	280	289	285	269	247	243	-2%	-14%
Portugal	116	123	109	104	112	115	108	106	106	106	0%	-9%
Romania	NE	NE	NE	NE	NE	47	46	130	142	132	-7%	
Russian Federation			561	576	647	591	613	522	475			
Serbia						NE	NE	NE				
Slovakia	45	48	41	37	33	47	41	35	34	33	-1%	-26%
Slovenia	19	19	19	18	18	19	18	18	17	16	-5%	-19%
Spain	144	143	145	143	142	140	135	138	122	109	-11%	-24%
Sweden	40	40	40	41	41	42	41	41	40	39	-3%	-2%
Switzerland	23	23	22	22	22	22	22	21	21	21	-1%	-10%
Turkey									0			
Ukraine		NO	3		119	131	NE	0	NA	NO		
United Kingdom	174	167	145	143	141	137	136	133	129	119	-8%	-32%
United States of America	20 901	21 266	19 346	19 335	19 322	19 275	17 533	15 762	13 028	10 232	-21%	-51%

Notes: *Blank cell indicates that no data have been reported to EMEP.*

NE: not estimated, NO: not occurring, NR: not relevant, NA: not applicable
Shaded cells (red) indicate increased emissions for the given period
Differences for Albania are between 2000 and 2008
Emissions in the row "Russian Federation" corresponds only to "Russian Federation in the former official EMEP domain"

1.1.3 *Contribution of GNFR[5] categories to total emissions*

In order to further improve the atmospheric monitoring and modelling under the Convention, it is important to identify categories that have a significant influence on total emissions. Such analysis helps identifying potential gaps in reporting.

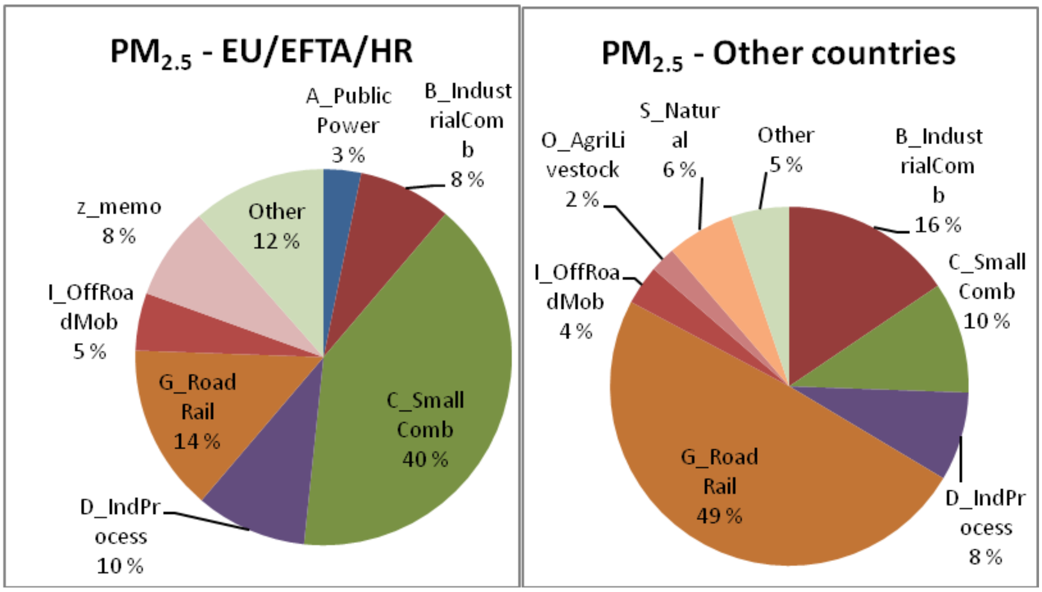

Figure 1.1: Top seven categories contributing to $PM_{2.5}$ 2009 emissions ***(GNFR categories).***

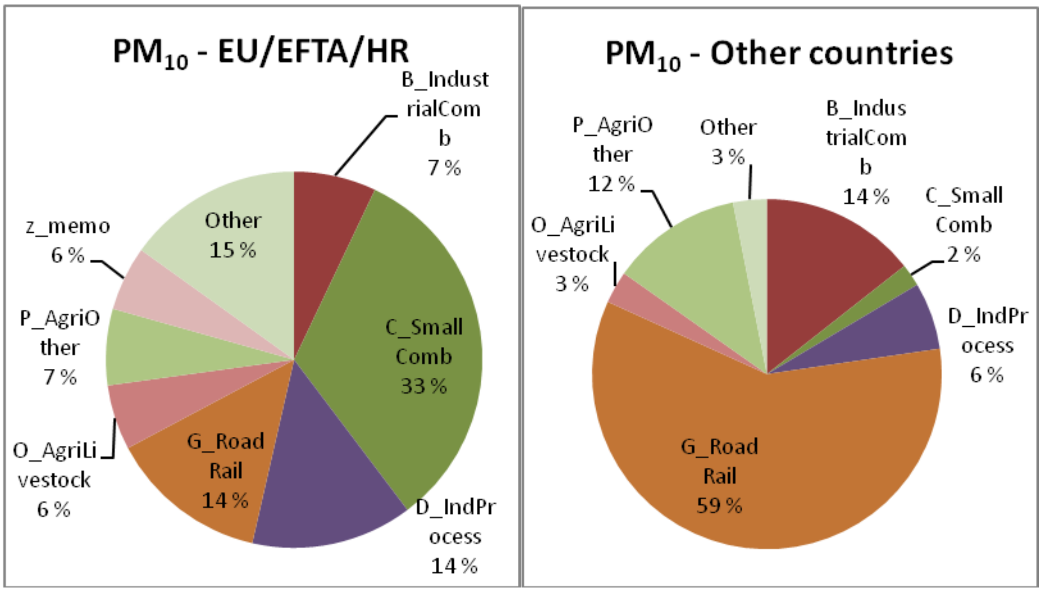

Figure 1.2: Top seven categories contributing to PM_{10} 2009 emissions ***(GNFR categories).***

Note: *If the total number of categories for a particular pollutant was more than seven or the contribution of a particular sector was < 2%, emissions were summed up in 'Other'*
'Memo items' represent emissions reported as international maritime navigation

---

[5] 21 GNFR categories are aggregated NFR09 categories, see (UNECE 2009) Annex IV at http://www.ceip.at/reporting-instructions/annexes-to-the-reporting-guidelines/, GNFR categories should be used for reporting of gridded emissions from 2012 onwards.

The different distribution of GNFR sectors between EU/EFTA/HR and “Other countries[6]”, especially the low contribution of “Small Combustion” in the total PM emissions of “Other countries” indicates that these emissions are significantly underestimated in this region (see Figure 1.1 and Figure 1.2). It has to be noted that in the group “Other countries” only Belarus, the Republic of Moldova and Montenegro reported PM emissions for 2009 and only these countries are included in the shown distribution. High PM emissions reported in “memo items” are due to emissions from ‘international navigation’ reported by Germany. This might indicate the importance of shipping as a source of PM, but also gaps in reporting of shipping emissions by other countries.

1.1.4 Uncertainties in primary PM emissions

The uncertainties in modelling transboundary primary PM are primarily related to uncertainties in the emission data. When considering whether national PM inventories are sufficiently robust to provide useful input for European policy purposes, it is clear that there are still a number of uncertainty-related issues that affect the overall quality of PM inventory data.

A major issue continues to be incomplete reporting. In 2011, only 35 of 49 Parties reported at least some PM data in the required NFR reporting format. Compared to the emissions of gaseous pollutants covered by the Gothenburg Protocol, fewer countries report emissions of primary PM. Officially reported data by the countries constitutes only about 30% of the PM emissions in the extended EMEP domain for 2009 (33% for $PM_{2.5}$ and 28% for PM_{10}), while the remaining 70% of PM emissions are expert estimates. The corresponding figure for NO_x is 47% and for SO_x 33%, whereas it is 54% for NH_3 and 58% for NMVOC.

As was the case in 2006[7], there is still strong evidence indicating that of those countries that did report PM emission not all Parties reported emissions from all sectors in which releases of PM are likely. Some of the sectors in which non-reporting appears common (e.g. agriculture or small combustion sources) may be significant sources with respect to national totals, therefore a general under-reporting of PM emissions to LRTAP from these sectors seems likely. It was also pointed out that there is still a noticeable difference in the number of sectors for which PM emissions are reported in EU27/EFTA/HR and ”Other countries” (Figure A1 and A2).

In addition to the problem of incomplete national inventories, the emission factors used to develop the emission estimates are still a source of uncertainties. Uncertainty associated with the use of recommended emission factors arises from variability in process measurements due to between plant variance and within plant variance as well as with uncertainties associated with the analytical methodology itself. Emission factors may also be subject to systematic bias, e.g. due to assumptions made about the abatement measures used or about the relationships between TSP and PM_{10} and $PM_{2.5}$.

---

[6] Other parties in this chapter refer to Albania, Armenia, Azerbaijan, Belarus, Bosnia and Herzegovina, Georgia, Kazakhstan, Kyrgyzstan, FYR of Macedonia, Republic of Moldova, Monaco, Montenegro, Russian Federation, Serbia, Turkey and Ukraine

[7] See “Transboundary particulate matter in Europe, Status report 4/2006”.

There is a significant range of variability of the uncertainty estimates between the individual countries. The largest uncertainty in PM emission estimates is reported by Denmark: 302% for PM_{10} and 364% for $PM_{2.5}$ emissions (which is an improvement compared to 2006 when Denmark reported 432% uncertainty for PM_{10} and 445% for $PM_{2.5}$). For the United Kingdom, the estimated uncertainty in PM_{10} and $PM_{2.5}$ emissions were (-20)–(+30)%. In Finland, the reported uncertainty of the 2009 emissions is (-43)–(+55)% for $PM_{2.5}$ and (-33)–(+35)% for PM_{10} emissions. The reported uncertainty for PM_{10} emissions is 43% in Ireland and 17% in Switzerland. For the individual sectors, the largest uncertainties in the PM emission inventories are reported to be due to fugitive emissions from industrial processes (e.g. metal production), quarrying, agriculture (agricultural soils, manure management etc.), constructions etc. Emission estimates for fuel combustion in transport, power production, industrial and commercial sectors are generally considered more reliable. However, significant uncertainties are associated with PM emissions from bio fuel combustion in the residential sector.

Additional uncertainties in $PM_{2.5}$ emissions can be due to the uncertainties in particle size distribution when $PM_{2.5}$ emissions are derived as a fraction of the corresponding PM_{10} emissions. However, the overall uncertainties of $PM_{2.5}$ emissions can be smaller than for PM_{10} emission inventories since much of $PM_{2.5}$ is emitted from fuel combustion sources (mobile sources, residential/commercial and industrial combustion). From those sectors, the estimates of traffic emissions are believed to be more reliable than e.g. the emissions from residential heating. Emissions of coarse PM are associated with rather significant uncertainties due to a larger contribution of fugitive emissions of coarse PM from industrial processes, constructions and agricultural activities, which are difficult to measure. Also, coarse PM emissions from residential combustion should be considered.

The fluctuations of reported PM emissions during the last ten years also indicate high uncertainty of these data. Figure 1.3 and Figure 1.4 show variations of $PM_{2.5}$ emissions for 2000 in selected countries as an example. The red bars present the latest emissions reported in 2011 and the black vertical line shows the range of submitted and resubmitted emission values from 2002 to 2011.

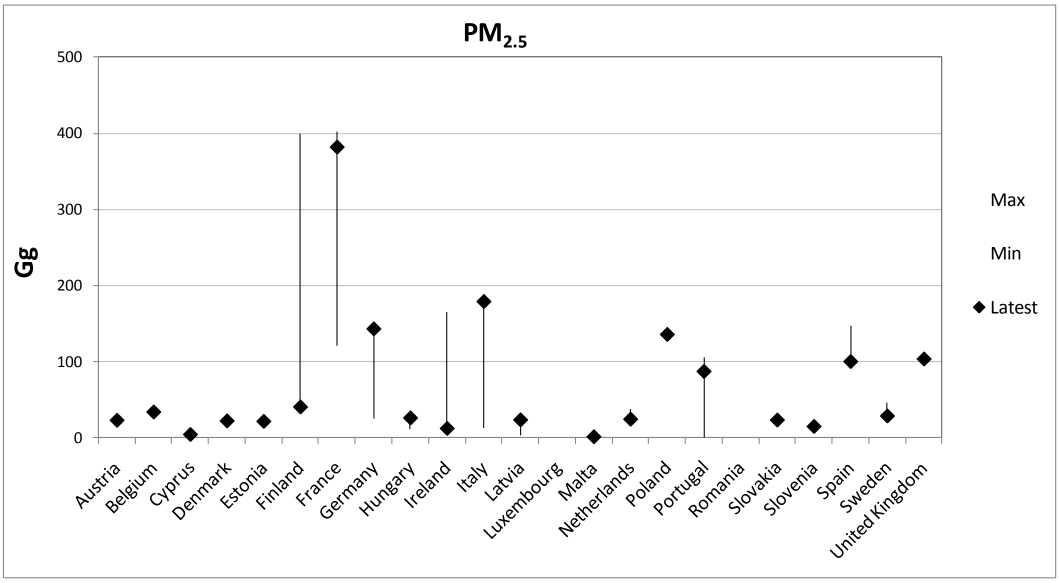

Figure 1.3: Variations in $PM_{2.5}$ emissions for the year 2000 reported in 2002–2011.

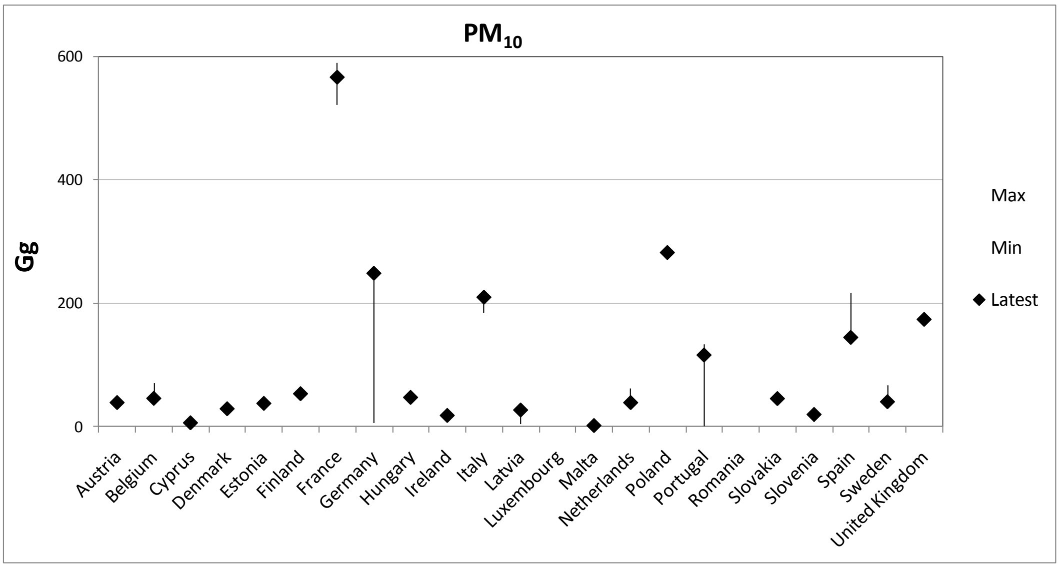

Figure 1.4: Variations in reported PM_{10} emissions for the year 2000 in 2002–2011.

The following tables (Table 1.3 and Table 1.4) show the PM emissions in Gg for selected countries for the year 2000 as reported from 2011 to 2002, whereas for every year the latest emission value available at that time is given. The last two columns indicate the range; the maximum deviation from the latest submitted value among the whole reporting timeline.

Table 1.3: PM$_{2.5}$ emissions (Gg) reported for the year 2000 between 2002 and 2011.

Country/ Year reported	2011	2010	2009	2008	2007	2006	2005	2004	2003	2002	Deviation from latest submitted value	
Austria	22.6	22.5	23.0	23.5	26.3	25.9	24.7	24.7	27.4		-1%	21%
Belgium	33.5	33.2	33.1	35.2	35.2	35.2	35.1	40.4	36.0		-1%	21%
Cyprus	3.9	2.8	2.3	0.5	0.5						-89%	0%
Denmark	21.8	22.5	24.2	24.2	24.3	22.9	23.2	14.8	13.3	12.1	-44%	12%
Estonia	21.2	21.0	21.2	21.2	21.2						-1%	0%
Finland	40.1	36.6	36.6	36.6	399.9						-9%	897%
France	381.3	378.3	402.5	400.1	121.3	341.6	281.4	290.2	299.3	304.0	-68%	6%
Germany	142.7	136.8	125.7	126.0	25.7	115.1	32.3	32.4			-82%	0%
Hungary	25.7	25.7	25.7	25.7	10.7	25.7	25.7	25.7	25.7	20.2	-59%	0%
Ireland	11.9	11.8	11.3	10.2	165.6						-14%	1295%
Italy	178.6	160.2	160.9	165.7	12.2						-93%	0%
Latvia	23.2	23.0	11.2	11.3		11.0	3.0	2.9	NE		-87%	0%
Luxembourg	NR	NR	NR									
Malta	1.0	1.0	1.0	1.0							-2%	0%
Netherlands	24.1	25.3	25.5	25.6	27.3	28.8	28.9	30.9	37.3		0%	55%
Poland	135.3	135.3	135.3	135.3	135.3	135.3	135.3	135.3	135.3	135.3	0%	0%
Portugal	86.8	97.8	105.3	105.7	95.1	95.1	0.1	0.1	NE		-100%	22%
Romania	NE	NE	NE									
Slovakia	22.9	31.7	32.6	26.0	26.0	26.0	NE	NE	NE		0%	42%
Slovenia	14.5	14.2	6.4	6.4	6.5	6.5					-56%	0%
Spain	99.7	126.5	131.1	130.8	135.0	136.6	139.5	146.7	0.0		-100%	47%
Sweden	28.2	28.3	30.7	36.2	32.1	46.1	44.7	44.5	45.0		0%	63%
United Kingdom	103.1	102.9	100.3	111.6	111.9	108.2	100.3	102.3	108.2		-3%	9%

Notes: *The table includes only Parties which reported PM emissions or notation keys at least for one year NE: not estimated; NR: not relevant. Red shaded cells indicate deviations of more than 50%*

Table 1.4: PM$_{10}$ emissions (Gg) reported for the year 2000 between 2002-2011.

Country/ Year reported	2011	2010	2009	2008	2007	2006	2005	2004	2003	2002	Deviation from latest submitted value	
Austria	38.7	36.7	43.4	43.9	45.5	44.3	44.1	38.3	47.4		-5%	23%
Belgium	45.5	47.6	47.5	66.4	66.4	66.4	64.9	70.0	65.4		0%	54%
Cyprus	5.9	4.7	3.5	0.8	0.7						-88%	0%
Denmark	28.6	29.7	35.5	35.5	35.6	30.9	31.3	22.4	19.9	27.1	-30%	24%
Estonia	37.3	36.6	36.8	36.8	36.8						-2%	0%
Finland	53.0	46.9	46.9	46.9							-12%	0%
France	566.1	566.0	590.2	587.7	589.2	549.5	521.5	534.7	545.4	566.0	-8%	4%
Germany	248.3	236.5	230.0	215.1	210.4	192.9	6.3	NE			-97%	0%
Hungary	47.0	47.0	47.0	47.0	47.0	47.0	47.0	47.0	47.0	45.8	-3%	0%
Ireland	17.8	17.8	16.9	12.6	13.1						-29%	0%
Italy	209.5	191.6	192.3	199.8	199.3	192.5	192.5	185.3			-12%	0%
Latvia	26.6	24.1	12.7	12.9	13.8	13.5	4.6	4.2	NE		-84%	0%
Luxembourg	NR	NR	NR									
Malta	1.4	1.4	1.6	1.6							0%	11%
Netherlands	38.6	43.6	43.7	44.3	46.2	48.0	48.0	49.0	62.5		0%	62%
Poland	281.9	281.9	281.9	281.9	281.9	281.9	281.9	281.9	281.9	281.9	0%	0%
Portugal	115.7	127.1	133.8	130.6	119.3	119.1	0.1	0.1	NE		-100%	16%
Romania	NE	NE	NE									
Slovakia	45.1	39.0	39.7	40.4	40.4	40.4	NE	NE	NE		-13%	0%
Slovenia	19.4	18.1	8.3	8.3	8.7	8.7					-57%	0%
Spain	144.3	170.5	173.2	173.0	177.3	204.5	208.3	216.9	0.0		-100%	50%
Sweden	40.0	40.3	42.8	48.4	51.5	67.8	66.1	65.7	66.1		0%	70%
United Kingdom	173.5	171.7	170.2	184.0	184.0	180.4	167.6	178.9	178.0		-3%	6%

Notes: *The table includes only Parties which reported PM emissions or notation keys at least for one year. NE: not estimated; NR: not relevant. Red shaded cells indicate deviations of more than 50%*

A number of countries reported significant variations in revised PM$_{2.5}$ emission: e.g. Ireland (+1295%), Finland (+897%), Portugal and Spain (both -100%), Cyprus (-89%), Latvia (-87%), Italy (-93%), Germany (-82%), France (-68%), Netherlands (+55%) and Denmark (-44%). Some of these countries reported also big variations in the PM_{10} emissions for the year 2000 (e.g. Cyprus, Germany, Latvia, Portugal and Spain).

The tables indicate that in a number of countries the completeness of PM emission reporting for 2000 has improved between 2002 and 2011. However, there are still Parties with no PM reporting (e.g. Greece, Luxembourg and Romania) or no improvements in PM historical data (e.g. Poland where no recalculations have been performed since 2002).

1.1.5 Emission data prepared for modelers

Modellers use $PM_{2.5}$ and PM_{coarse}[8] ($PM_{10-2.5}$) emissions distributed in the 50 x 50 km² PS EMEP grid[9]. The extended EMEP domain comprises approximately 20 000 grid cells, but PM sectoral data is reported for less than 50% of this area. More or less complete emissions are available for Europe, except for some Balkan countries. No PM emissions were reported by a number of EECCA countries, Turkey and for the “Russian Federation extended EMEP domain”.

To make submitted emission data usable for modellers, emissions reported in NFR09 categories are converted to 10 SNAP sectors, whereas missing information (not reported by Parties) has to be filled in[10].

Gap-filled and gridded data can be accessed via the CEIP homepage at http://www.ceip.at/emission-data-webdab/emissions-as-used-in-emep-models/ and gridded data can also be visualized in Google Maps/Earth at http://www.ceip.at/emission-data-webdab/gridded-emissions-in-google-maps/.

1.1.6 Update of historical gridded emissions used in EMEP models (2000–2008)

To provide modellers with historical data that is consistent with the latest (recalculated) data reported by Parties, CEIP has re-gridded data from previous years (from 2000 to 2008). In 2011, the years 2000 to 2004 were re-gridded using the RG tool[11] to keep the distribution of these years. The years 2005 to 2008 were re-gridded using the same distribution as for 2009. These updated emissions are used in the source-receptor models in the year 2011.

Revised data show only small changes in $PM_{2.5}$ and PM_{coarse} emissions for the years 2000 and 2005 for the whole EMEP area (see Table 1.5). For some countries the differences in revised emissions have been significant. For example, Cyprus’ updated $PM_{2.5}$ emissions increased by 41% in 2000, whereas for Spain (-25%) and Slovakia (-28%) they decreased. PM_{coarse} emissions increased in Finland by 25% in the year 2000, whereas in 2005 they decreased by -28%. In

---

[8] PMcoarse emissions are not reported but estimated as the difference between PM_{10} and $PM_{2.5}$

[9] Information regarding the gridding procedure can be downloaded at http://www.ceip.at/fileadmin/inhalte/emep/pdf/gridding_process.pdf

[10] Basic principles are described in the EEA, 2009 *Proposed gap-filling procedure for the European Community LRTAP Convention emission inventory.*

[11] CEIP has developed a software “RG tool” for distributing resubmitted emissions which uses the given spatial distribution of a particular year. It was developed in 2010 to re-grid air pollutants reported to UNECE on SNAP 10 sector level.

Croatia, Latvia and Slovenia revised PM_{coarse} emissions increased significantly for the whole timeline from 2000 to 2008. These major revisions of historical data indicate high uncertainty of PM emissions.

Table 1.5: Total differences between PM emissions gridded in 2010 and re-gridded in 2011 for the years 2000 and 2005.

	2010 expert data	**2011 expert data**	**Difference [Gg]**	**Difference [%]**
$PM_{2.5}$ Total 2000	3 636	3 623	-13	-0.37%
$PM_{2.5}$ Total 2005	2 966	2 943	-23	-0.77%
PM_{coarse} Total 2000	1 967	1 984	17	0.88%
PM_{coarse} Total 2005	1 602	1 606	4	0.26%

A table listing the differences between gridded emissions from 2000 to 2008 used in models in 2010 and re-gridded in 2011 (per country/pollutant/year and expressed both as a percentage and in Gg) can be downloaded at http://www.ceip.at/fileadmin/inhalte/emep/xls/2011/Diff_gridded_regridded_2011.xls.

1.2 Updated GAINS emission estimates from road transport sector (SNAP 7)

By Jens Borken-Kleefeld and Zbigniew Klimont

The major upgrade of the reporting period is the implementation of the latest emission factors for road vehicles in European countries. These factors now correspond to the latest version of COPERT IV and have been supplied by LAT (Thessaloniki) directly. This upgrade comes with several improvements:

- Emission factors refer to real world driving (as described by the so-called ARTEMIS driving cycles), not to limit values.
- Previously emission factors for each vehicle category were calculated as the product of a base factor referring to the so-called ‘no-control technology’ and the so-called removal efficiency, specific to each exhaust emission control stage (Euro norm). The no-control factor was specific to each country and reflected the then fleet mix in terms of vehicle sizes and ages, while the removal efficiencies differed only for the technology, not the country.
  Now, emission factors for all vehicle categories and emission control stages are country specific, thus better reflecting the different developments of fleet mix.
- Total emissions are still calculated as the product of fuel consumption times the energy specific emission factor, with the exception of non-exhaust particulate matter. However, vehicle mileage and vehicle numbers have been carefully revised and harmonized with the respective fuel consumption in European countries. This means, that implied ratios e.g. for the specific fuel consumption per vehicle category or the average annual vehicle mileage are now consistent

and validated with latest data, essentially as collected in the FLEETS project[12] exactly for the purpose of emission calculations.

As a consequence, non-exhaust emissions of particulate matter depending on the actual vehicle mileage are now much more consistent. Furthermore, cost estimates have been improved as they depend on the vehicle number.

- Furthermore, the fleet turnover modelling has been revised at the same time as the vehicle stock numbers. Again, this draws on the data from the TREMOVE/COPERT database for the European countries and thus ensures consistency across countries and with the other pertinent data. In consequence, the fleet mix by technology, i.e. the so-called control strategy, has been improved.

In terms of emissions, the most important change concerns NO_x emissions from diesel passenger cars: According to measurements, vehicles certified according to Euro III emission standards have actually higher emissions in real world driving than older vehicles, and reductions for vehicles according to Euro 5 and Euro 6 are by far not as large as stipulated by the respective limit values. Hence, overall NO_x emissions from road transport in EU27 will decline less and will be about 28% higher in 2020 than previously anticipated[13].

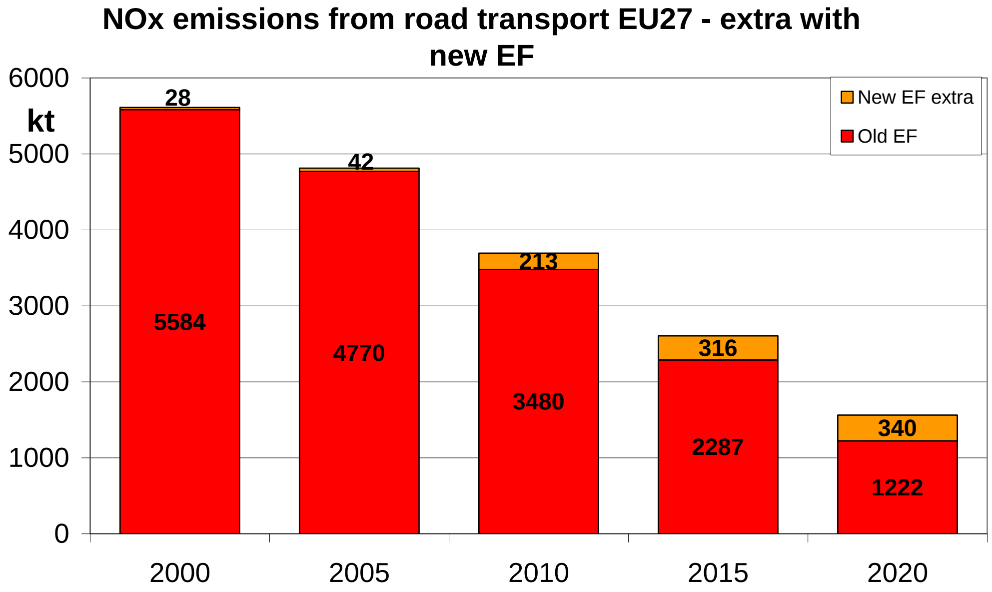

Figure 1.5: NO_x emissions from road transport in EU27: The extra contribution as a consequence of revised real world emission factors is highlighted. It becomes the more relevant the bigger the share of the more vehicles (Euro 4/IV and 5/V) becomes. (Source: IIASA-GAINS: Latest EC4MACS scenario using the PRIMES 2009 Baseline scenario against NEC 4 scenario.)

---

[12] "European Database of Vehicle Stock for the Calculation and Forecast of Pollutant and Greenhouse Gases Emissions with TREMOVE and COPERT", funded by EC – DG Environment http://www.emisia.com/tools/FLEETS.html

[13] This increase is partially offset by reductions in other sectors so that total NO_x emissions in EU27 in 2020 will be about 2% higher than previously estimated. Latest EC4MACS scenario using the PRIMES 2009 Baseline scenario against NEC 4 scenario.

Finally, the upgrade of emission factors affected also CO, NMVOC, CH_4, N_2O, PM_{10}, $PM_{2.5}$, BC and OC emissions. However, changes to previous values, though large for individual vehicle categories and countries, are small when all sectors are summed up.

As already discussed in the last year report (EMEP, 2010; *the Status Report 4/2010*), assessment of the role of high emitting vehicles (including off-road land machinery) has been included in GAINS. The work on refining and validating the approach continues but to date the results for all primary PM components are similar to those discussed in the last report for black carbon, indicating that these vehicles are estimated to contribute about 10-15% of emissions and might be often neglected in official emission inventories. It has to be noted that current methodology shows that for NO_x and CO the contribution of high emitting vehicles might be larger, i.e., 15-20%. CIAM is working with University of Illinois (US) on update of the methodology and its extension for the whole world. The results of this work will be implemented in GAINS in the next months and we will report on this in the next report.

1.3 Feedback from the work of the UNECE Expert Group on Black Carbon

By Zbigniew Klimont

CIAM is continuing efforts to update and harmonize estimates of black carbon and other primary PM components in the GAINS model. Within the work of the UNECE Expert Group on Black Carbon that concluded its work in December 2010, CIAM provided detailed national modelling results from GAINS to the national experts for their evaluation and possible use in own inventories. It is encouraging to see that following this collaboration, also stimulated by the involvement of CIAM in the work of the Arctic Council Task Force on short-lived climate forcers, Denmark pursued a first national BC inventory which has been recently published (Winther and Nielsen, 2011); this forthcoming paper has been drawing on GAINS methodology making use of the most recent national data as well as data specifically developed for the project.

We have received comments from several countries, specifically: Denmark, Finland, Norway, Switzerland, UK, US, and Canada. We work on the inclusion of them in the model and the results will be used in the current round of calculations for the revision of the Gothenburg Protocol.

Discussion with few of the national experts and the new data they have collected for domestic sector underlines the importance of this sector for emissions but even more so for the future emissions and therefore understanding of the technology transition in this sector is essential. What follows is a need for better understanding of emissions of various primary PM species from the new technologies that are expected to represent a significant share of the activity in the near future. The work will continue under the new UNECE HTAP mandate.

2 Measurement and model assessment of particulate matter in Europe, 2009

2.1 PM mass concentrations

By Svetlana Tsyro, Karl Espen Yttri and Wenche Aas

2.1.1 Introduction

The current assessment of the concentration levels of regional background PM_{10} and $PM_{2.5}$ in 2009 has been made based on EMEP model calculations and data from the EMEP monitoring network. In this chapter, we present the recent estimates of PM_{10} and $PM_{2.5}$ concentrations for 2009 and outline the main changes in calculated PM_{10} and $PM_{2.5}$ for 2009 compared to those for 2008. Furthermore, calculated exceedances of the WHO Air Quality Guidelines by the regional background PM_{10} and $PM_{2.5}$ concentrations in 2009 are presented. Finally, the summary results of the model evaluation for PM_{10} and $PM_{2.5}$ and aerosol components with EMEP observations in 2009 are provided and the status of model performance is discussed.

2.1.2 The measurement network

The observed annual mean concentrations of PM_{10}, $PM_{2.5}$ and PM_1 for 2009 at European rural background sites can be found in Hjellbrekke and Fjæraa (2011). For 2009, mass concentrations of PM are reported for 65 regional or global background sites (61 for PM_{10} and 40 for $PM_{2.5}$); two more than in 2008. There are four new sites in 2009 compared to 2008: ES0001, ES0017, FR0018 and NL0011, but two sites from 2008 have not reported data for 2009: DE0043G and SE0035. The same number of Parties reported aerosol mass data in 2009 and 2008 (25). It is worth noting that although the number of sites has increased the last years, several sites have unsatisfactory data coverage. In 2009, 51 of the 61 PM_{10} sites have data completeness higher than 75%. For $PM_{2.5}$ there are 33 of the 40 sites with satisfactory data coverage. PM_1 was reported for 6 sites in 2009, compared to 7 for 2008.

2.1.3 The EMEP model and runs set-up

The calculations presented in this report have been performed with the EMEP/MSC-W model, earlier referred to as the ‘Unified EMEP model’. A detailed description of the EMEP MSC-W model can be found in Simpson et al. (2003), Fagerli et al. (2004) and Tsyro (2008) and in last year EMEP Status Report 1/2010. The most recent developments of the EMEP MSC-W model (version v. 2011-06) are documented in EMEP Status Report 1/2011 and Simpson et al. (2011).

The meteorological data used in the model simulations for 2009 was produced using the ECMWF-IFS meteorological model (Integrated Forecast System).

The national emissions of SO_x, NO_x, NH_3, NMVOC, PM_{10} and $PM_{2.5}$ for the year 2009 were prepared by EMEP/CEIP.

2.1.4 Annual PM_{10} , $PM_{2.5}$ and PM_1 concentrations in 2009

The lowest measured concentrations of PM_{10} were observed in the northern and north-western parts of Europe, i.e. the Nordic countries, British Isles, and for high altitude sites (> 800 masl) on the European mainland (Figure 2.1). The highest concentrations are found in the Netherlands, Hungary and Italy. The regional distributions of PM_{10} and $PM_{2.5}$ are very similar. These measurements have been combined with the EMEP/MSC-W model to create annual mean concentration fields of regional background PM_{10} and $PM_{2.5}$ (Figure 2.2).

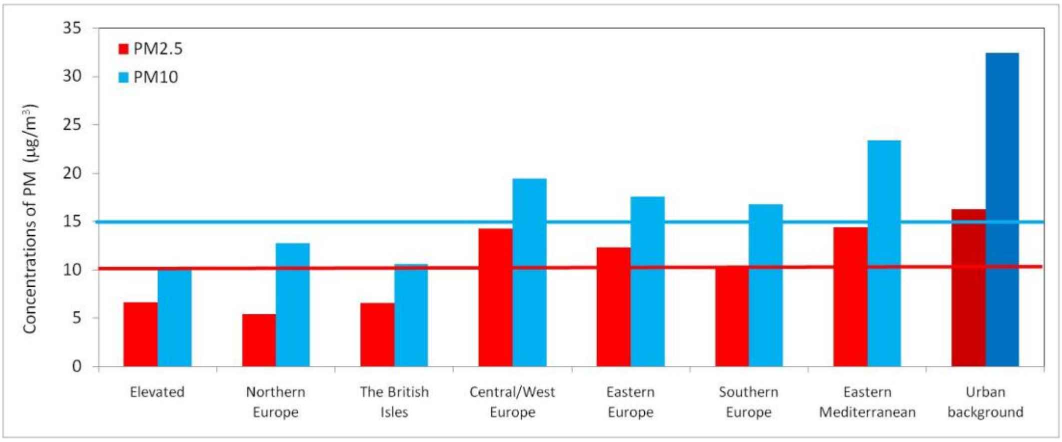

Figure 2.1: Annual mean concentrations of PM_{10} and $PM_{2.5}$ for various regions of the EMEP domain in 2009 ($\mu g\ m^{-3}$). Solid blue and red lines denote the average concentrations for all sites. Annual mean concentrations for European urban background sites (from AirBase) are included for comparison.

The following procedure has been used to generate the combined maps shown in Figure 2.2: For each measurement site with PM data in 2009, the difference between the measured value and the modelled value in the corresponding grid cell has been calculated. The differences for all sites have been interpolated spatially using radial base functions, thus providing a continuous 2-dimensional function describing the difference in any cell within the modelled grid. The combined maps have been constructed by adjusting the model results with the interpolated differences, giving larger weight to the observed values close to the measurement site, and using the model values in areas with no observations. The range of influence of the measured values has been set to 500 km.

These combined maps (Figure 2.2), have a pronounced north to south gradient in PM concentrations, with the annual mean PM_{10} varying from 1-5 $\mu g/m^3$ in Northern Europe to 10-25 $\mu g/m^3$ in Southern Europe.

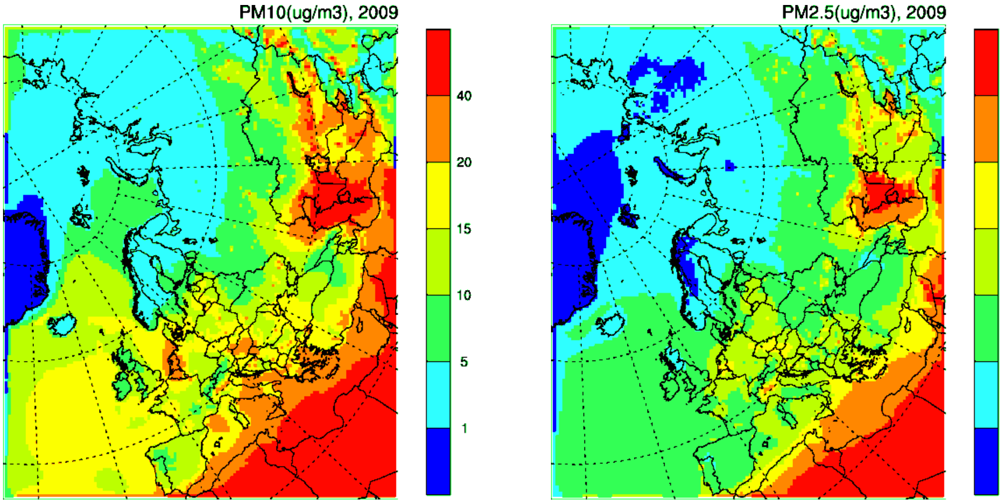

Figure 2.2: Annual mean concentrations of PM_{10} *(left) and* $PM_{2.5}$ *(right) in 2009 based on EMEP/MSC-W model calculations and EMEP observation data.*

The average concentration of PM_{10} for all sites was 15.0 $\mu g/m^3$, shown as the blue line in Figure 2.1. The concentration levels in Southern, Eastern and Western Europe are notably higher than in Northern Europe and reflect both population density and major anthropogenic sources. The lowest observed annual mean PM_{10} concentration was recorded at the high altitude global site Jungfraujoch (CH0001G, 2.7 $\mu g/m^3$). For regional sites the lowest concentration was observed at Hyytiälä (FI0050R, 4.5 $\mu g/m^3$), situated in the boreal forest of Finland, whereas the highest were recorded at the Italian site Montelibretti (IT0001R, 29.9 $\mu g/m^3$) and Hungarian site K-puszta (HU0002R, 27.9 $\mu g/m^3$). The mean European urban background concentration of PM_{10} measured at AirBase sites has been included in Figure 2.1 to give an idea of the rural background influence, which generally appears to be 50% of urban concentrations.

The average concentration of $PM_{2.5}$ for all sites was 10.1 $\mu g/m^3$, shown as the red line in Figure 2.1. The annual mean concentrations of $PM_{2.5}$ range from 3-7 $\mu g/m^3$ in Northern Europe to 8-19 $\mu g/m^3$ in Southern Europe (Figure 2.1). The highest annual means were measured at Vredepeel (NL0010) and Ispra (IT0004R) with concentrations just above 19 $\mu g/m^3$. The lowest levels were exclusively associated with sites in Northern Europe and the British Isles or elevated sites in continental Europe. The lowest annual mean $PM_{2.5}$ concentration was observed at the Norwegian site Birkenes (3.5 $\mu g/m^3$). More than 60% of the urban background concentration is likely to be attributed to the mean rural background concentration of $PM_{2.5}$ (Figure 2.1).

The annual mean concentration of PM_1 was reported for six sites. The highest annual mean was observed at the Austrian site Illmitz (AT0002R, 11.5 $\mu g/m^3$), and was more than three times higher than lowest annual mean measured at Hyytiälä in Finland (FI0050R, 3.2 $\mu g/m^3$).

2.1.5 PM_{10} and $PM_{2.5}$ in 2009 compared to 2008

50% of the sites which reported concentrations of PM_{10} both for 2008 and 2009 had lower annual means in 2009 compared to the previous year, meaning that the levels in 2009 and 2008 are quite comparable. On average there was a small decrease of 4%, which follows the decreasing trend from the previous years. However, there are large variations between sites, and the largest relative decrease was at the British site Narberth (GB0043), were the annual mean went from 17.6 $\mu g/m^3$ in 2008 to 11.5 $\mu g/m^3$ in 2009 (35% decrease). The largest relative increase of 28% (from 7.2 to 9.2 $\mu g/m^3$) was seen at the German site Schauinsland (DE0003).

For $PM_{2.5}$ the average concentration levels in 2008 and 2009 are similar, and the same number of sites had a decrease or increase. The highest decrease was seen at the Spanish site Penausend (ES0013), with a change from 6.6 $\mu g/m^3$ in 2008 to 5.2 $\mu g/m^3$ in 2009 (20% decrease) , and the highest increase of 32% was found at Schauinsland (DE0003), same site as for PM_{10}

Also for PM_1, the annual mean concentrations observed for 2009 were on average comparable to the previous year, ranging from a decrease of 12% to an increase of 11%.

When comparing the calculated PM_{10} and $PM_{2.5}$ concentrations from the EMEP/ MSC-W model from 2009 with the previous year, the differences are in the range of 10-20%, as reported in Report 4/2010 (EMEP, 2010). The general tendency is that PM_{10} and $PM_{2.5}$ concentration levels go up somewhat in the northern of the EMEP area (Fennoscandia and north-western Russia), while they decrease in Central and Southern Europe in 2009 compared to 2008. Both changes in emissions and meteorological variability are the reasons for the differences in calculated PM concentrations. The model development since last year reporting has also some effect on calculated PM concentrations. No model calculations of PM_1 concentrations are available.

Changes due to emissions. Reductions in the emissions of gaseous precursors and primary PM have been reported for most of EMEP countries in 2009 compared to 2008. Just to note the most important emission changes, reductions by 21-36% in SO_x emissions are reported by twelve European countries; the largest NO_x emissions reductions occurred in Spain (-23%), the UK (-23%), Ukraine (-36%) and Latvia (-25%); $PM_{2.5}$ emissions decreased by 20-38% in four countries and coarse PM emissions went down by 36% in Belgium and by 35% in Bulgaria. In addition, the emissions of SO_x and PPM from shipping in the North and Baltic Sea decreased by around 30%. Significant emission increases have been reported by Belarus (91%), Latvia (44%), Iceland (24%) and Croatia (21%) for SO_x, by Czech Republic (26%) for NH_3 and by Albania (102%) and Italy (18%) for $PM_{2.5}$, and by Albania (51%), Slovenia (59%), Latvia (306%) and Lithuania (32%) for coarse PM. For further details see EMEP Report 1/2011 (EMEP, 2011).

As a result of the reported emission changes, the $PM_{2.5}$ concentrations are lower in 2009 than in 2008 by 5-15% over most of EMEP area, with the largest decrease in Spain (20-30%). The only exception is Iceland and Montenegro, where $PM_{2.5}$ concentrations increased by 5-10% from 2008 to 2009. PM_{10} concentrations show similar changes from 2008 to 2009, only the decreases are slightly lower than for $PM_{2.5}$.

***Changes due meteorological conditions*.** Due to differences in meteorological conditions in 2009 and 2008, there are changes up to 20% in the annual mean concentrations of PM_{10} and $PM_{2.5}$. There is a pronounced belt of enhanced PM concentrations, stretching south-west to north-east, from Spain, through France, Austria, Czech Republic and Germany, to Scandinavia and northern Russia. Here the annual mean concentrations of all $PM_{2.5}$ and SIA are 10-20%, whereas PM_{10} is 5-15% higher in 2009 than in 2008. The main apparent reason is less precipitation in this area in 2009 compared to 2008. An additional reason is lower temperatures in Central Europe, Scandinavia and Russia, which facilitated formation of secondary aerosols in 2009 compared to 2008. Outside this belt, PM concentrations are 5-10% lower in 2009 than in 2008, in particular in the UK, Mediterranean region, in Balkan and EECCA countries.

Model changes. Recent updates in model description of several processes caused moderate, mostly within ±10%, changes in calculated PM_{10} and $PM_{2.5}$ concentrations. Calculated with the present model version (v. 2011-06) of the EMEP/MSC-W model, $PM_{2.5}$ is 5-10% lower in Central and Eastern Europe, southern Russia and EECCA countries, whilst it is 5-10% higher in the north and south of the EMEP area compared with the previous model version. The $PM_{2.5}$ changes are mostly driven by SIA components and are due to the lower calculated values of NO_3^- and NH_4^+ in central Europe, whereas SO_4^{2-} concentrations are 2-10% higher. Changes in PM_{10} are in general within 5% due to model updates, with the exception of Central Asian countries, where calculated windblown dust is about 20-30% lower compared to that from the previous model version. This change is due to the adjustments of windblown scheme to ECMWF-IFS data for soil moisture.

2.1.6 Trends in PM_{10} and $PM_{2.5}$

The longest time series of PM data reported to EMEP goes back to 1997; i.e. for four Swiss sites and one British. Profound inter annual variations in the PM concentrations are observed of which those associated with the peak in 2003 is the most pronounced (Figure 2.3). However, there is also a relatively clear decrease in the mass concentration for several of the sites. Trend analysis, using the Mann Kendall test, of data from seventeen sites, having more than nine years of measurements and sufficient data coverage, show a significant decrease at ten of these and no sites with increase. The average decease for these ten sites was 21%.

For $PM_{2.5}$, there is a significant decrease at three (ES13, IT04, DE03) of the eight sites having at least nine years with measurements, meaning trend analysis can be done. No sites have a significant increase. The average decrease is 27% for these three sites.

The downward tendency in the observed annual mean concentration of PM, corresponds to a rather broad reduction in the emissions of primary PM and secondary PM precursors in Europe in the actual period.

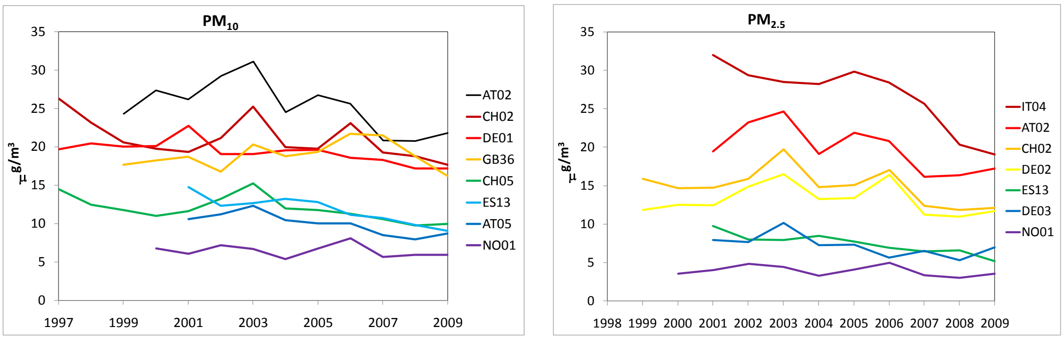

Figure 2.3: Time series of PM_{10} and $PM_{2.5}$ at selected EMEP sites.

Figure 2.4 shows model calculated and observed changes in annual mean PM_{10} and $PM_{2.5}$ concentrations between 2005 and 2009. Here, the concentrations are averaged over all EMEP sites with at least 75% data for each of the years. Except from enhanced PM level in 2006 (especially for PM_{10}), the model calculates a downward “trends” in PM_{10} and $PM_{2.5}$ towards 2009 corresponding with the observations.

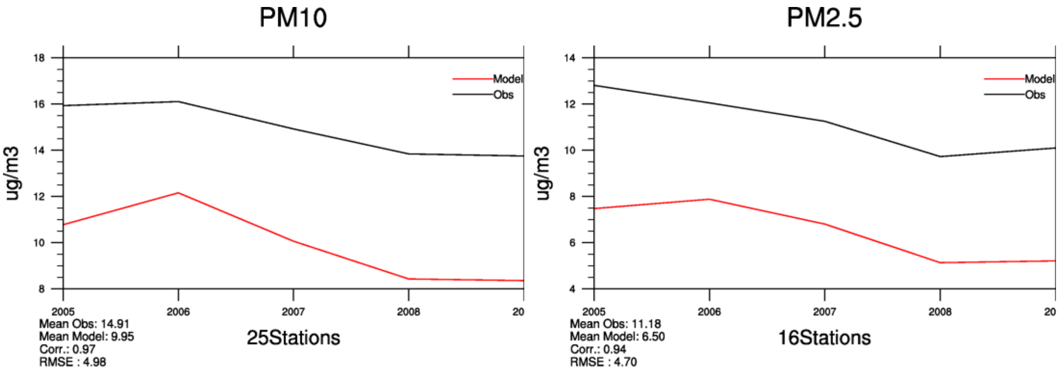

Figure 2.4: Time series of PM_{10} and $PM_{2.5}$ from the EMEP/MSC-E model calculated for selected EMEP sites, 2005-2009.

2.1.7 PM size fractions

Table 2.1 shows the annual mean $PM_{2.5}$ to PM_{10} ratio at EMEP sites based on observational data and model calculations for 2009. The ratios have been calculated for common days, i.e. when both observational and modelled concentrations of $PM_{2.5}$ and PM_{10} were available. Further, only sites with similar methods for both size fractions are used, i.e. sites with TEOM for one size fraction and gravimetric for the other has not been included due to the large differences the choice of methodology may cause. Notice that not all the sites have measurements for a complete year.

On average, there is a good agreement between model calculations and measured data regarding the fraction of $PM_{2.5}$ in PM_{10}. Over all sites, the observed $PM_{2.5}$ to PM_{10} ratio is 0.62, while the model calculations give a ratio of 0.58.

Table 2.1: Observed and model calculated annual mean PM *ratios at EMEP sites in 2009.*

		Site	$PM_{2.5}/PM_{10}$		PM_1/PM_{10}	$PM_1/PM_{2.5}$
			Obs	Mod	Obs	Obs
Northern Europe	Norway$^{1)}$	NO01$^{1)}$	0.51	0.53		
	Sweden	SE11$^{3)}$	0.51	0.55		
		SE14	0.46	0.50		
	Finland	FI50	0.85	0.60	0.69	0.80
The British isles	Great Britain	GB36	0.56	0.49		
		GB48	0.56	0.45		
Central /Western Europe	Austria	AT02	0.75	0.74	0.54	0.72
	Switzerland	CH02	0.66	0.65	0.46	0.71
		CH05	0.69	0.65	0.57	0.77
	Czech Rep.	CZ03$^{2)}$	0.87	0.74		
	Germany	DE02	0.72	0.63	0.45	0.63
		DE03	0.74	0.68		
		DE44	0.73	0.69		
	France	FR09	0.66	0.63		
		FR13$^{2,3)}$	0.59	0.51		
		FR15$^{2,3)}$	0.56	0.56		
		FR18$^{2,3)}$	0.58	0.48		
Eastern Europe	Latvia	LV10$^{2)}$	0.64	0.59		
		LV16$^{2)}$	0.54	0.66		
	Poland	PL05	0.77	0.63		
Southern Europe	Spain	ES01	0.54	0.49		
		ES07	0.58	0.42		
		ES08	0.57	0.56		
		ES09	0.54	0.55		
		ES10	0.48	0.44		
		ES11	0.50	0.46		
		ES12	0.48	0.55		
		ES13	0.57	0.56		
		ES14	0.60	0.59		
		ES16	0.58	0.60		
		ES1778				0.81
	Slovenia	SI08	0.75	0.76		
Eastern Mediterranean	Cyprus	CY02	0.58	0.58		
Average			0.62	0.58	0.54	0.74

1) Estimated based on weekly data; 2) Less than 75% data coverage; 3) Based on hourly data

Both the observations and the model indicate that the fine fraction in PM_{10} is largest in central Europe (0.6-0.8), which is due to the dominating role of anthropogenic sources. The fraction of fine PM is on average smaller (0.4-0.6) at the sites in southern Europe, where windblown dust has a large influence. Relatively low $PM_{2.5}$ to PM_{10} ratios (0.5) are derived from model results and observational data for Norwegian, Swedish and British sites. This could be due to the presence of coarse sea salt particles, as the sites are located relatively close to the coast, and relatively high influence of primary biogenic aerosols (PBAP) at some sites. However, these compounds are not included in the emissions, and the relatively low ratio also for the model results can therefore not be explained by PBAP.

2.1.8 Exceedances of EU limit values and WHO Air Quality Guidelines in the regional background environment in 2009

The EU limit values for PM_{10} (Council Directive 1999/30/EC) are 40 $\mu g/m^3$ for the annual mean and 50 $\mu g/m^3$ for the daily mean, not to be exceeded more than 35 days per calendar year.

The WHO Air Quality Guidelines (AQGs) (WHO, 2005) are:
for PM_{10}: < 20 $\mu g/m^3$ annually, 50 $\mu g/m^3$ 24-hour (99th perc. or 3 days per year)
for $PM_{2.5}$: < 10 $\mu g/m^3$ annually, 25 $\mu g/m^3$ 24-hour (99th perc. or 3 days per year).

EU limit values for PM for protection of human health and WHO Air Quality Guidelines for PM apply to PM concentrations for so-called zones, or agglomerations, in rural and urban areas, which are representative of the exposure of the general population. The EMEP model is designed to calculate regional background PM concentrations. Clearly, rural and urban PM levels are higher than background levels due to the influence of local sources. However, comparison of model calculated PM_{10} and $PM_{2.5}$ with EU limit values and WHO AQGs can provide an initial assessment of air quality with respect to PM pollution, flagging the regions where the regional background PM already has exceeded the critical values.

The combined model and observation maps show that the annual mean regional background PM_{10} concentrations in 2009 were below the EU limit value of 40 $\mu g/m^3$ over all of Europe, with the exception of small areas in the EECCA countries (Figure 2.2). However, the annual mean PM_{10} concentrations calculated by the model exceed the WHO recommended AQG of 20 $\mu g/m^3$ in Benelux, Hungary and the Po Valley. Calculated PM_{10} concentrations were also found to be in excess of 20 $\mu g/m^3$ in the southern parts of the Mediterranean basin and in the Caucasus and the EECCA countries due to the influence of windblown dust from deserts and semi-arid soils. The regional background annual mean $PM_{2.5}$ concentrations were above the WHO recommended AQG value of 10 $\mu g/m^3$ in many parts of Central, Eastern and South-Eastern Europe, in the Po Valley and EECCA area.

The maps in Figure 2.5 show the model calculated number of days exceeding 50 $\mu g/m^3$ for PM_{10} and 25 $\mu g/m^3$ for $PM_{2.5}$ in 2009. To illustrate the relative importance of man-made and natural particulates in the deterioration of air quality, Figure 2.6 shows the corresponding exceedance maps for anthropogenic PM_{10} and $PM_{2.5}$. For most of Europe, except from southern parts of Spain, Italy and Greece, and parts of Turkey and EECCA countries, PM_{10} did not exceed 50 $\mu g/m^3$ more than 35 days in the rural background (i.e. the EU limit value) in 2009. However in large areas in the south of the EMEP territory, PM_{10} exceeded 50 $\mu g/m^3$ more than 3 days recommended by WHO. Furthermore, the WHO AQG for $PM_{2.5}$ is exceeded by regional background concentrations for more than 3 days in most EMEP countries, except in Finnoscandia and Northern and Eastern Russia. Figure 2.6 indicates for the anthropogenic fraction of regional background PM, exceedances of the EU limit value occurred for PM_{10} in less than 10 days in a very few small areas. However for anthropogenic $PM_{2.5}$, we have calculated between 3 and 20 days with exceedances on a rather large territory, and even 20-40 days (up to 100) in the Po Valley and in the grid cells in Poland, Romania, Bulgaria and on the Uzbekistan-Kyrgystan/Tajikistan border. Comparison of Figure 2.5 and Figure 2.6 reveals the significant contribution from natural dust to the calculated exceedances of the EU limit values and the AQGs for PM_{10} and $PM_{2.5}$ in many EMEP areas.

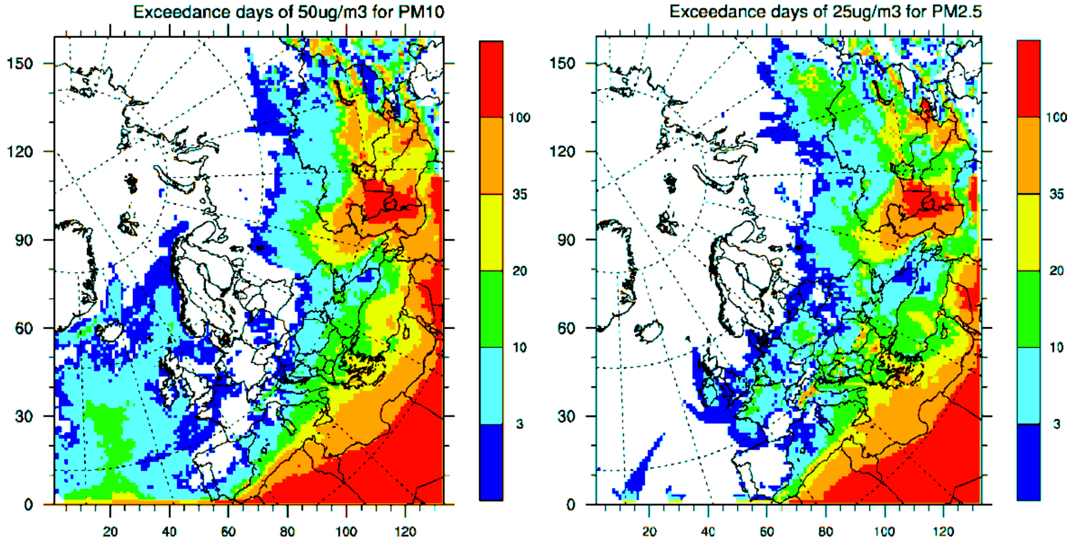

Figure 2.5: Calculated number of days with WHO AQG exceedances in 2009: PM_{10} exceeding 50 $\mu g/m^3$ (left) and $PM_{2.5}$ exceeding 25 $\mu g/m^3$ (right). Note: EU Directive requires that no more than 35 days exceed the limit value, while the WHO AQG recommendation is not to be exceeded more than 3 days.

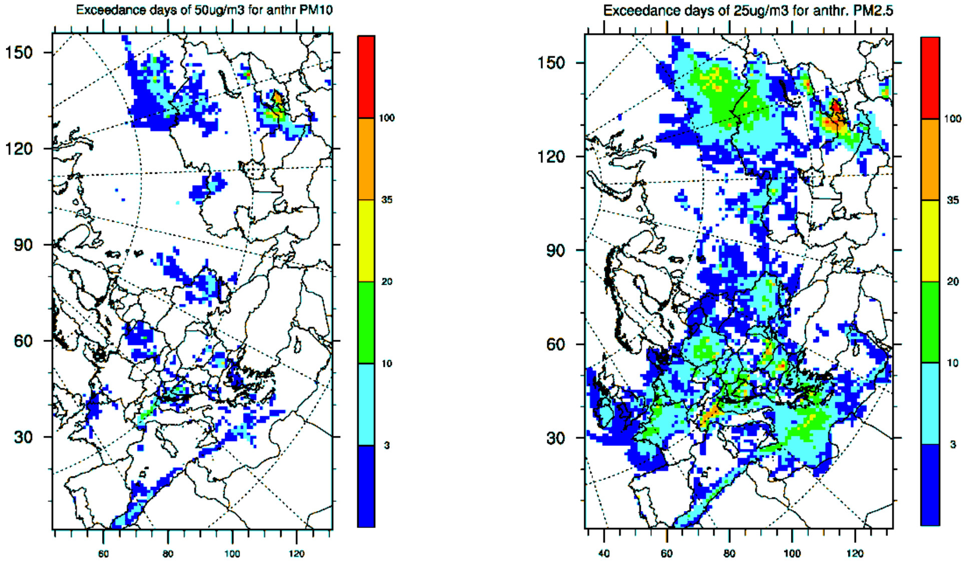

Figure 2.6: Calculated number of days with WHO AQG exceedances in 2009: same as Figure 2.5 but for anthropogenic PM_{10} (left) and anthropogenic $PM_{2.5}$ (right).

Table 2.2: Number calculated and observed days exceeding the WHO AQGs (50 $\mu g\ m^{-3}$ for PM_{10} and 25 $\mu g\ m^{-3}$ for $PM_{2.5}$) at EMEP sites.

	PM_{10}				$PM_{2.5}$			
	Obs	Model	Common	Hit ratio	Obs	Model	Common	Hit ratio
AT02	23	1		0	62	8	5	8
AT05	0	0						
AT48	0	0						
CH01	0	0						
CH02	4	0		0	38	7	5	13
CH03	6	0		0				
CH04	0	0						
CH05	0	0			6	5	2	33
CY02	18	32	14	78	22	22	8	36
CZ01*	0	0						
CZ03*	5	0		0	17	1	1	6
DE01	2	0		0				
DE02	4	0		0	25	3	2	8
DE03	0	0			4	2	0	0
DE07	0	0						
DE08	2	0		0				
DE09	1	0		0				
DE44	11	0		0	50	7	5	10
DK05	7	0						
DK41	4	0						
ES01	1	1	0	0	0	0		
ES07	4	15	1	25	4	2	0	0
ES08	7	3	0	0	9	4	2	22
ES09	0	0			0	0		
ES10	0	0			0	2		0
ES11	0	5	0	0	0	0		
ES12	2	1	0	0	1	0		0
ES13	0	0			0	0		
ES14	0	2		0	4	1	0	0
ES16	0	0			5	0	0	0
ES17	4	2	1	25				
FI50	0	0			0	0		
GB36	2	0		0	19	3	3	16
GB48	0	0			5	1	1	20
GR02	0	84		0				
IT01	20	5	3	15				
IT04					87	10	6	7
LV10*	11	0		0	60	0		0
LV16*	11	0		0	15	0		0
NL09*(PM2.5)					18	0		0
NL10					75	12	12	16
NL11					56	12	12	21
NL91					43	10	8	19
MD13	11	7	0	0				
PL05	6	0		0	31	3	3	10
SE14	4	0		0	1	0		0
SI08	5	2	1	20	16	9	6	38
FR09	12	2	2	17				
FR13*	0	0						
FR15*	6	1	1	17				
GR02*	1	13	1	100				
HU02	30	1	0	0				
IE31					1	2	0	0
MK07*	1	8	0	0				
SE11	0	0			2	1	0	0
SE12*(PM210)	0	0			3	0		0

Hit ratio (%) shows the percentage of observed exceedance days correctly predicted by the model (common_days/obs_days x100%). The shadowed cells show the sites where hourly measured PM concentrations have been averaged to obtain daily values. *Sites with less than 75% data completeness.

Based on model and measurement data, we have calculated the number of days with exceedances of the WHO AQGs at EMEP sites in 2009. The observed and calculated numbers of exceedance days, as well as the number of common exceedance days, i.e. the days for which observed PM exceedances are also predicted by the model, are presented in Table 2.2.

For most of the sites, the model under-predicts the number of exceedance days for PM_{10} and $PM_{2.5}$. The model does not calculate any exceedance for PM_{10} at 15 out of 51 sites, at which exceedances occurred in fewer than 11 days in 2009. For $PM_{2.5}$, the model calculates the occurrences of exceedance at practically all sites where they were observed, but not all of the actual exceedance days are predicted. The most severe model under-prediction of the exceedances are at AT02, IT01, SI08, FR09 and HU02 (for PM_{10}), and CH04, DE44, GB36, GB38, IT04, PL05 and three NL sites for $PM_{2.5}$.

The “Hit ratio” in Table 2.2 shows the percentage of observed exceedance days correctly predicted by the model. The hit ratios vary a substantially (from 0 to 100%) between the sites, and more non-zero hit ratios are achieved for $PM_{2.5}$ than for PM_{10}.

2.1.9 Evaluation of the model performance for PM in 2008

The ability of the EMEP model to reproduce PM concentrations measured at EMEP monitoring sites in 2009 has been evaluated. The model has been evaluated for PM_{10}, $PM_{2.5}$ and also individual aerosol components and the main result are summarised in this section and in Appendix. Note that secondary organic aerosols (SOA) are not included in this model evaluation. The preliminary PM calculations including SOA are presented in the Chapter 2.4.2.

Overall statistic analysis Table 2.3 provides a summary of annual and seasonal statistical analysis of model results versus EMEP monitoring data for 2009. Statistical parameters shown are the mean observed and modelled values, the relative bias, the root mean square error, the correlation coefficient and the index of agreement (IOA). Just to remind, IOA can be interpreted as a difference measure of the degree to which the observed value is accurately estimated by the calculated value. The IOA describes the degree to which the model predictions are error free and varies from 0.0 (theoretical minimum) to 1.0 (perfect agreement).

On average in 2009, PM_{10} and $PM_{2.5}$ are underestimated by 41% and 52%. The $PM_{2.5}$ underestimation is fairly flat for all seasons, while it is somewhat larger in spring-summer compared to autumn-winter seasons for PM_{10}. The annual mean spatial correlation between calculations and measurements is 0.59 for PM_{10} and 0.57 for $PM_{2.5}$.

Secondary inorganic aerosols (SIA) are rather underestimated for 2009 by the model. On the annual average, the model underestimates SO_4^{2-} by 45%, NO_3^- by 27% and NH_4^+ by 39%. The annual mean spatial correlations are 0.67, 0.77 and 0.63 respectively. The model performance for SO_4^{2-} is quite similar in all seasons, for NO_3^- and NH_4^+ the bias and correlations are somewhat worse in spring. Modelled sodium from sea spray compares quite well with measured Na^+

concentrations. The annual (and seasonal) mean calculated Na^+ is practically unbiased and nicely correlates with observed values.

The index of agreement (IOA) shows that model reproduces observed PM_{10} and $PM_{2.5}$ concentrations with an accuracy of 0.59 and 0.57 respectively. For SIA compounds, the IOA is 0.67 for SO_4^{2-}, 0.77 for NO_3^- and 0.63 for NH_4^+. These results are considered to be rather good (Elbir, 2003).

More discussion on uncertainties of model calculated PM and on potential sources of the inaccuracies in model results is given in Chapter 7.

Individual stations. Statistical analysis of model calculated PM_{10} and $PM_{2.5}$ versus daily observations at individual sites are summarised in Tables A.1 and A.2 in the Appendix. Beside daily measurements of PM_{10} and $PM_{2.5}$, also hourly and weekly measurements were available at a number of sites in 2009. The hourly concentrations have been averaged to 24-hourly concentrations.

Averaged over all sites, the model bias is -49% for $PM_{2.5}$ and -35% for PM_{10}, and the temporal correlation between calculated and measured concentrations is 0.64 and 0.56 respectively.

The model performance is quite variable for different sites. The bias varies from -20% (GB48) to -76% (LV10) for $PM_{2.5}$ and from +116% (GR02) to -71% (LV10) for PM_{10}. However, model calculated concentrations lie within ±50% of observed values at 70% and 50% of the sites; and within ±30% of observed value at 20% and 5% of the sites for PM_{10} and $PM_{2.5}$ respectively.

The major outlier is the Greek site GR0002R. However, the observations are available only from for the second half of 2009. During that period, the model calculates severely enhanced PM concentrations for 15-31 December. Otherwise, the model bias is 44% for the period from 1 July to 15 December. The greatest model underestimation is found for two Latvian sites (LV0010R and LV0016R), where the correlation is also poor. The time-series for those sites show numerous episodes, with observed PM_{10} concentrations reaching 60-70μg/m^3. This suggests that the sites may be frequently affected by some strong local sources, unaccounted for in the EMEP emission database.

Table 2.3: Annual and seasonal comparison statistics between EMEP model calculations and EMEP observed concentrations of PM_{10}, $PM_{2.5}$, SIA, SO_4^{2-}, NO_3^- and NH_4^+ for 2009. Note that in "Yearly mean", only sites with the data capture above 50% are included.

Period	N sites	Obs (μg/m^3)	Mod (μg/m^3)	Rel.Bias, %	RMSE	R	IOA
PM_{10}							
Annual mean	41	14.46	8.60	-41	7.10	0.62	0.59
Daily mean	41	14.52	8.72	-40	12.08	0.51	0.66
Jan-Feb	41	15.56	10.39	-33	8.91	0.48	0.60
Spring	41	15.70	9.01	-43	8.00	0.52	0.54
Summer	41	14.18	7.35	-48	8.19	0.63	0.60
Autumn	41	13.48	8.53	-37	6.24	0.69	0.62
PM_{25}							
Annual mean	31	10.71	5.15	-52	6.48	0.78	0.57
Daily mean	31	10.79	5.25	-51	9.49	0.63	0.64
Jan-Feb	31	14.44	6.60	-54	10.3	0.81	0.61
Spring	31	11.88	5.74	-52	7.28	0.73	0.55
Summer	31	8.53	4.06	-52	5.13	0.48	0.49
Autumn	31	9.22	4.71	-49	5.26	0.76	0.58
SO_4^{2-}							
Annual mean	53	1.81	0.99	-45	1.00	0.77	0.67
Daily mean	53	1.82	1.00	-45	1.70	0.60	0.70
Jan-Feb	53	2.25	1.34	-40	1.50	0.67	0.69
Spring	53	1.95	1.03	-47	1.09	0.71	0.60
Summer	48	1.68	0.85	-50	1.00	0.79	0.63
Autumn	48	1.56	0.80	-49	1.00	0.72	0.68
NO_3^-							
Annual mean	24	1.97	1.44	-27	1.25	0.85	0.77
Daily mean	24	1.98	1.44	-27	5.03	0.33	0.41
Jan-Feb	24	2.47	2.17	-12	1.97	0.65	0.73
Spring	24	2.99	1.66	-44	3.39	0.62	0.54
Summer	24	1.30	0.84	-35	0.95	0.68	0.72
Autumn	24	1.47	1.31	-11	0.89	0.67	0.78
NH_4^+							
Annual mean	27	1.08	0.66	-39	0.60	0.66	0.63
Daily mean	27	1.08	0.65	-40	1.64	0.44	0.52
Jan-Feb	27	1.48	1.01	-32	0.93	0.52	0.61
Spring	27	1.42	0.76	-46	1.15	0.52	0.51
Summer	27	0.77	0.42	-45	0.51	0.45	0.55
Autumn	27	0.83	0.54	-35	0.47	0.52	0.64
Na^+							
Annual mean	25	0.75	0.74	-2	0.50	0.83	0.91
Daily mean	25	0.76	0.75	-2	2.11	0.41	0.51
Jan-Feb	25	0.67	0.74	11	0.59	0.77	0.87
Spring	25	0.97	0.82	-15	1.10	0.63	0.73
Summer	25	0.62	0.59	-5	0.39	0.84	0.91
Autumn	25	0.79	0.84	7	0.46	0.88	0.93

Here, N sites – the number of stations, Obs – the measured mean, Mod – the calculated mean, Bias is calculated as Σ(Mod-Obs)/Obs x 100%, RMSE – the Root mean Square Error= $[1/Ns\Sigma(Mod-Obs)^2]^{1/2}$, R – the tempo-spatial correlation coefficient between modelled and measured daily concentrations and spatial correlation for seasonal mean concentrations. $IOA=1-(\Sigma(Mod-Obs)^2 / \Sigma(|Mod-<Obs>|+\Sigma|Obs-<Obs>|)^2)$

2.2 Contribution of primary particles, secondary inorganic aerosols (SIA), sea salt and base cations to PM mass

By Wenche Aas and Svetlana Tsyro

The modelled PM_{10} and $PM_{2.5}$ concentrations include primary PM and secondary inorganic aerosols (SIA) from anthropogenic precursor emissions, sea-salt and windblown dust from natural sources and particulate water. Note that the model calculated PM does not include secondary organic aerosols (SOA), causing a bias in the calculated relative contribution of SIA and the other inorganic species to PM mass.

In the EMEP measurement programme, speciation of PM has historically focused on the secondary inorganic constituents (SIA), which are known to have a long range transport potential; i.e. sulphate, ammonium and nitrate. Thus, the majority of the EMEP Parties have measured these ions for decades. In 2009, concurrent measurements of sulphate and PM_{10} are performed at a total of 38 sites. At the majority of these sites, SO_4^{2-} is collected using a sampler with an undefined cut-off, whereas at a few sites a sampler with a PM_{10} inlet is applied. The sampling conditions are similar for nitrate and ammonium, but these variables are collected at somewhat fewer sites, 27 for NO_3^- and 18 for NH_4^+. However, this does not reflect the total picture of the number of sites performing reactive nitrogen measurements, as there are 50 sites measuring nitrate as the sum of NO_3^- and HNO_3 and 46 measuring ammonium as the sum of NH_4^+ and NH_3; though not all of these sites do have concurrent PM measurements. For details see the EMEP/CCC data report (Hjellbrekke and Fjæraa, 2011). It should be noted that only IT01 and Netherlands measure NO_3^- and NH_4^+ using the recommended denuder method. The method used at the other sites may give a positive artefact due to absorption of NH_3 or HNO_3 or a negative artefact due to evaporation of NH_4NO_3. Also base cations, sea salt ions and mineral dust are part of the monitoring programme, but only a few countries are currently reporting data. 10 sites measure one or all three major sea salt ions (Na^+, Cl^- and Mg^{2+}) in PM_{10}; though 37 sites report sea salt ions in aerosols (Hjellbrekke and Fjæraa, 2011). Mineral dust is mainly measured during intensive measurement periods and typically at sites in southern Europe.

Figure 2.7 compares the importance of primary and secondary aerosols in PM concentrations, as calculated with the model for 2009. On average, the levels of secondary inorganic aerosols exceed those of primary particles in PM_{10}. However, the relative importance of primary PM increases significantly in the vicinity of major urban agglomerates due to substantial emissions from traffic and residential heating. Furthermore, SIA accounts for more than 30 % of $PM_{2.5}$ in most of Europe. Its largest contribution to $PM_{2.5}$ of 50-60% is calculated for Central and Eastern Europe, whereas on the easternmost part of the EECCA region it is substantially smaller (10-20%).

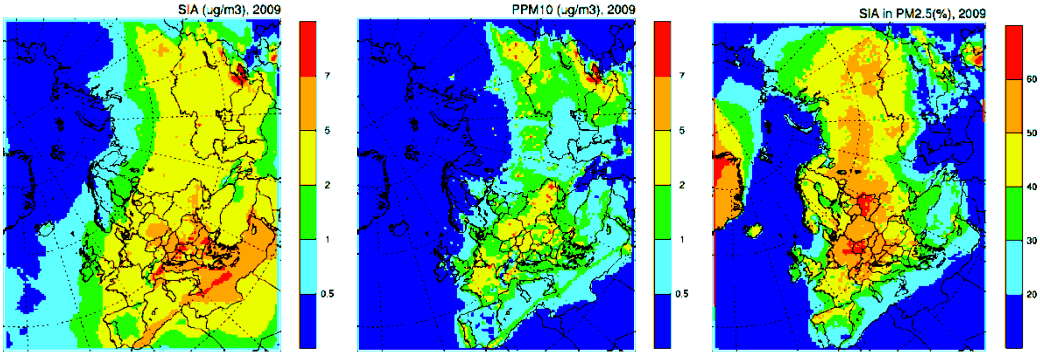

Figure 2.7: Annual mean concentrations of SIA (left), primary PM_{10} (middle), and relative contribution (in %) of SIA to $PM_{2.5}$ (right) for 2009, calculated using the EMEP/MSC-W model.

The relative contributions of SIA and primary PM to PM_{10} and $PM_{2.5}$ vary during the year, and shows different geographical distribution in different months. Typically, SIA's portion in PM is greatest in the cold season and during the periods of manure application in agriculture in spring (and to some extend in autumn), when it makes up between 50 and 80% of PM_{10} mass. In the summer, the contribution is mostly in a range of 40 to 60%. Geographically, the largest SIA contributions to PM_{10} mass are found in Central Europe and Central Russia most on the year, and also in Eastern/South-Eastern countries especially in the warm season.

The average relative contribution of SO_4^{2-} to PM_{10} and NO_3^- to PM_{10} based on the data reported for 2009 are quite comparable; i.e. 13±3% for SO_4^{2-} and 14±8% for NO_3^-, though the spatial distribution of sulphate and nitrate is somewhat different. For NH_4^+ the relative contribution to PM_{10} based on observations was 7±3%. The contribution of sea salt is very dependent on distance to the sea, i.e. 0.4% at the continental site Illmitz (AT02) in Austria and around 15% at the coastal sites in Norway (NO01), Denmark (DK05) and the Netherlands (NL91).

There are only four sites with a full year of chemical speciation in the fine fraction, and only one site with measurements in both size fractions (DE44). The relative contribution of SIA is somewhat lower for PM_{10} than for $PM_{2.5}$. This is to be expected as most of these ions reside in the fine fraction of PM_{10}

Time series of the relative contribution of the individual SIA constituents to PM_{10} were examined for the three sites reporting such data for a period of seven years or more, Figure 2.8. The relative contribution of SO_4^{2-} was found to be rather consistent until the last two-three years where it seems to be a reduction, though not seen at the Austrian sites AT02. There is a relatively large inter-annual variability of the relative contribution of sulphate to PM_{10} and even more so for nitrate and ammonium.

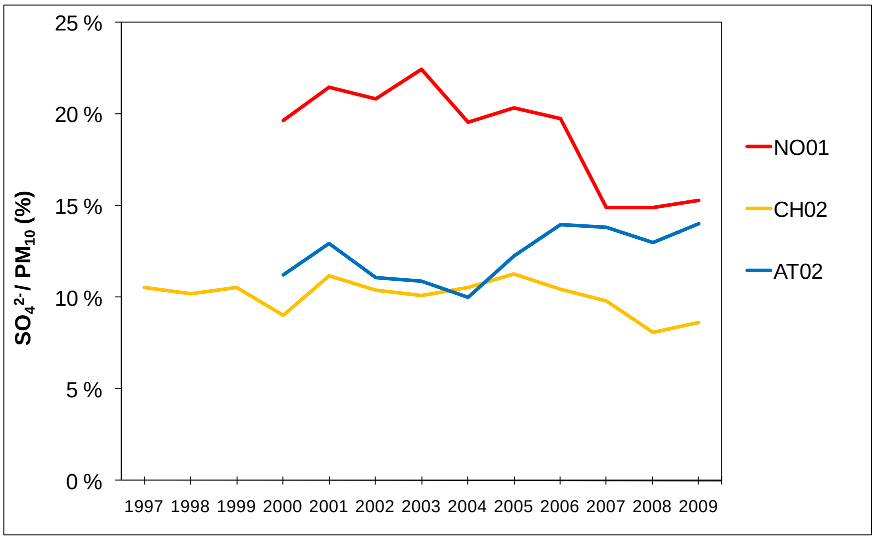

Figure 2.8: Time series showing the observed relative contribution of SO_4^{2-} to PM_{10}.

2.3 Measurements of carbonaceous matter

By Karl Espen Yttri

2.3.1 Status of sampling and measurement, and quality of observation data

The lack of comparable EC/OC data in Europe has hampered the possibility to address the spatial and temporal variation of these variables on the regional scale. Exceptions are the EMEP EC/OC campaign (Yttri et al., 2007), and the CARBOSOL project (Pio et al., 2007), with data for the period 2002 – 2004, which can be used for such a purpose. More recent measurements are needed to get an overview of the current situation, and to validate the progress made with respect to model development.

Table 2.4: Sites reporting EC and OC for 2009, including size fractions and sampling period.

Site (Country)	**EC**	**OC**	**PM_1**	**$PM_{2.5}$**	**PM_{10}**	**Period**
Aspvreten (Sweden)	x	x			x	2008, 2009
Birkenes (Norway)	x	x		x	x	2001, 2002, 2003, 2004, 2005, 2006, 2007, 2008, 2009
Finokalia (Greece)	x	x	x			2009
Harwell (UK)	x	x			x	2009
Ispra (Italy)	x	x		x		2002¹⁾, 2003²⁾, 2004²⁾, 2005²⁾, 2006, 2007, 2008, 2009
Košetice (Czech Rep.)	x	x		x		2009
Melpitz (Germany)	x	x		x	x	2006, 2007, 2008, 2009
Montseny (Spain)	x	x		x	x	2007, 2008, 2009
Pay de Dome (France)	x	x		x		2008, 2009
Vavihill (Sweden)	x	x			x	2008, 2009

1. EMEP EC/OC campaign
2. Both $PM_{2.5}$ and PM_{10}.

An increased number of countries and sites have been expected to start reporting levels of EC and OC following from the development of the EUSAAR protocol. Ten countries reported measurements of EC and OC for 2009, which are two more than for 2008. Measurements performed at the sites Finokalia (Greece), Harwell (UK) and Košetice (Czech Republic) are reported for the first time for 2009. See Table 2.4 for all sites reporting levels of EC and OC for 2009. In addition, total carbon (TC) was reported for the Hungarian site K-Puszta.

Nine of the ten sites listed in Table 2.4 quantified EC and OC according to a thermal-optical method protocol. Further, seven of these nine sites followed the EUSAAR-2 protocol, being an important step towards harmonized and comparable data for EC and OC within EMEP. Indeed, the EUSAAR-2 protocol has been adapted as standard method for analysis of EC/OC within EMEP. A detailed description of the EUSAAR-2 protocol and its performance can be found in Cavalli et al. (2010). Work is currently in progress to finalize the standard operating procedure (SOP) for subsequent inclusion to the EMEP manual. A challenge still remains with respect to how to handle samples which are impacted by carbonate carbon, however guidelines for how to deal with such samples will be developed and provided in the SOP.

The EUSAAR-2 protocol has already been used for other site categories than rural background, and is one of the candidate methods to be tested for a standardized method for EC/OC measurements within CEN. With EMEP adapting the EUSAAR-2 protocol, we hope this can be in favour of the choice of this protocol also within CEN.

Particular concern should be made regarding EC/OC data obtained by other than thermal-optical analysis methodology, which do not account for charring of OC during analysis. For 2009, this concerns the German site Melpitz, only, for which the EC concentration is grossly overestimated.

Only the analytical part of the EUSAAR unified protocol is considered finalized at present, as some challenges still remain concerning the design of the “artefact-free” sampling train. Comparable data, in particular for OC, require that both the analytical and the sampling protocol are harmonized, which currently is not the case. The finalization of the EUSAAR best affordable, “artefact-free” sampling train, will take place within the EU funded project ACTRIS, which started in April 2011. The variability amongst the various sampling approaches used is apparent from the variables listed in Table 2.5. Most sites sample for 24 hours, whereas the sampling time range from 48 hours to one week for low loading sites such as Birkenes and Pay De Dome. From the datasets it is apparent that the combination of low ambient levels and 24 hour sampling time cause poor data capture for certain sites, particularly with respect to EC. Three sites (Aspvreten, Ispra and Vavihill) attempted to account for both positive and negative sampling artefacts, whereas one used the QBQ-approach (Quartz-behind-Quartz) to account for positive artefacts. 6 of the 10 sites did not address sampling artefacts on a regular basis, but some addressed the positive sampling artefacts based on results from intensive measurements periods.

3 of the 10 sites performed measurements of EC and OC in PM_{10} and $PM_{2.5}$, hence providing valuable information on the size distribution of these variables, which also add to the understanding of sources and atmospheric processes. An overview of the annual mean EC/OC/TC concentration reported for 2009 are shown in Table 2.6.

Table 2.5: Sampling equipment and analytical approach used at the sites reporting EC and OC to EMEP for 2009.

Site (Country)	**Sampling time/frequency**	**Filter face velocity**	**Sampling equipment**	**Analytical approach**
Aspvreten (Sweden)	24 hr, daily	55 cm s^{-1}	Denuder/Backup filter pos/neg artifact	Sunset TOT (EUSAAR-2)
Birkenes (Norway)	7 days, weekly	54 cm s^{-1}	Single filter (no correction)	Sunset TOT (EUSAAR-2)
Finokalia (Greece)	Irregular, irregular	131 cm s^{-1}	Single filter (no correction)	Sunset TOT (EUSAAR-1)
Harwell (UK)	24 hr, daily	20 cm s^{-1}	Single filter (no correction)	Sunset TOT (Quartz)
Ispra (Italy)	24 hr, daily	20 cm s^{-1}	Denuder/Backup filter Pos/neg artifact	Sunset TOT (EUSAAR-2)
Košetice (The Czech Rep.)	24 hours, weekly	20 cm s^{-1}	QBQ (pos. artifact)	Sunset TOT (EUSAAR-2)
Melpitz (Germany)	24 hr, daily	20 cm s^{-1}	Single filter (no correction)	VDI 2465 Part 2
Montseny (Spain)	24 hours, irregular	74 cm s^{-1}	Single filter (pos. artefact/camp)	Sunset TOT (EUSAAR-2)
Pay de Dome (France)	48 hours, weekly	69 cm s^{-1}	Single filter (pos. artifact/camp)	Sunset TOT (EUSAAR-2)
Vavihill (Sweden)	Irregular, irregular	55 cm s^{-1}	Denuder/Backup filter pos/neg artifact	DRI (EUSAAR-2)

Table 2.6: Annual mean concentrations of EC, OC and TC for 2009. Only sites which reported for more than 6 months have been included.

	EC PM_{10} (µg C m^{-3})	**OC PM_{10} [1)] (µg C m^{-3})**	**TC[1)] PM_{10} (µg C m^{-3})**	**EC/TC (%)**	**EC $PM_{2.5}$ (µg C m^{-3})**	**OC $PM_{2.5}$ [1)] (µg C m^{-3})**	**TC $PM_{2.5}$ [1)] (µg C m^{-3})**	**EC/TC (%)**
Aspvreten (Sweden)	0.21	1.5	1.7	17				
Birkenes (Norway)	0.11	0.83	0.94	12	0.09	0.63	0.73	14
Finokalia[2)] (Greece)					0.25	0.84	1.1	25
Harwell (UK)	0.51	2.3	2.8	21				
Ispra (Italy)					1.4	6.8	8.3	19
Košetice (Czech Rep.)					0.60	2.9	3.5	20
Melpitz (Germany)	1.4	2.7	4.1	32	1.1	2.0	3.4	37
Pay de Dome (France)					0.10	1.3	1.4	10
Montseny (Spain)	0.32	1.8	2.1	17	0.22	1.2	1.4	16
Vavihill (Sweden)	0.20	1.5	1.7	12				

1) Both sampling-artefact-corrected and uncorrected concentrations of OC and TC are here denoted “OC” and “TC”

2) EC and OC were measured on PM_1 filter samples.

Since 2008, i.e. data from 2007, EC/OC data are reported to EBAS according to the EUSAAR format. This appears to be somewhat more challenging than with the previous format, given its complexity and inclusion of quite a few meta-data. The meta-data is needed to evaluate the comparability of various dataset. We are continuously working to improve this, but reporting of EC and OC will not be substantially easier until a unified protocol for EC and OC is ready. As previously mentioned, this will take place within the project ACTRIS.

An effort to establish a large and harmonized dataset which goes beyond the ordinary EC/OC/TC measurements when addressing the carbonaceous content, and its sources, of the European rural background aerosol, has been made in the two most recent EMEP intensive measurement periods (EIMPS). These data are currently being interpreted and discussed for subsequent publication in a peer reviewed paper (Yttri et al., in progress). Some recently published papers covering the same topic, but for different geographical areas, and using a similar methodology can be found in Yttri et al. (2011 a, b), and Gilardoni et al. (2011).

2.3.2 Observed levels of EC and OC in 2009

EC

Annual mean concentrations of EC

The levels of EC (including both PM_{10} and $PM_{2.5}$) varied by a factor of 15 between the site reporting the lowest (0.09 µg C m^{-3} at Birkenes, Norway) and the highest annual mean concentration of EC (1.4 µg C m^{-3} at Ispra, Italy) (see Table 2.6). The lowest concentrations were observed in Scandinavia (0.09 – 0.21 µg C m^{-3}), at certain high altitude European continental sites in western/south-western Europe (0.10 – 0.32 µg C m^{-3}), as well as for the Finokalia site (0.25 µg C m^{-3}) in the Eastern Mediterranean. The annual mean EC concentrations observed at Košetice and Melpitz in Eastern Europe, Harwell in the UK, and Ispra in northern Italy (0.51 – 1.4 µg C m^{-3}), were substantially higher than for the other sites. Although EC levels at the Melpitz site are overestimated due to the analytical method used (VDI 2465 part 2), it is more likely that the “true” EC level at this site falls within the upper rather than the lower range reported in Table 3.

Seasonality of EC

The four high-EC-loading-sites all experienced an increase in the EC concentration during winter (see Figure 2.9). This was particularly pronounced for Ispra, at which the EC concentration increased by a factor of 4 in winter compared to summer, whereas the corresponding factor for the other three sites ranged from 1.4 – 1.6. These increased levels are likely to reflect both increased emissions, e.g. preliminary results from the EIMPs 2008/2009 show a substantial influence of wood burning emissions in winter, as well as meteorological conditions preventing dispersion of the air pollution; i.e. inversion. The wintertime increase in the EC concentration was shared by the Scandinavian countries (EC increased by a factor of 1.2 – 1.7), whereas it was found to be reduced (Puy de Dome) or unchanged (Montseny and Košetice) for the rest.

Size distribution of EC

Three sites performed concurrent measurements of EC and OC in two size fractions (here: PM_{10} and $PM_{2.5}$). At Birkenes, 88% of EC in PM_{10} could be attributed to EC in $PM_{2.5}$, underlining that EC is associated mainly with fine particles, resulting from incomplete combustion of fossil fuels and biomass. The corresponding percentage for Melpitz was 75% (percentage is based on < 60% of the samples due to $EC_{PM10} < EC_{PM2.5}$). At Montseny, collection of PM_{10} and $PM_{2.5}$ filter samples for subsequent analyses of EC and OC was not performed on the same days, thus complicating the calculation of a similar percentage. By assuming that the annual averages of EC in PM_{10} and $PM_{2.5}$ are representative for the entire year, no more than 69% of EC in PM_{10} could be attributed to $PM_{2.5}$. Further inquiries into the causes of this rather low percentage based on the current dataset would be speculative only.

Annual mean EC/TC ratio

The annual mean EC/TC ratio showed that 10–25% of the ambient aerosol TC content could be attributed to EC; i.e. for the sites analysing according to a thermal-optical protocol (here: EUSAAR and Quartz.par). This range corresponds with that reported by Yttri et al. (2007) (12–24%) for the EMEP EC/OC campaign, using Quartz.par. For Melpitz, using the VDI (2465 part 2) protocol, EC accounted for 32% (PM_{10}) and 37% ($PM_{2.5}$). The EC/TC ratio for the Scandinavian sites and the western/south-western European high altitude sites were all <17%, whereas it ranged from 19–25% for Finokalia, Harwell, Košetice, and Ispra. EC was found to be a more pronounced fraction of TC in winter compared to summer, except for the sites Košetice and Puy de Dome where no change between seasons were observed. The increased fraction of TC attributed to EC in winter is in accordance with that observed during the EMEP EC/OC campaign (Yttri et al., 2007).

Changes in annual mean concentration of EC from 2008 to 2009

7 out of 10 sites reporting annual mean concentrations of EC for 2009 did also report this variable for 2008. However, only the sites Birkenes, Ispra, and Melpitz had a sampling time and frequency which covered the entire year. In cases where sampling is performed once a week for a period of e.g. 24 hours, the data coverage is no more than 14% per year. Consequently, the variability of the annual mean is increased and the comparability of the annual mean from one year to the other correspondingly reduced. Further, irregular sampling frequency, e.g. covering the entire heating season but only a minor part of the non-heating season and vice versa the consecutive year, is another potential bias, hampering the comparability on an annual basis.

For Birkenes, EC was reduced by 21 % (in PM_{10}) and 25% (in $PM_{2.5}$) going from 2008 to 2009. A substantial 18% reduction was also observed for Ispra during. For Melpitz, EC showed a modest 8% increase for PM_{10}, while it was found to be reduced by 15% for $PM_{2.5}$. For the other sites reporting EC, but with a less data coverage (<30%), it is found that the annual mean EC concentration at Puy de Dome was reduced by 44% from 2008 to 2009. At Puy de Dome, situated 1465 m asl., one should not exclude the possibility that annual changes in the relative time that the site reside in the planetary boundary layer versus the free troposphere might have a pronounced influence on the observed variability of the annual mean concentrations.

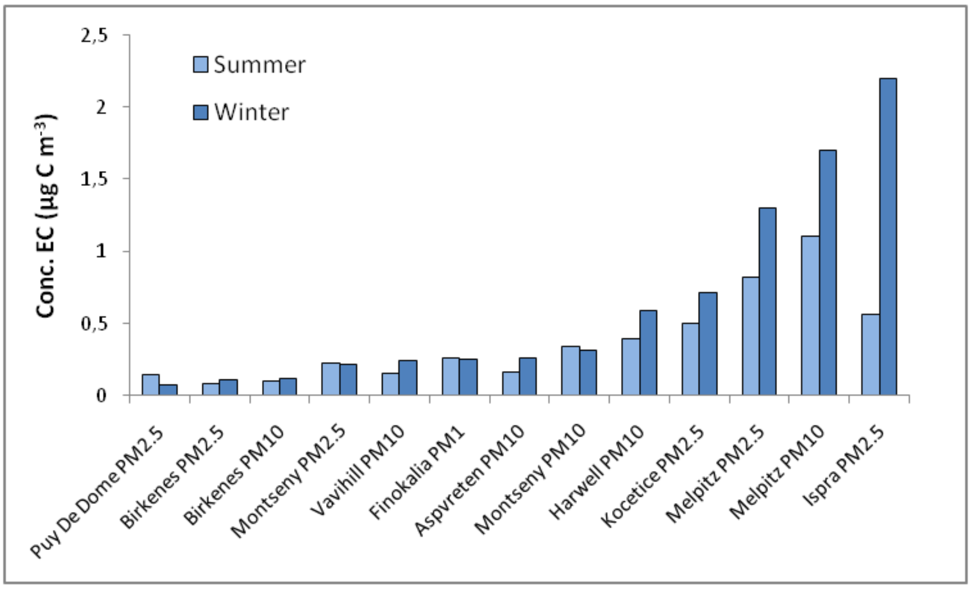

Figure 2.9: Mean summer and winter time concentrations of EC in PM_{10} and $PM_{2.5}$ at EMEP sites in 2009. The sites are ranked according to increasing winter time concentration of EC.

OC

For the sake of simplicity sampling-artefact-corrected OC (OC_p) and uncorrected levels of OC have been denoted as “OC” in Table 3, and subsequently discussed and compared in following section as OC.

Annual mean concentrations of OC

Amongst the sites using a thermal-optical method for analysis of EC/OC, the annual mean concentration of OC in PM_{10} ranged from 0.83 µg C m^{-3} at the Norwegian site Birkenes to 2.3 µg C m^{-3} at the UK site Harwell, corresponding to a difference of a factor of approximately 2.5. For $PM_{2.5}$, the corresponding range was 0.63 µg C m^{-3} (Birkenes in Norway) to 6.8 µg m^{-3} (Ispra in Italy). The VDI 2465 part 2 method used to quantify EC and OC at the Melpitz site underestimates the samples level of OC by not accounting for charring of OC to EC, thus the level of 2.7 µg C m^{-3} of OC observed for PM_{10} and 2.1 µg C m^{-3} of OC observed for $PM_{2.5}$ at this site should likely be higher.

As for EC, the lowest levels of OC (here: considering OC in both PM_{10} and $PM_{2.5}$) were observed in Scandinavia (0.63–1.5 µg C m^{-3}), at the Eastern Mediterranean site Finokalia (0.84 µg C m^{-3}), and at certain high altitude European continental sites in western/south-western Europe (1.3–1.8 µg C m^{-3}). For Košetice and Melpitz in Eastern Europe, Harwell in the UK, and Ispra in northern Italy, the annual mean OC concentration ranged from 2.3–6.8 µg C m^{-3}, thus being substantially higher than for the other sites. This is particularly true for Ispra, for which the annual mean OC concentration is more than twice that observed at Košetice, which observed the second highest annual mean OC concentration.

Seasonality of OC

The sites in Scandinavia (except Vavihill), the high altitude European continental sites in western/south-western Europe, the eastern Mediterranean site Finokalia, and the UK site Harwell all experienced increased levels of OC in summer compared to winter by a factor of 1.1–2.5 (see Figure 2.10). The particularly pronounced increase observed for Finokalia (factor of 2.5), could be influenced by the low number of samples, and for summer in particular, potentially biasing the result. Increased summer time concentrations of OC have typically been associated with formation of secondary aerosol, both from anthropogenic and natural precursors. It has also been shown that primary biological aerosol particles (PBAP) could contribute to increased levels of OC in summer, at least for certain regions. Typically, increased summer time OC concentrations was observed for the sites experiencing the lowest carbonaceous aerosol loading, suggesting they are situated in areas less perturbed by anthropogenic sources. One could not exclude the possibility that sampling artefacts could have an influence on observed seasonal cycles of OC, and this ought to be examined in further detail.

It is interesting to note that the summertime increase for OC was larger for PM_{10} than for $PM_{2.5}$ at the sites Birkenes and Montseny performing measurements of both size fractions indicating the influence of coarse OC, of which PBAP most likely is the major contributor. As previously stated, collection of PM_{10} and $PM_{2.5}$ filter samples at the Montseny site was not performed on the same days, making this finding less robust than for the Birkenes site. Further insight into the contribution of PBAP to OC in the Nordic environment can be found in Yttri et al. (2011a, b). For Melpitz, OC in $PM_{2.5}$ was found to be higher in winter than for summer, whereas it was a marginal difference between summer and winter for OC in PM_{10}.

Size distribution of OC

Concurrent measurements of EC and OC in two size fractions (here: PM_{10} and $PM_{2.5}$), were performed at three sites. At Birkenes, 73% of OC in PM_{10} could be attributed to OC in $PM_{2.5}$ on an annual basis, the corresponding percentage for Melpitz was 72%. As previously stated, collection of PM_{10} and $PM_{2.5}$ filter samples for subsequent analyses of EC and OC was not performed on the same days at the Montseny site, thus complicating the calculation of a similar percentage. By assuming that the annual averages of OC in PM_{10} and $PM_{2.5}$ are representative for the entire year, no more than 67% of OC in PM_{10} could be attributed to $PM_{2.5}$

At all three sites, levels of OC in $PM_{10-2.5}$ were found to be increased in summer. This was particularly pronounced at Birkenes, at which the summer time concentration was three times higher than that observed in winter, whereas for Montseny the summer time concentration was estimated to be twice that observed in winter. For Melpitz, the concentration of OC in summer was no more than 1.3 times higher in summer compared to winter.

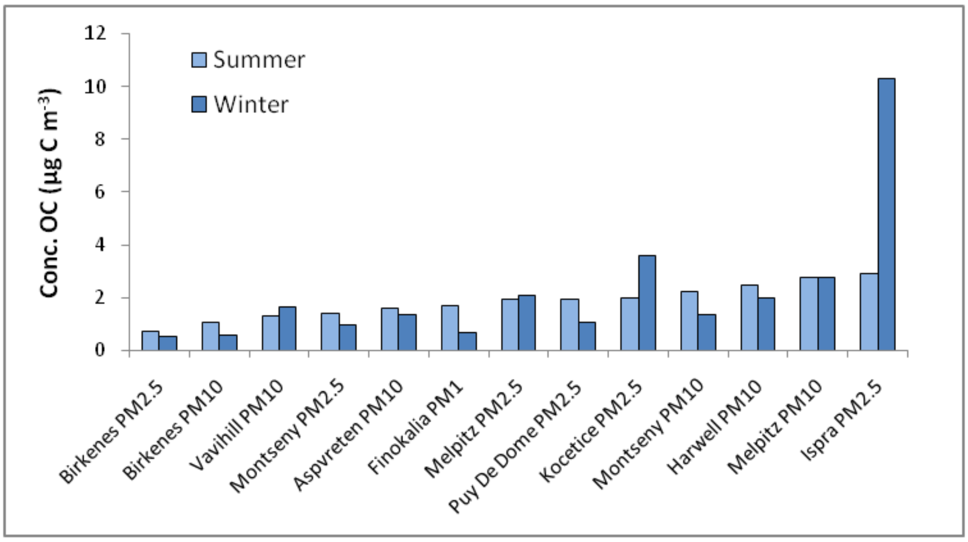

Figure 2.10: Mean summer and winter time concentrations of OC in PM_{10} and $PM_{2.5}$ at EMEP sites in 2009. The sites are ranked according to increasing summertime time concentration of OC.

2.3.3 Levels of EC and OC at sites reporting for the first time in 2009

In the 2009 EMEP status report on PM (EMEP, 2010), a description of EC and OC, including levels, size distribution, and seasonality, was provided for each site reporting these two variables. In the following, a similar description is provided for the sites reporting levels of EC and OC for the first time, only; these are, Košetice (Czech Republic), Harwell (UK) Finokalia (Greece).

EC and OC levels at the Greek site Finokalia (GR0002R)

Measurements of EC and OC in PM_1 was performed at the site Finokalia (GR0002R) (150 m asl) located at the island of Crete, thus representing an important extension of the EMEP monitoring network with respect to EC/OC, covering the Eastern part of the Mediterranean Basin. Sciare et al. (2008) described in his informative paper how this region is influenced by emissions of carbonaceous aerosol from countries surrounding the Black Sea, focusing in particular on biomass burning, and is recommended to the interested reader.

The data series of EC and OC reported for 2009 are based on highly irregular sampling, including no measurements for June and July. This introduces substantial uncertainty to the annual mean concentrations of EC and OC, hampering any comparison with other sites. The annual mean EC concentration (0.25 µg C m^{-3}) at Finokalia was slightly higher than the highest annual means observed for the Scandinavian countries and comparable to that observed for the Spanish site Montseny. It should be noted that the laboratory at which the samples from Finokalia were analyzed reported EC values which were on average 1.7 times higher than the mean of all participants in the most recent EUSAAR intercomparison (Chapter 3). Consequently, it cannot be excluded that the mean EC concentration reported in Table 2.6 is affected as well. The rather high mean EC/TC ratio (25%) observed at Finokalia, which was the highest value amongst all sites using thermal-optical analysis, further contributes to this suspicion.

The annual mean OC concentration (0.84 µg C m^{-3}) was rather low, even compared to the Scandinavian sites, and only the level observed at the Birkenes site was lower. Given the poor data coverage, including the total absence of sampling for two entire months, the annual mean concentration of OC have a substantial uncertainty, which makes it hard to compare with other sites.

EC and OC levels at the UK site Harwell (GB0036R)

The Harwell (GB0036R) monitoring site is located is a rural area in central southern England, within the grounds of the Harwell Science Centre. The surrounding area is generally open with mown grass and agricultural fields. The nearest road is a minor road located approximately 140 metres from the station, whereas the nearest town (20 000 inhabitants) is around 5 km to the north east.

With a 24 hour sampling time, daily sampling frequency, and a rather good data capture the EC and OC time series for Harwell provides an important asset to the EMEP monitoring network with respect to EC and OC. Although the measurement of EC and OC was performed using thermal-optical analysis, a different thermal program (Quartz.par) was used than for the majority of the sites (EUSAAR2), thus hampering the comparison. According to the latest EUSAAR EC/OC inter comparison (Chapter 3), the lab performing the analysis for the Harwell site reported EC levels which on average were 50% larger than the average EUSAAR_2 values for all but two samples. Slightly lower EC levels *"should be expected"* compared to EUSAAR2 given the higher temperature during the He-mode of the Quartz.par.

The annual mean concentration of EC at Harwell (0.51 µg C m^{-3}) should be considered medium high compared to what was reported for the European rural background environment in 2009 (see Table 2.6). I.e. the mean EC level at Harwell was substantially higher than for the Scandinavian sites and the high altitude sites in western/south-western Europe, but less than that reported for Eastern Europe and the Italian sites Ispra. The mean EC concentration observed during winter was approximately 50% higher than during summer at the Harwell site (see Figure 2.11). Also the EC/TC ratio was increased in winter (23%) compared to summer (17%), showing that EC accounted for a larger fraction of the carbonaceous aerosol during the cold season.

The annual mean OC concentration at Harwell is in the upper range of those listed in Table 2.6, but still a factor of three less than the annual mean observed at Ispra (6.8 µg C m^{-3}). OC was found to be increased in summer compared to winter (by nearly 25%), thus deviating from that observed for EC. The summer time increase in OC is shared with other low loading sites e.g. in Scandinavia.

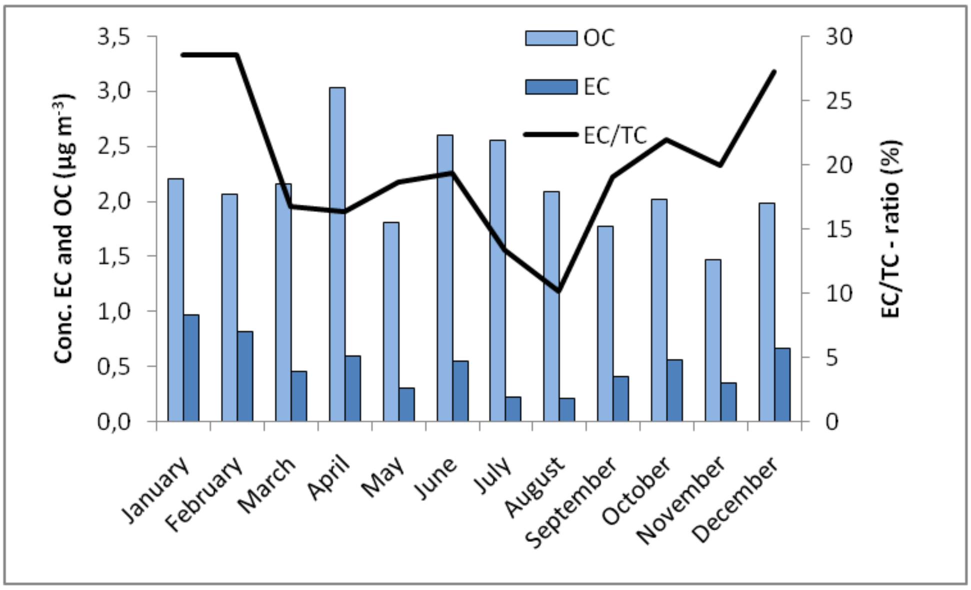

Figure 2.11: Seasonal variation of EC, OC and the EC/TC ratio obtained from PM_{10} filter samples collected at the UK site Harwell (GB0036R) during 2009.

EC and OC levels at the Czech Republic site Košetice (CZ0003R)

The Czech Republic site Košetice (CZ0003R) (534 m asl) is situated in the Czech-Moravian Highlands, approximately 80 km southeast from Prague. Forests dominated by conifer trees account for approximately 50% of the land use in the vicinity of the site, whereas the remaining 50% is attributed to meadow (25%) and agricultural areas (25%). The nearest town (15 000 inhabitants) is located 25 km south of the station. Air samples collected at the Košetice observatory reflects the general background level of air quality in the Czech Republic.

The annual mean concentration of EC at Košetice (0.60 µg C m^{-3}) should be considered in the upper range of what has been reported for the European rural background environment in 2009 (See Table 2.6). Although the annual mean EC concentration is substantially less than what has been observed for the Italian site Ispra (1.4 µg C m^{-3}) (notoriously high) and Melpitz (1.3 µg C m^{-3}) (analytical method overestimating EC), it is higher compared to the levels observed for the other sites listed in Table 2.6, in particular the Scandinavian countries (0.09–0.21 µg C m^{-3}) and certain high altitude European continental sites (0.10–0.32 µg C m^{-3}). The EC concentration increased by a substantial 40% during winter at the Košetice site. This increase was not reflected in the EC/TC ratio, which remained rather unchanged throughout the season; i.e. 19% in winter compared to 21% in summer.

The annual mean OC_p concentration (here: OC_p means corrected for the positive sampling artefact) (2.9 µg C m^{-3}) at Košetice is in the upper range of those listed in Table 2.6, although substantially less than the annual mean observed at Ispra (6.8 µg C m^{-3}). The positive artefact was found to be on average 22%, corresponding to an OC (uncorrected) level of 3.7 µg C m^{-3}. The winter time increase of OC_p was substantial (i.e. 78% compared to summer), thus being more pronounced than for EC (see Figure 2.12). The winter time increase in OC is shared with other relatively “high-loading” sites such as Ispra, and Melpitz, which likely is an indication of sites experiencing a substantial influence of anthropogenic emissions.

Košetice was one of the sites participating in the one year long EMEP EC/OC campaign conducted in 2002–2003. Despite slightly different temperature protocols and cut off size used during the EMEP EC/OC campaign (Quartz.par and PM_{10}) and for 2009 (EUSAAR2 and $PM_{2.5}$), there are indications that levels of EC has decreased from 2002/2003 (1.1 µg C m^{-3}) and till 2009 (0.60 µg m^{-3}) at this site. This is attributed to EC residing mainly in the $PM_{2.5}$ fraction and that the Quartz.par temperature program is more likely to cause premature burn-off than EUSAAR-2, thus underestimating EC compared to EUSAAR-2.

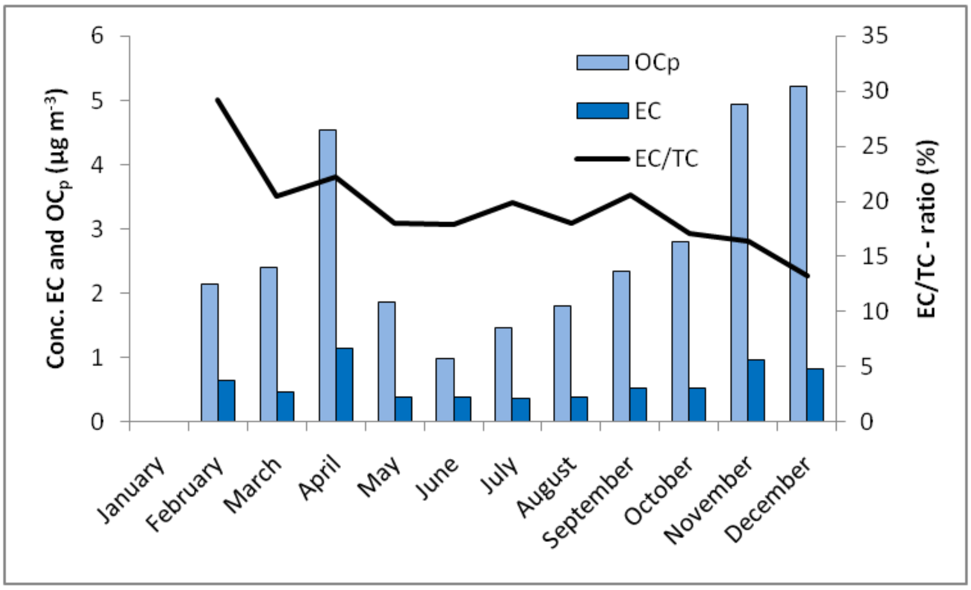

Figure 2.12: Seasonal variation of EC, OC and the EC/TC ratio obtained from $PM_{2.5}$ filter samples collected at the Czech Republic site Košetice (CZ0003R) during 2009.

2.3.4 Time series of EC and OC

Birkenes and Ispra are the only two sites with time series of EC and OC extending five years. At Birkenes, measurements go back to 2001, whereas for Ispra measurements started in 2003. Birkenes is somewhat unique in a European context as it has a continuous time series of EC and OC for both PM_{10} and $PM_{2.5}$, and that thermal-optical analysis has been applied for the entire period. At Ispra, parallel measurements of EC and OC in PM_{10} and $PM_{2.5}$ was performed for the period 2003 – 2005, whereas thermal-optical analysis was has been applied since 2005. Birkenes and Ispra represent two very different parts of the European rural background environment. Birkenes typically report the lowest annual mean concentrations for both EC and OC in Europe, while Ispra report the highest levels, by a fair margin. Birkenes has a strategic position well suited to monitor the outflow of air pollutants from the European continent. Consequently, Birkenes from time to time experience elevated concentrations. The very high level of the carbonaceous aerosol observed at Ispra is attributed to the severe regional air pollution characterizing the Po Valley region. EC and OC also differ with respect to seasonality at the two sites, as levels are high during summer at Birkenes and during winter at Ispra.

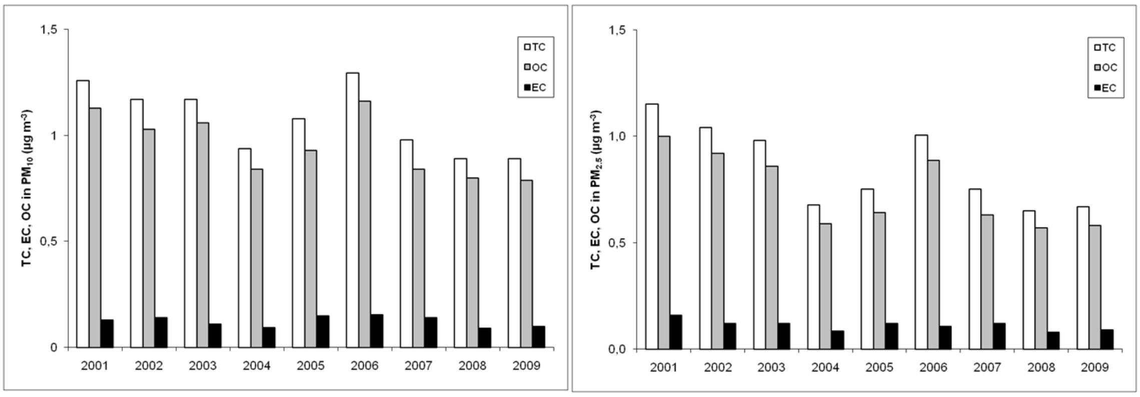

Figure 2.13: Annual mean concentrations of EC, OC and TC in PM_{10} (A) and $PM_{2.5}$ (B) at the Norwegian site Birkenes for the period 2001 – 2009.

The time series of EC and OC in PM_{10} and $PM_{2.5}$ at Birkenes look very similar (see Figure 2.13), however, the inter-annual variability is more pronounced for EC and OC in $PM_{2.5}$ compared to PM_{10}. For PM_{10} this is likely due to primary biological aerosol particles of mostly local origin. No stepwise up- or downward trend in the annual mean concentration of OC and EC is observed for the period 2001–2009. The time series are characterised by a drop in the annual mean concentrations from 2003 to 2004 and a maximum in 2006. For the period 2007–2009, only a modest annual variation is observed for OC, although more pronounced for EC. The time series of EC and OC for PM_{10} and $PM_{2.5}$ closely resemble that of the secondary inorganic constituents, as well as the mass concentration of PM_{10} and $PM_{2.5}$ observed at Birkenes. The annual mean OC concentration (both for OC in PM_{10} and $PM_{2.5}$) observed for 2009 was 30–40% less compared to the first year of sampling (2001). For EC the corresponding range was 20–40%.

The relative contribution of TCM [(TCM = Total carbonaceous matter (TCM = OC x 1.7 + EC x 1.1)] to PM_{10}, $PM_{2.5}$ and $PM_{10-2.5}$ at Birkenes for the time-period 2001–2009 is shown in Figure 2.14. The relative contribution of TCM to PM_{10} and $PM_{2.5}$ shows a modest annual variation, except from 2001–2002, ranging between 25–29% for PM_{10} and 30–36% for $PM_{2.5}$. The relative contribution of TCM-to-$PM_{2.5}$ has the same temporal pattern as for TCM-to-PM_{10}. The relative contribution of TCM to $PM_{10-2.5}$ ranged from 9–21% for the actual period. While the relative contribution increased substantially from 2001–2004, the contribution have declined slightly again from 2004 and onwards.

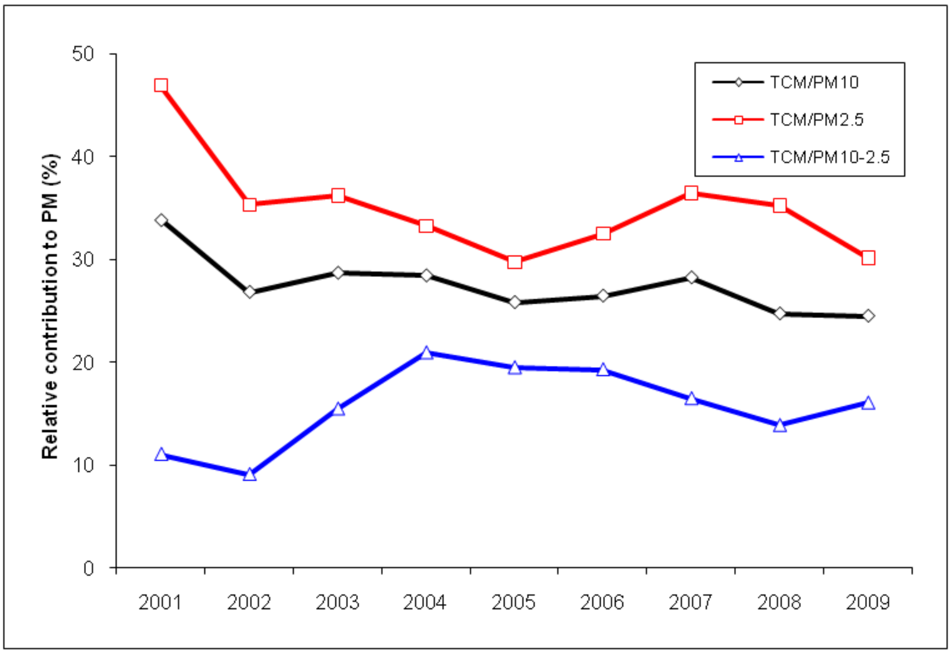

Figure 2.14: Relative contribution of TCM (Total Carbonaceous Matter) to PM_{10}, $PM_{2.5}$ and $PM_{10-2.5}$ at Birkenes for the period 2001 – 2009.

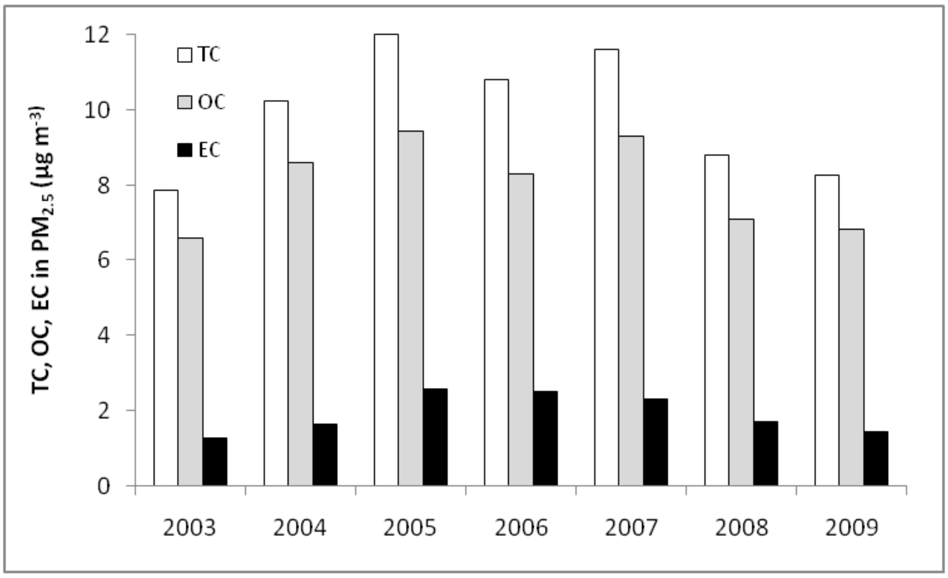

Figure 2.15: Annual mean concentrations of EC, OC and TC in $PM_{2.5}$ at the Italian site Ispra (IT0004R) for the period 2003 – 2009.

No stepwise up- or downward trend in the annual mean concentration of OC and EC is observed for the entire period 2003–2009 at Ispra. However, since 2005, i.e. the year thermal-optical analysis was introduced at Ispra, and until 2009, the annual mean EC concentration has decreased by a substantial 80%; with the greatest reductions taking place since 2007. The annual mean concentration of OC has a rather similar variation as seen EC, and for the period 2005 until 2009, a nearly 40% decrease has been observed. It should be noted that the sampling approach has been changed during this period, i.e. a denuder has been introduced into the sampling train, which is likely to have caused a reduction in the observed OC level.

For the interested reader, a more thorough presentation of the carbonaceous aerosol at the Birkenes and Ispra sites were provided in the last year Status report (EMEP Report 3, 2010).

2.3.5 Concluding remarks

The lack of a harmonized sampling- and analytical measurement protocol has been the main concern in our effort to establish a reliable picture of the regional distribution of the carbonaceous aerosol concentration within EMEP. For 2009, Seven out of ten sites reported levels of EC and OC using the recently developed EUSAAR2 thermal protocol, being an important step towards harmonized and comparable data for EC and OC within EMEP. Only *one* site reported levels of EC and OC, which were not obtained by thermal-optical analysis. Fully comparable data require that also the sampling protocol is harmonized, which is currently not the case. The finalization of the EUSAAR best affordable, “artefact-free” sampling train, will take place within the EU funded project ACTRIS.

The carbonaceous aerosol concentration was found to range by more than one order of magnitude within the European rural background environment. Elevated concentrations were observed in northern Italy and in Eastern Europe. Concentrations observed at sites in Scandinavia, the eastern Mediterranean and at high altitude sites in western/south-western Europe, were substantially lower. Levels observed in the UK should be considered intermediate. The spatial variation of the carbonaceous aerosol concentration for 2009 closely resembles that observed during the EMEP EC/OC Campaign conducted in 2002–2003.

Levels of EC were found to be increased during winter at most sites, reflecting increased emissions, e.g. from residential wood burning, as well as inversion, preventing dispersion of air pollution. Increased EC/TC ratios in winter show that EC was more pronounced in the carbonaceous aerosol in winter compared to summer. Increased summertime concentrations of OC were observed at most low and medium loading sites. Formation of secondary aerosol, both from anthropogenic and natural precursors, and primary biological aerosol particles, along with a low impact from anthropogenic OC are likely to explain the observed seasonal variation for the actual sites.

For sites with time series of EC and OC extending 7–9 years back in time, levels of EC and OC were found to be lower in 2009 compared to the year when the measurements were initiated.

2.4 Organic Aerosol modelling in EMEP

2.4.1 Recent Developments

By David Simpson and Robert Bergström

The EMEP model for particulate carbonaceous matter (PCM) is an extension of the standard EMEP MSC-W photochemistry model. In the EMEP PCM model, a scheme for secondary organic aerosol (SOA) formation, from biogenic and anthropogenic VOCs, and gas/particle partitioning of semi-volatile organic compounds, using the volatility basis set (VBS) approach, are added to the modelled primary emissions of elemental carbon (EC) and organic aerosol (POA). The VBS approach was introduced by Donahue et al. (2006) and has been applied by e.g. Lane et al. (2008) and Shrivastava et al. (2008).

The new VBS based EMEP PCM model was introduced in Simpson et al. (2009), extending the work of Andersson-Sköld and Simpson (2001) and Simpson et al. (2007). Further examples of EMEP-VBS approaches were presented in Bergström and Simpson (2010) and Kulmala et al. (2011). Over the last year the model has been updated with new BVOC emissions (Simpson et al., 2011). The model is also being compared to high time-resolution data from aerosol mass spectrometers, from the EMEP intensive measurement and EUCAARI field campaigns (Kulmala et al., 2011).

The model results are currently being written up for publication in a peer-review paper, but some main conclusions can be given:

I) Summertime levels are quite well captured by some versions of the VBS scheme. Those VBS schemes which include aging processes (reactions of OH with semivolatile compounds) seem to do a better (and reasonable) job of reproducing summertime OA levels than schemes without such a mechanism.

II) It is hard however to know if the BVOC emissions which are the major summertime precursor to SOA are correct – there are significant uncertainties in European BVOC estimates (e.g. Rinne et al., 2009).

III) There are problems matching wintertime OA levels, with the model in general underestimating. Some of these problems may stem from dispersion issues (in stable boundary layers), but there are signs that there are also problems with the emission inventories.

As mentioned in Kulmala et al. (2011), residential wood combustion was also shown to be a major source of wintertime OA at Ispra in northern Italy (Gilardoni et al., 2011) in Oslo and a nearby background site in southern Norway (Yttri et al., 2011), as well as at Vavihill in southern Sweden (Genberg et al., 2011). Despite these congruent observations, it is not possible to say at this stage if such contributions are a local problem or reflect more wide-spread problems with the wood-burning inventories. Further work with the emissions inventories and modelling are planned to follow up this problem.

This work with the EMEP VBS schemes was funded by the EU EUCAARI project, the Swedish Clean Air Programme (SCARP), as well as by EMEP under UNECE.

2.4.2 *Preliminary evaluation of the effect of Secondary Organic Aerosols (SOA) on model performance for PM*

By Svetlana Tsyro

The PM calculations for 2009 with the EMEP/MSC-W model have been combined with the results of a research model version for organic aerosols to complete the modelled PM mass with SOA as described above in Chapter 2.4.1Note that the SOA results used here are just one of a series of experimental SOA calculations and therefore should be regarded accordingly. The purpose of this section is to evaluate the potential improvements in calculated PM concentrations due to accounting for SOA.

We have compared the resulting concentrations of PM_{10} and $PM_{2.5}$ with observations in 2009. On the annual average, the contribution of SOM to PM mass varies from 0.5-1 $\mu g/m^3$ in the north to 1.5-2 $\mu g/m^3$ in the south of the EMEP area. The model also includes an assumed background OM concentration of 1 $\mu gC/m^3$ at the surface. There is a pronounced seasonal variation in the SOM concentrations. From October through March, monthly average SOM is mostly below 2 $\mu g/m^3$, while in the warm period SOM concentrations are 2.5-3.5 $\mu g/m^3$ over most of Europe (0.2-1 $\mu g/m^3$ in the northern parts), and up to 5-7 $\mu g/m^3$ in southern European countries.

Compared to standard calculations (Table 2.3), there is a clear improvement in modelled PM_{10} and $PM_{2.5}$ concentration levels (Table 2.7 and Figure 2.16). The annual mean bias is now only -24% for PM_{10} and -31% for $PM_{2.5}$; the RMSE has significantly decreased, whereas the spatial correlation and the Index of Agreement are slightly lower. The annual mean modelled PM_{10} and $PM_{2.5}$ are now within 30% of observed value at almost all of the sites with measurements.

Table 2.7: Annual and seasonal comparison statistics between EMEP model calculated and EMEP observed concentrations of PM$_{10}$ and PM$_{2.5}$ for 2009 (compared to Table 2.3, SOM and background OC are included in the calculated PM)

Period	N sites	Obs µg/m^3	Mod µg/m^3	Rel.Bias, %	RMSE	R	IOA
PM$_{10}$							
Annual mean	41	14.46	10.94	-24	5.28	0.64	0.69
Daily mean	41	14.52	11.07	-24	11.68	0.50	0.68
Jan-Feb	41	15.56	11.91	-23	8.22	0.47	0.62
Spring	41	15.70	11.16	-29	6.32	0.52	0.61
Summer	41	14.18	10.55	-26	5.68	0.69	0.75
Autumn	41	13.48	10.87	-19	4.65	0.67	0.73
PM$_{25}$							
Annual mean	31	10.71	7.37	-31	4.71	0.72	0.65
Daily mean	31	10.79	7.50	-31	8.61	0.59	0.69
Jan-Feb	31	14.44	8.07	-44	9.17	0.80	0.63
Spring	31	11.88	7.83	-34	5.66	0.68	0.62
Summer	31	8.53	7.20	-16	3.06	0.51	0.70
Autumn	31	9.22	6.90	-25	3.53	0.73	0.72

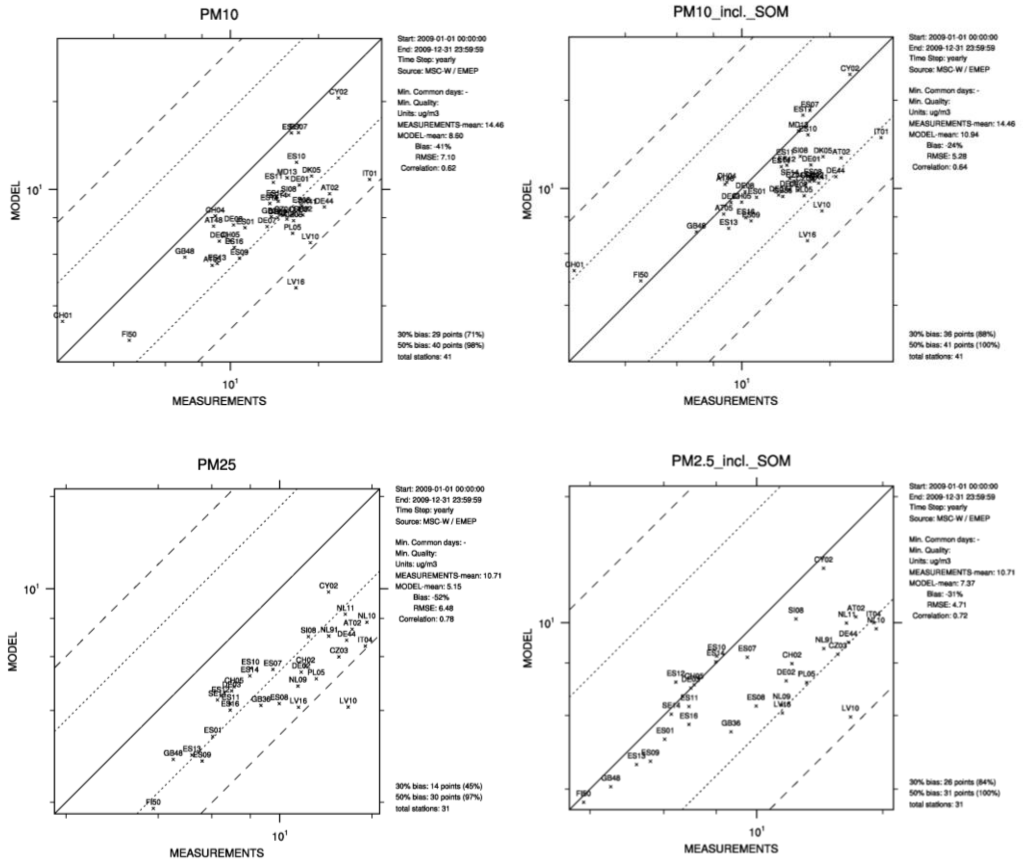

Figure 2.16: Annual mean scatter-plots for calculated versus measured PM$_{10}$ and PM$_{2.5}$ in 2009, excluding (left panels) and including (right panels) SOM and background OM in the calculated PM.

3 Results of the 2010' intercomparison of TC, OC and EC analytical methods

By Fabrizia Cavalli and Jean-Philippe Putaud

Intercomparisons of organic carbon (OC) and elemental carbon (EC) measurements by laboratories in charge of analysing samples collected at EMEP stations have been organized on a regular basis for the last 5 years as a part of EUSAAR, and will be organized for the next four years as a part of ACTRIS in 2010. The Institute for Environment and Sustainability of the EC - Joint Research Centre has been in charge of distributing the samples as well as interpreting the results.

3.1 Samples

Ambient PM_{10} aerosol samples were collected on two 150 mm diam. quartz fiber filters at each of the following 4 sites: Birkenes (NO01), K-Puszta (HU02), Ispra (IT04), and Montseny (ES1778). A 4 cm^2 punch from each of these filters was provided to LGGE, PSI, ITM, JRC, IfT, NILU, ECPL-UoC, FMI, ACUV, CMHI, ULund, UBham, and a 2 cm^2 punch to CNR-IIA, UBA-Germany, ISCIII, and EMPA. It was asked to participants to determine the organic carbon (OC) and elemental carbon (EC) or total carbon (TC) content in µgC/cm^2 of these punches, by applying the analytical protocol in-use in their own laboratory. The actual analytical protocols used by the participants are listed in Table 3.1.

Table 3.1: Analytical protocol used by the 16 institutes involved in the intercomparison.

	Participant	EMEP Station(s)	Method	Charring corection
1	LGGE	FR30	EUSAAR_2	Transmittance
2	PSI	CH01	EUSAAR_2 short	Transmittance
3	ITM	SE12	EUSAAR_2	Transmittance
4	JRC	IT04	EUSAAR_2	Transmittance
6	IfT	DE44	VDI 2465	N/A
7	NILU	NO01	EUSAAR_2	Transmittance
11	ECPL-UoC	GR02	EUSAAR_1	Transmittance
12	FMI	FI50	EUSAAR_2	Transmittance
13	ACUV	HU02	680°C in O2	N/A
14	CMHI	CZ03	EUSAAR_2	Transmittance
17	UBham	GB36	Quartz	Transmittance
19	ULund	SE11	EUSAAR_2	Transmittance
21	CNR-IIA	IT01	EUSAAR_2	Transmittance
22	UBA	DE-xx	EUSAAR_2	Transmittance
23	ISCIII	ES-xx	Quartz	Transmittance
24	EMPA	CH-xx	EUSAAR_2	Transmittance

Data for the latest inter comparison were reported to JRC by October 1st, 2010, as requested, by 15 laboratories. No data were reported by Participant #12, because they experienced technical problems with their instrument at the time of this intercomparison.

3.2 TC measurements

TC measurements (in µgC cm^{-2} units) reported by 15 participants are shown in Figure 3.1. These levels would correspond to atmospheric TC concentrations ranging from approx. 2 to 12 µg C m^{-3} for a face velocity of 20 cm s^{-1} and a sampling time of 24 hr. For each of the 8 samples, TC values determined by Lab. #2 deviated from the average value (including all participants) by more than 1 standard deviation (SD), and were therefore excluded to estimate the reference values, calculated as the average over the remaining laboratories. It should be noted that Participant #2 was the only laboratory using a Semi-Continuous Field Analyzer.

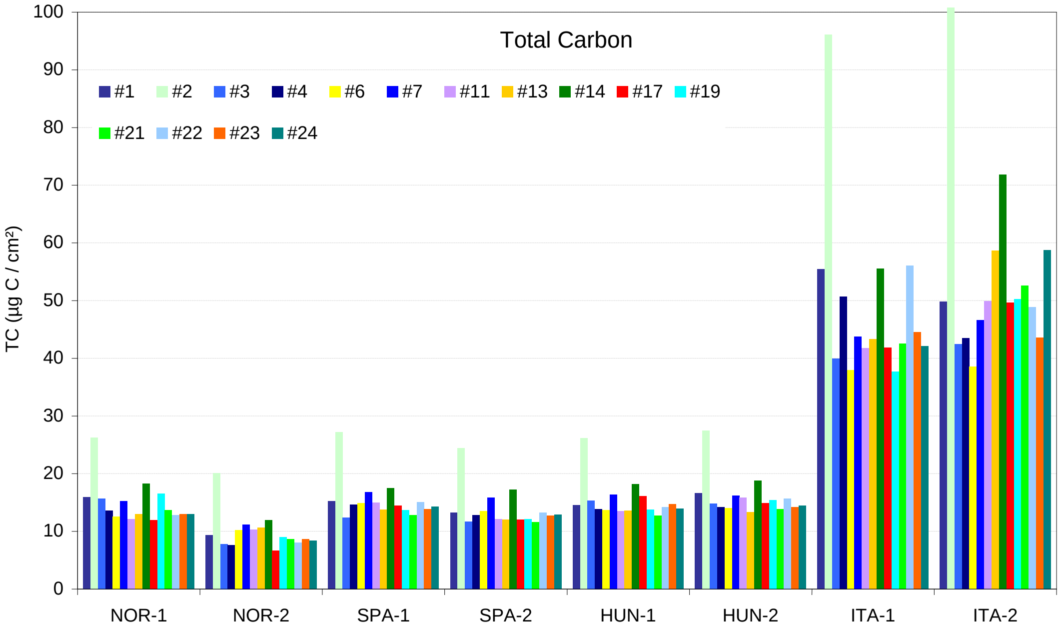

Figure 3.1: Levels of TC (in µgC/cm²) reported by all participant for each of the eight ambient aerosol filters used for the latest intercomparison. The colour of the bars' reflect the kind of analytical method implemented (blue-green: EUSAAR_2 protocol, red: NIOSH-like protocol, yellow: thermal analysis without optical correction)

Figure 3.2 shows the ratio between the TC values reported by individual laboratories and the reference values for each sample. Thirteen participants among 15 determined TC within ± 10% of the reference value, on average. Laboratories 2 (not shown) and 14 systematically overestimated TC concentrations. The other participants did not systematically (i.e. for all samples) over- or underestimate TC. The discrepancies we observed therefore probably result from both systematic and random errors.

Systematic biases could come from an inaccurate calibration of the instrument. Twelve participants submitted data related to the external calibration performed with organic standards, e.g. sucrose or potassium phthalate. Reported deviations from the expected value ranged between -4% and +9%, and could not always account completely for the largest deviations observed in this intercomparison exercise. For instance, Participant 7 underestimated the concentration in the external standard by 4%, and reported TC values 9% larger than the reference value, on average. In contrast, Participant 23 reported TC values 7% smaller than the reference value (on average), in line with their underestimation by 6% of the external standard. This suggests that the concentration value assigned to the standard solution employed to determine the calibration constant was not accurate. This can be checked by using other independent standards, like e.g. known micro-volumes of CO_2.The accuracy of Partners 2 and 14 instrument's calibration could not be assessed, since data related to external calibration were not submitted.

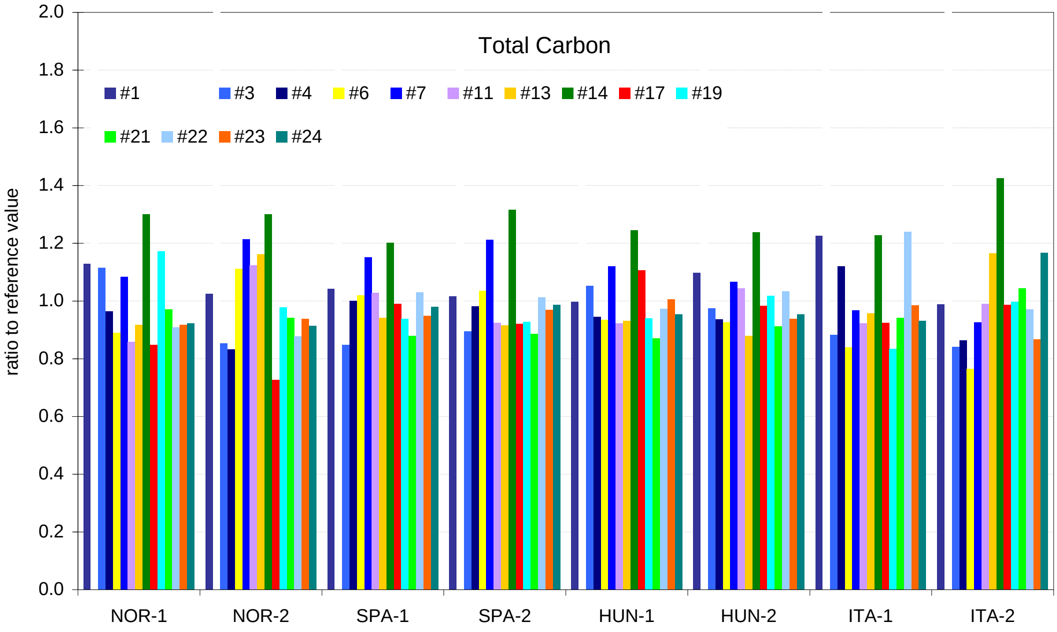

Figure 3.2: TC reported value divided by the reference value (see text), 1 outlier excluded. See Figure 3.1 caption for details regarding the colour codes.

In order to evaluate the role of random errors in the observed discrepancies, the repeatability for TC measurements was calculated as the average relative standard deviation of the mean values reported by laboratories that replicated analyses of the intercomparison filters. The average repeatability for Partners 1, 3, 4, 6, 7, 11, 13, 17, 19, 21, 22, 23 and 24 ranged between 4% and 10%. The analytical repeatability (due to random uncertainties inherent to the technique, inhomogeneities of the deposit on the punch delivered to each participant, error in the dimension of the analysed filter punch) can contribute to random errors. Contaminations and/or material loss and inhomogeneities of the deposit on the large filters collected at the 4 EUSAAR sites could also contribute to the deviations observed.

3.3 EC measurements and EC/TC ratios

The EC measurements reported by 15 laboratories are shown in Figure 3.3. No value was reported by PSI for the sample NOR-1. On average, reported EC amounts ranged from 0.9 µg C cm^{-2} to 4 µg C cm^{-2}, corresponding to atmospheric concentrations ranging from 0.5 to 2 µg m^{-3} collected over 24h at a face velocity of 20 cm s^{-1}.

The thermal method VDI 2465, used by Participant 6 (does not include any optical correction for charring), provided significantly higher EC levels for all samples – by 210% on average – than the average values including all participants. Laboratories 2 and 11 also reported EC values that were on average 1.7 times greater than the mean over all participants. The deviation with respect to average of the EC results reported by Participant 2 is consistent with their results for TC, and is therefore not EC specific. In contrast, the large EC data reported by Laboratory 11 cannot be explained by a bias in TC determination, but rather by an improper determination of the OC/EC split point. It should be noted that Participant 11 was the only one implementing the protocol EUSAAR_1 (whereas most others used EUSAAR_2), however this cannot be the reason for this discrepancy as the EUSAAR1 and EUSAAR2 protocols have proven to vary only to a minor extent with respect to the EC/OC split point (Cavalli et al., 2010). The EC amounts obtained by the Laboratories 17 and 23, both applying a NIOSH-type protocol, are not consistent among them: Lab. 23 reported EC values that are, as expected, significantly lower than the average EUSAAR_2 values (on average by a factor of 2), but Partner 17 reported EC values which are, on average, 50% larger than the average EUSAAR_2 values for all samples but two (SPA-1 and SPA-2).

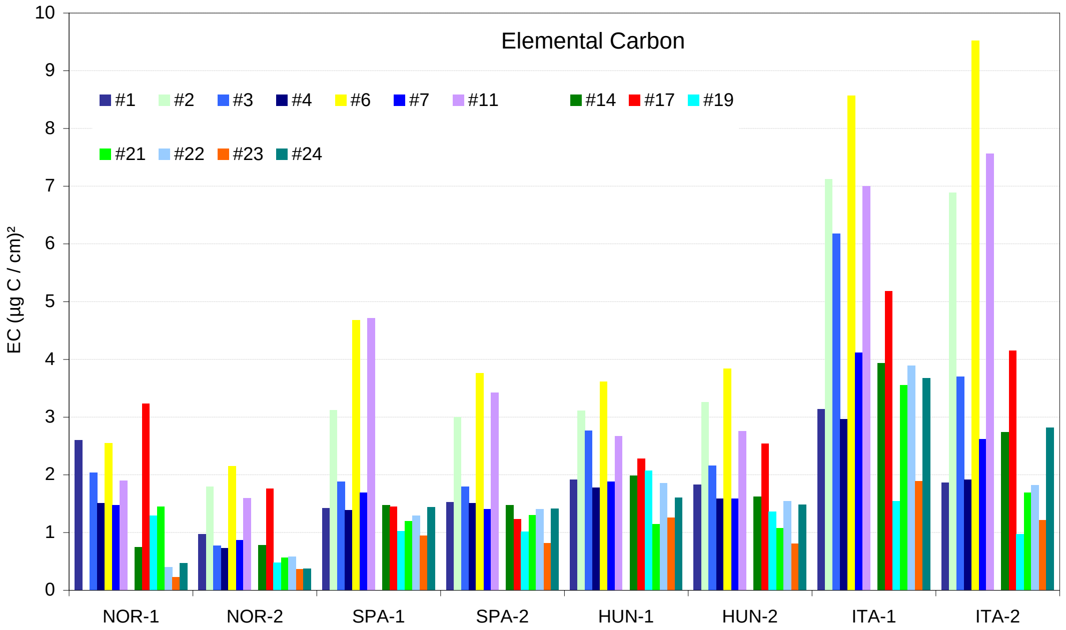

Figure 3.3: Amounts of EC (in µgC/cm²) reported by 14 participants. See Figure 3.1 caption for details regarding the colour codes.

The observations for EC were confirmed by the EC/TC ratios (Figure 3.4) which are independent of the possible spatial heterogeneities in filter loadings and of the accuracy of the standard used for calibration. The EC/TC ratios reported by all participants differ by a factor of 3 to 13, whereas those reported by the participants applying the EUSAAR_2 protocol differ by a factor of 1.8 to 4.5

"only". Among the participants applying an analytical protocol that corrects for charring, Laboratory 11 reported EC/TC values exceeding the average EC/TC by more than 1 SD. Therefore, the reference EC/TC values for this inter-comparison was calculated over the results obtained by all participants who delivered EC and TC data, except from Laboratories 6 and 11.

Figure 3.5 shows EC/TC ratios relative to these reference values. On average, EC/TC was determined within ±22% of the reference value by 9 among 15 participants. All of them used the EUSAAR_2 protocol. Although Laboratory 3, who also run the EUSAAR_2 protocol, overestimated the EC/TC by 50% with respect to the reference value, this result demonstrates that the use of the optimized analytical protocol such as EUSAAR_2 improves the comparability in EC determinations. Let us recall that Laboratories 6, 11, 19 and 23, implementing other analytical protocols, obtained mean EC/TC ratios differing from the reference values by (on average) factors of 2.9, 2.2., 1.6, and 0.5, respectively.

To further reduce the discrepancies in EC/TC ratio determination by laboratories implementing a common thermal optical protocol, it is again recommended to check the instrument's response in the 2 modes by injecting known volumes of pure C-containing gases during the two modes of the analysis. Differences in the flame ionization detector (FID) response in the He- and the He/O_2-mode of the analysis (due to a significant difference in the total carrier gas flow rate in these 2 modes) can indeed lead to systematic differences in EC/TC determination by different instruments. Investigating other instrumental malfunctions related to i) the correction of the laser drift with temperature and/or to ii) the inaccuracy of the temperature experienced by the filter with respect to the temperature set point in the He-mode (i.e. 650°C) could be envisaged once this simple test is performed and leads to satisfactory results.

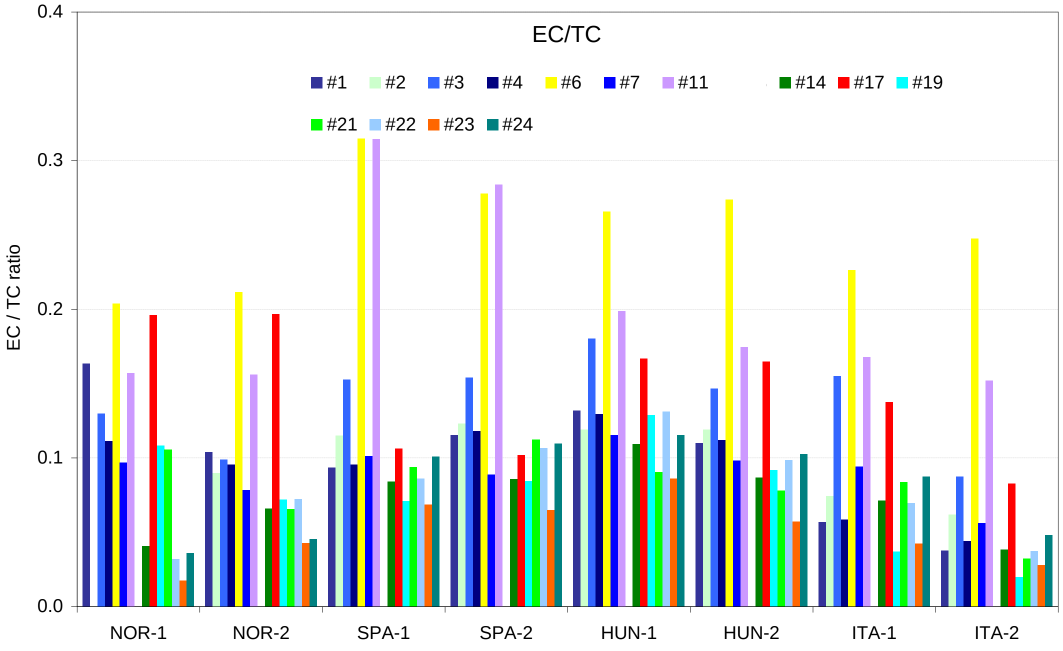

Figure 3.4: EC/TC ratios derived from the results reported by 14 participants. See Figure 3.1 caption for details regarding the colour codes.

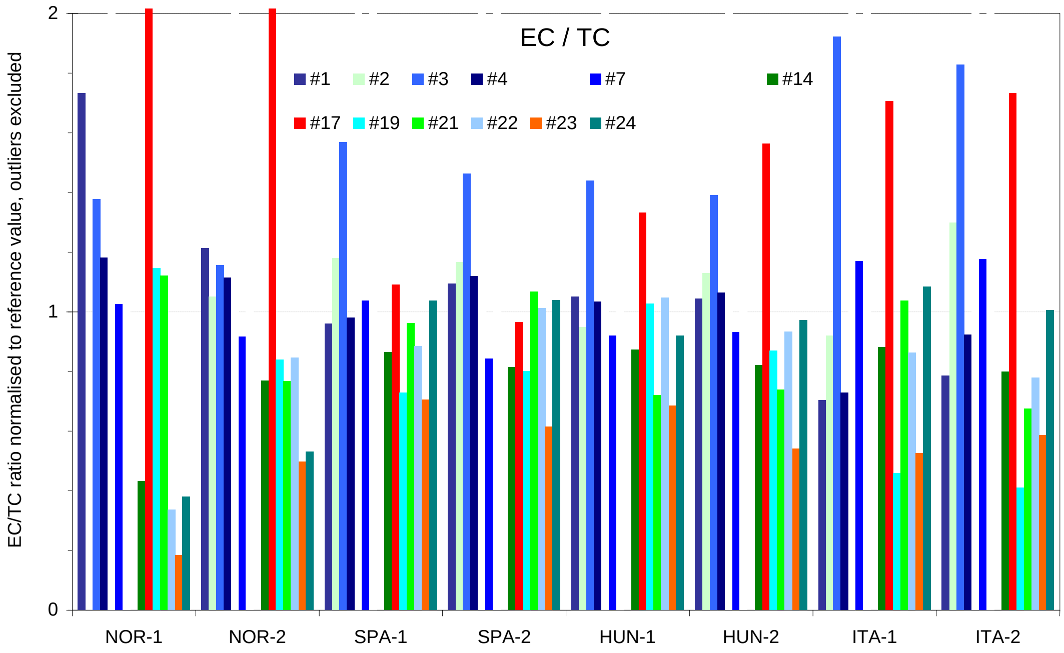

Figure 3.5: EC/TC ratio normalized to the reference value (see text). See Figure 3.1 caption for details regarding the colour codes.

3.4 Conclusions and recommendations

Among the 15 laboratories that participated in this inter-comparison, 13 determined the TC content of ambient PM_{10} collected on quartz fibre filters within ± 10% on average of the reference values, calculate as the average over all participants; outliers.

Systematic deviation from average could be investigated and corrected by:

- verifying the accuracy of the concentration value attributed to the standard reference solution employed to determine the calibration constant and afterwards to check the accuracy of the measurements;
- performing calibration and periodical checks by injection of well defined micro-volumes of CO_2.

Analytical repeatability (4%-10%), inhomogeneities of the filter deposits, precision of the dimension of the analysed filter punch, and contaminations / loss of material from the filters, can contribute to the random errors.

Nine participants among 14 could determine EC/TC ratio within ±22% (on average) of the reference EC/TC values, calculated as the average over all data obtained with analytical protocols correcting for charring. These nine participants all applied the EUSAAR_2 protocol. Results obtained with an analytical protocol that does not account for charring are systematically biased high (by more than a factor of 2). However, comparable biases can also affect data obtained with thermal method with optical correction of charring.

Recommendations for improving the comparability of EC measurements include:

- using the EUSAAR_2 analytical protocol;
- removing O_2 traces in the He carrier gas using an Oxygen trap;
- checking the detector response in the He and He+O_2 analytical mode by spiking known volumes of CO_2 in both modes.

We recommend that:

- The participation in the annual OCEC intercomparison should be compulsory for all institutes delivering such data to EMEP.
- The OC and EC data delivered to EMEP should be traceable to calibration data and intercomparison exercise results.
- EMEP should demand that the OC and EC data files delivered to them include in the metadata the analytical technique used to produce these data.

4 EMEP and the Project *EUropean Supersites for Atmospheric Aerosol Research* (EUSAAR): a Collaboration for Mutual Benefit

By Markus Fiebig, Paolo Laj, Alfred Wiedensohler, Ann Mari Fjæraa

4.1 Introduction

Collaboration and integration with other networks and frameworks working on monitoring of atmospheric constituents is a paramount theme in the EMEP monitoring strategy (ECE/EB.AIR/GE.1/2009/15). With respect to atmospheric aerosol, the strategy points out that the chemical aerosol properties, which are traditionally considered when looking at aerosol air quality and health effects, are inherently linked to the microphysical and optical aerosol properties which are considered in addition when looking at the aerosol climate effects. Aerosols exerting these effects share the same emission sources, long-range transport pathways, and managing these effects benefits from the same abatement strategies. At the national level, monitoring efforts targeted at aerosol air quality and health effects oftentimes share the infrastructures with respective efforts targeted at the aerosol climate effects. The same synergies hold for the modelling tools needed to interpret the data and source attribute pollution events. Modern chemistry transport models (CTMs) or Earth system models (ESMs) include representations of the aerosol particle phase to a level of detail that render them equally suitable for modelling aerosol climate, health, and air quality effects. Even though the strategy notes the increasing importance of the aerosol climate effect to society in addition to the air quality and health effects, it also states that resources to install additional monitoring capacities in terms of further sites and parameters are limited. This contrasts with the increasing expectations of governmental agencies and policy makers, e.g. concerning data provision with near-real-time for more efficient decision making in the “Global Monitoring for Environment and Security” (GMES) initiative. Co-operations of EMEP with other projects and frameworks, bringing together infrastructures targeting the aerosol climate, air quality, and health effects, are the logical consequence of this situation.

A text book example of such a co-operation is the one between EMEP and the project “EUropean Supersites for Atmospheric Aerosol Research” (EUSAAR). EUSAAR is a 5-year project conducted between April 2006 and March 2011 and funded by the European Union under Framework Programme 6. The EUSAAR network of ground sites conducting long-term monitoring of climate and air quality relevant aerosol parameters originally consisted of 20 stations distributed over whole Europe, which were in the course of the project joined by further 15 associate sites, Figure 4.1. The projects main objectives were:

- to provide easy and efficient access to the data collected within the network by establishing data reporting structures to a common data centre, which itself should be easily accessible over the web.
- to improve the quality of the data provided by the network by establishing standard operating procedures (SOPs), conducting station audits, and arranging inter-comparisons with other, international networks.

- to extend the network capacities by bringing methodologies so far considered research grade to the operational and routine use level.
- to provide trans-boundary access to the participating stations and research facilities.

The aerosol parameters covered as core variables by EUSAAR focus on the aerosol climate effects, but have synergy with the air quality and health effects and are contained in the EMEP strategy as advanced aerosol parameters:

- Concentration of total carbon and its partitioning into organic and elemental carbon (OC / EC), measured by thermo-optical analysis.
- Sub-micrometer particle number size distribution measured by Scanning and Differential Mobility Analysis (SMPS / DMPS)
- Aerosol optical depth measured by sun-tracking filter radiometer.
- Aerosol scattering coefficient measured by integrating nephelometer.
- Aerosol absorption coefficient measured by filter absorption photometer techniques.

In addition, EUSAAR worked on bringing the following research methods to the operational level:

- Measurement of the aerosol profile by Multi Axis Differential Optical Absorption Spectroscopy (MAXDOAS), in synergy with providing selected trace-gas profiles.
- Measurement of the hygroscopic water uptake of aerosol particles by Hygroscopicity Tandem Differential Mobility Analysis (HTDMA).
- Collecting, processing, and disseminating data of advanced aerosol parameters in near-real-time (NRT) with less than 3 hours delay.

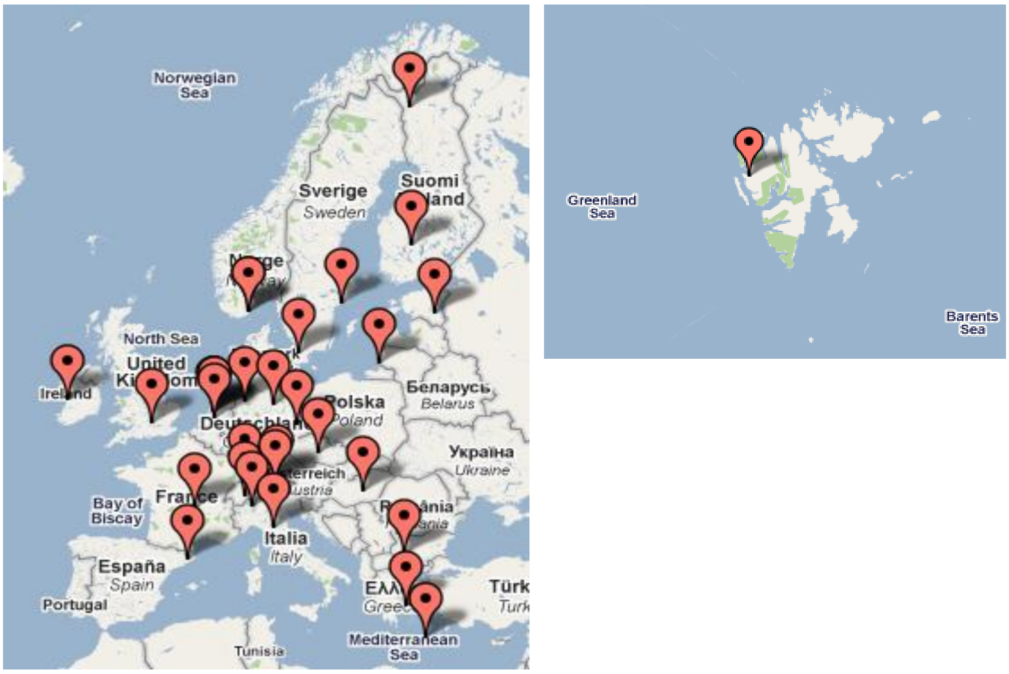

Figure 4.1: Map depicting the locations of the original EUSAAR stations and the European associate stations.

Already the 2004-2009 EMEP monitoring strategy made provisions for including these observation types by introducing three levels of EMEP stations. While a typical level 1 station measures the core EMEP variables on aerosol particle and precipitation, a level 2 station extends this observation programme with selected other variables such as volatile organic compounds (VOCs), particle number size distribution, optical aerosol properties, further heavy metals, and persistent organic pollutants (POPs). The strategy sets the aim that each member country should at least contribute one such level 2 station. The programme of a level 3 station is extended even further, e.g. by lidar profiling, and may also be campaign-based. By this definition, the EUSAAR stations qualified as level 2 supersites. Many of them already participated in EMEP and other networks such as the WMO Global Atmosphere Watch (GAW) aerosol programme. To formalise the collaboration and to ensure the political support of EMEP, all EUSAAR stations were registered as EMEP level 2 sites where this wasn't already the case and the sites where defined as joined EMEP/GAW supersites. In addition, it was agreed that EUSAAR and EMEP should share the data centre facilities at the EMEP Chemical Co-ordinating Centre (CCC) at the Norwegian Institute for Air Research (NILU).

The following sections give an overview of the key benefits provided by EUSAAR from an EMEP perspective. Though, we will focus on the optical and physical properties of aerosols even though development of reference method for EC/OC also has been a core activity in EUSAAR. The thermo-optical analysis using the defined EUSAAR-2 protocol (Cavalli et al., 2010) has been adapted as standard method for analysis of EC/OC within EMEP. Work is currently in progress to finalize the standard operating procedure (SOP) of EC/OC measurements for subsequent inclusion to the EMEP manual. Furthermore, the EMEP manual needs include guidelines on measurements of physical and optical properties, and these will be based on the standard operation procedures as outlined in the following chapters.

4.2 Standard operating procedures for sub-micrometer particle number size distribution

The particle number size distribution (PNSD) is probably the most fundamental property of an aerosol. Via the strong dependence of the particle scattering cross-section on particle size, it determines the aerosol optical properties and thus its direct climate effect to a much larger degree than particle chemical composition (Bohren and Huffman, 1983). The same holds for the indirect aerosol climate effect, i.e. the influence of atmospheric aerosol on cloud reflectivity and lifetime (Dusek et al., 2006). It is the size of an aerosol particle that determines where it is deposited in the human respiratory system, and how large its effect on human health is (Seaton et al., 1995). The PNSD may not explain every detail about an aerosol, but assessing its physical state without it isn't possible. Despite this fundamental role, measurements of the particle number size distribution, more specific for particle diameters < 1µm, are not part of the regular observation programme at EMEP sites (level 1 stations) due to the level of sophistication demanded. Even though instruments measuring this property are commercially available from several manufacturers, operating these instruments in a network routinely and long-term to give reliably comparable results across the network so far has not been successful because the commercial instruments were not designed for this purpose.

To understand the underlying challenges, a few words are warranted on how the PNSD in the ≈0.01 µm–1 µm particle diameter range is measured. The instrument type most commonly used for this purpose at ground sites is the Differential or Scanning Mobility Particle Sizer (DMPS / SMPS). In these instruments, the PNSD is scanned step-wise or continuously by selecting a size fraction of particles from the sample. A Differential Mobility Analyser (DMA), a cylindrical capacitor, is used for this purpose. The inner and outer electrodes of the DMA are separated by a continuous, laminar flow of particle-free air flowing lengthwise through the DMA (sheath flow). The sample is introduced on one end of the DMA at the outer electrode. The sample exit slit is located at the opposite end of the DMA in the inner electrode. When a defined electrical tension is applied to the DMA, only singly charged particles with a certain electrical mobility, which is a function of particle diameter, make their way to the sample exit slit. The particle concentration in the resulting almost monodisperse sample is measured by a Condensation Particle Counter (CPC). Prior to entering the DMA, the particle sample is brought into a thermal charge equilibrium by exposing it to a radioactive source. To arrive at the PNSD as final result, the data collected need to be processed by an inversion algorithm.

The above description of the operation principle suggests that the method leaves room for multiple sources of error:

- To interpret the data accurately, the flows in the system need to be known to within 1-2% accuracy, also under long-term operating conditions.
- The sample needs to be low in relative humidity. Otherwise, the process of charge equilibration doesn’t proceed as defined.
- The counting efficiency of the CPC is particle size dependent and drifts as the instrument ages.
- The sheath flow needs to be dry and at room temperature, which may be a challenge if the flow is circulated in a closed loop, a common instrument design.
- Temperature and pressure inside the instrument need to be exactly known for accurate data interpretation.
- The high-voltage supply used for generating the electrical tension on the DMA needs to be accurate over 4 orders of magnitude. Current designs tend to drift over time.
- The whole system needs to be leak-tight, even though it involves a considerable amount of joints that may vibrate due to pump activity.
- The inversion algorithm used to interpret the data needs to be certified, i.e. error free and producing results comparable to other such algorithms.

Since no currently commercially available instrument of this type takes into account all the above mentioned points, the instruments used so far at the European monitoring stations are research grade and largely self-build by the maintaining research institution. Proper operating conditions concerning the above mentioned points are imperative for producing reliably comparable results. On the other hand, experience shows that these instruments operate stably once these operating conditions are established, and the process of establishing these may even be (semi-)automated. The method is thus not inherently more unmanageable than other instrument types.

EUSAAR took on the task of transferring a cluster of well-distributed, custom-built, and research grade DMPS and SMPS systems producing data of unknown quality into a well-organised, centrally accessible network of such instruments producing data of known, inter-comparable, and traceable quality. Three workshops were held for this purpose, where each instrument in the network participated in at least one. Inter-comparisons were conducted on monodisperse laboratory test aerosols as well as ambient aerosol. After identifying all critical points in operating DMPS and SMPS instruments, it was demonstrated by Wiedensohler et al. (2010) that the networked instruments agree in terms of particle concentration within 10%, and in terms of particle size within 3%. The critical aspects of designing and operating DMPS and SMPS instruments were collected and specified in a detailed design and standard operating procedure, including check-lists for routine maintenance. A hierarchy of data format templates from annotated raw to finally processed hourly averages, including uncertainties, was defined in order to establish traceability. All inversion algorithms used in the network, as well as volunteering commercial inversion algorithms, were inter-compared and quality assured. If necessary, the instruments were upgraded to meet the common quality standards. The process of including these quality standards in the relevant CEN and ISO guidelines has been started, as well as a dialog with manufacturers in order to make a DMPS/SMPS instrument meeting the EUSAAR quality standards commercially available.

As a result, EUSAAR created all prerequisites for including the PNSD as a central parameter in understanding atmospheric aerosol processes in a more central role in the EMEP observation programme.

4.3 Standard operating procedures and network inter-comparisons for aerosol optical properties, notably black carbon

In terms of aerosol optical properties, the EUSAAR efforts on improving data quality assurance and comparability within the network and to other networks included the following variables:

- Aerosol optical depth (AOD)
- Aerosol scattering coefficient
- Aerosol absorption coefficient, being linked to black carbon (BC) mass

There currently exist two networks for monitoring of aerosol optical depth with global coverage: 1) the Precision Filter Radiometer (PFR) network, operated by the Physical-Meteorological Observatory Davos (PMOD) hosting the GAW World Optical Depth Research and Calibration Centre (WORCC); 2) the AErosol RObotic NETwork (AERONET), operated by the U.S. National Aeronautics and Space Administration (NASA) and its European branch, the PHOTONS network, operated by the French National Observatory for Aerosol at the University of Lille 1. The two networks use the same measurement principle, but different instrumentation and different operating procedures, e.g. continuous measurement in the PFR network versus 15 minute sample intervals in AERONET. Driven by the significance of AOD data for the climate modelling community, there have previously been a few singular inter-comparisons between these networks (e.g. McArthur et al., 2003). To avoid a drift of calibrations between these networks, these inter-comparisons would need to be repeated more often while at the same time, the downtime of instruments due to calibrations would need to be limited. The purpose of the work within EUSAAR was to achieve both goals by setting up a travelling standard of the PFR network. After procurement of the PFR travelling standard, it was used for inter-comparisons at the AERONET sites Birkenes in Southern Norway, and Leipzig, Germany. In both cases, the deviations were at the 0.001–0.002 level of absolute AOD, which is remarkable considering that deviations of 0.005 are often accepted (McArthur et al., 2003).

The aerosol scattering coefficient is part of the core set of aerosol variables observed at the EMEP-EUSAAR / GAW sites. It is measured with an instrument called integrating nephelometer. This instrument type uses a Lambertian light source to illuminate a defined volume filled with dried sample aerosol, where the sample is continuously shifted. The light scattered by the sample is optically integrated, ideally over the whole solid angle sphere, which would require an instrument of infinite length. Due to the finite length of any real instrument, the data needs to be corrected for angular truncation. The value desired, the scattering coefficient of the aerosol particle fraction, is the difference of scattering by the total aerosol and the scattering of a particle free sample. Zero offset and span of the instrument therefore need to be calibrated regularly with particle free air and a particle free span gas, commonly carbon dioxide. The first commercially available multi-wavelength integrating nephelometer, the TSI 3563, came on the market in 1991. It has been widely used at EUSAAR and GAW sites, and has been extensively characterised in terms of Lambertian characteristics, wavelength characteristics, calibration, accuracy, precision (all in Anderson et al., 1996), and correction of angular truncation (Anderson and Ogren, 1998). Since then, the TSI 3563 underwent two redesigns due to discontinued components, and competing instruments such as the ECOTECH Aurora 3000 entered the market, both warranting an update of the earlier characterisation work. EUSAAR conducted a nephelometer inter-comparison workshop already early in the project, which is reported in Müller et al. (2009). The workshop showed the long-term stability of the instruments used in the network, and extended the characterisation work to the newly introduced types, which may now safely be used yielding data of the same accuracy and precision as the remaining parts of the network.

The third optical aerosol parameter considered by EUSAAR, the aerosol absorption coefficient, is most commonly measured in monitoring networks with an instrument type called filter absorption photometer. In these instruments, the decrease in optical transmissivity of a filter is measured at several wavelengths across the visible spectrum while the filter is loaded with aerosol particles. Since the scattering of the sample/filter system is dominated by scattering of the filter and thus almost constant, the method is mostly sensitive to absorption of the aerosol particle fraction. By applying Lambert-Beer's law, the decrease in transmissivity can be translated into an aerosol absorption coefficient. While the method is mostly sensitive to aerosol absorption, the dependence on aerosol scattering is too large to be neglected. The commercially available instruments of this type handle this effect to a varying degree of accuracy. For the oldest such instrument type, the Magee Scientific Aethalometer, exist a number of articles proposing correction schemes, but no agreement could be reached within the community on this issue. This situation is unfortunate since the Aethalometer is widely used and by default providing the concentration of black carbon mass, a property derived from the aerosol absorption coefficient on the grounds of assuming a mass absorption efficiency, which thus suffers from the same systematic uncertainty. Another widely used instrument type is the Radiance Research Particle Soot Absorption Photometer (PSAP), which has received community attention concerning its correction to particle scattering and can be considered as sufficiently well understood (Bond et al., 1999). The third instrument type in this group is the Multi-Angle Absorption Photometer (MAAP) (Petzold and Schönlinner, 2004). The MAAP is designed for taking the method's dependence on particle scattering explicitly into account while measuring the aerosol absorption coefficient and the derived BC mass concentration. It does so by monitoring not only the filter transmissivity, but also the reflectivity while loading the filter, and applies an online inversion for the system of sample and filter, but features unfortunately a measurement only at one wavelength. The situation of three different instrument types with vastly varying degree of scientific understanding being used in one network for measuring aerosol absorption coefficient and BC mass concentration is far from ideal and leaves many open questions concerning comparability. EUSAAR conducted 2 absorption photometer inter-comparison workshops addressing the described issues, involving all named instrument types. During the workshops, the instruments sampled lab generated test aerosols with varying particle size and imaginary refractive index. The goal is to find a common, unified correction scheme applicable to all filter absorption photometers, which will be a significant advancement in accuracy and comparability of absorption coefficient and BC mass concentration data available. The work is ongoing and will be finished in the EUSAAR follow-up project.

4.4 Improved access to EMEP / EUSAAR data by web-portal and establishing near-real-time data collection and dissemination services

The mutual co-benefit between EMEP and EUSAAR is most obvious considering aspects of data collection, archiving, and dissemination, even for non-experts in the various measurement techniques. Right from the start, EUSAAR could build on the existing EMEP data infrastructure at its Chemical Co-ordinating Centre (CCC) at the Norwegian Institute for Air Research (NILU) with its EBAS database. Already before EUSAAR, the extended application of the EBAS database by users outside the traditional EMEP community led to a growing number of repeated demands concerning additional features and services:

- The EBAS database was accessible directly only for selected EMEP bodies, otherwise only by e-mail requests to the CCC. A user driven web interface was missing.
- EMEP data documentation and metadata standards were designed with the original applications for the CLRTAP in mind. Users in the climate and air quality forecasting community enquired about additional information concerning data quality, traceability, and SOPs used, specifically a measure of variability within an averaging period, so the observation method permits.

- A formal collaboration with other frameworks in terms of data access and use as outlined by the 2010-2019 EMEP strategy was not in place.
- Near-real-time (NRT) services for policy makers and air quality forecasting require also the data to be reported and processed in near-real-time.

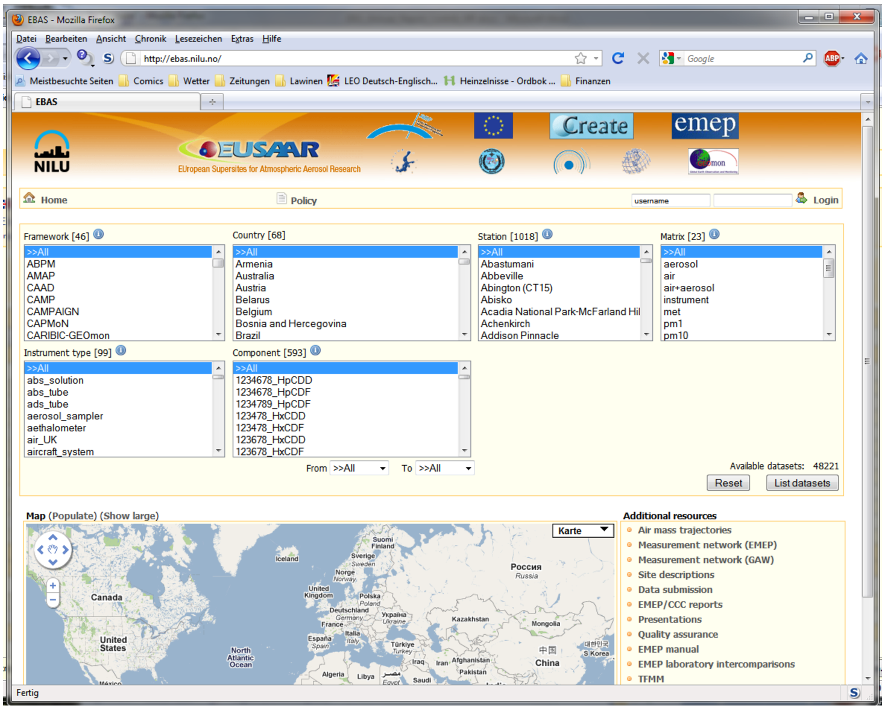

username

Framework [46]
>>All
ABPM
AMAP
CAAD
CAMP
CAMPAIGN
CAPMoN
CARIBIC-GEOmon

Country [68]
>>All
Armenia
Australia
Austria
Belarus
Belgium
Bosnia and Hercegovina
Brazil

Station [1018]
>>All
Abastumani
Abbeville
Abington (CT15)
Abisko
Acadia National Park-McFarland Hil
Achenkirch
Addison Pinnacle

Matrix [23]
>>All
aerosol
air
air+aerosol
instrument
met
pm1
pm10

Instrument type [99]
>>All
abs_solution
abs_tube
ads_tube
aerosol_sampler
aethalometer
air_UK
aircraft_system

Component [593]
>>All
1234678_HpCDD
1234678_HpCDF
1234789_HpCDF
123478_HxCDD
123478_HxCDF
123678_HxCDD
123678_HxCDF

From >>All To >>All

Available datasets: 48221

Reset
List datasets

Additional resources
- Air mass trajectories
- Measurement network (EMEP)
- Measurement network (GAW)
- Site descriptions
- Data submission
- EMEP/CCC reports
- Presentations
- Quality assurance
- EMEP manual
- EMEP laboratory intercomparisons
- TFMM

Figure 4.2: Screenshot of the new web-interface for EMEP's database EBAS at NILU, accessible at http://ebas.nilu.no.

Within the EUSAAR project, a user-driven web interface for the EBAS database was developed, which is accessible at http://ebas.nilu.no (see Figure 4.2). The web-interface allows users to search the database with framework, location, instrument, and data type related search criteria, and visualise the spatial coverage with a map tool. Datasets matching the selected search criteria may be plotted as time series or downloaded for user specified time intervals. On the result page, links to other dataset specific products exist, e.g. to back-trajectory or retro-plume products. Datasets may be access restricted by their project association, allowing access only with a user-specific password, e.g. for data already submitted to EBAS, but not yet released. Access restricted datasets may still be discovered, but only accessed being logged-in as authorised user.

EUSAAR also provided a concept for improved documentation of data submitted to the EBAS database. Additional metadata items were defined referring to standardised SOPs used for collecting and processing the data, along with items describing station setting and situation of instrument and sample intake. Furthermore, an architecture for establishing data traceability to the source similar to concepts used for satellite data was defined. The architecture uses four data levels with pertaining format templates specific for each type of instrument and observation:

Level 0: Annotated raw data as close to parameters provided by instrument as possible, format instrument specific, “native” time resolution.

Level 1: Data processed to final physical variable, property specific format, “native” time resolution.

Level 1.5: Data aggregated to hourly averages, property specific format, includes information on atmospheric variability along with average, generated automatically.

Level 2: As level 1.5, but manually quality assured. This data level is also used for regular, annual data reporting.

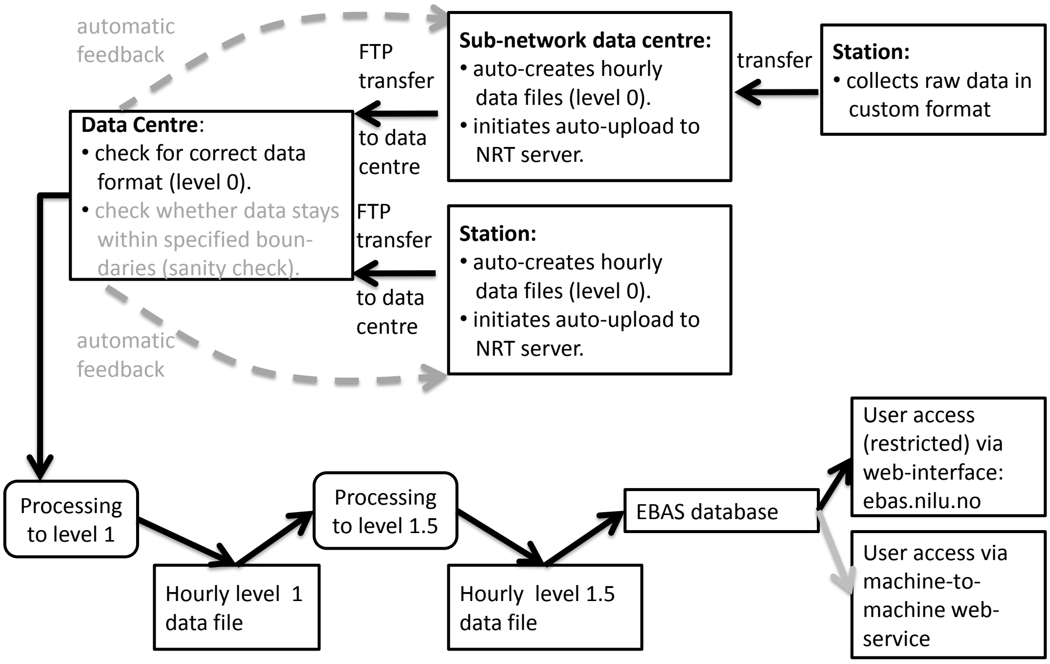

Figure 4.3: Screenshot of the new web-interface for EMEP’s database EBAS at NILU, accessible at http://ebas.nilu.no.

All format templates are formulated in the EBAS NASA-Ames format used previously for data reporting within EMEP, and are backwards compatible. Only level 2 data are available to the data users by default. Levels 1.5 and 2 include information on atmospheric variability within the averaging period, a feature long requested by users in the modelling community. Having the other levels available and stored either with the data provider or at the data centre allows to trace the data back to the point when it was acquired (level 0), and opens the possibility of reprocessing it if new research offers improved data quality.

EUSAAR also worked towards implementing EMEP’s strategy of collaboration between networks and frameworks. The features offered by the EMEP data centre as augmented and improved by EUSAAR led the Global Atmosphere Watch (GAW) programme of the World Meteorological Organisation (WMO) to approach the data centre to assume the responsibility of World Data Centre for Aerosol (WDCA). In this function, the EMEP data centre now collects data on microphysical, optical, and chemical aerosol properties not only from European sites, but from all sites contributing to the GAW programme globally. This can be seen as a successful collaboration and synergy of resources between EMEP run by the UN Economic and Social Council, and WMO as UN agency.

Prior to EUSAAR, near-real-time (NRT) data collection and dissemination services existed only for aerosol parameters like online PM_{10} or $PM_{2.5}$ mass that have to be used as provided by the instrument. For parameters like particle number size distribution (PNSD), aerosol scattering or absorption coefficient, NRT services were considered not feasible due to the level and sophistication of processing involved in arriving at a usable data product. EUSAAR nevertheless managed to set up such a service with a centralised data collection and processing facility, thereby making use of the newly defined data documentation architecture (see Figure 4.3). The data are uploaded to a designated FTP server at the data centre as level 0 files. At the data centre, the data are processed via level 1 to level 1.5, imported into the EBAS data base while being clearly marked as automatically processed. Sending the data to the data centre in level 0 (annotated raw data) has the advantage that users registered as instrument owners can check not only the processed data, but also the instrument status parameters like flags, supply voltages, etc. A separate online tool allows only these users to flag data they deem of doubtful quality as invisible to other users. The observables and instrument types included in the NRT network were chosen for their use to the anticipated user community and their degree of agreement in the community in terms of data processing:

- Particle number size distribution, measured by:
    - Differential Mobility Particle Sizer
    - Scanning Mobility Particle Sizer
- Aerosol optical depth, measured by:
    - Precision Filter Radiometer
- Aerosol scattering coefficient, measured by:
    - Integrating nephelometer
- Aerosol Absorption Coefficient, measured by:
    - Particle Soot Absorption Photometer
    - Multi-Angle Absorption Photometer

The network currently comprises 23 stations, submitting data of 39 individual instruments that pertain to 6 different instrument types, Figure 4.4. Users interested in obtaining access to NRT data are requested to send an e-mail to ebas@nilu.no.

Figure 4.4: Global distribution of stations participating in the EMEP/EUSAAR/ GAW aerosol near-real-time network.

4.5 Conclusion and outlook

Access to NRT data is currently restricted to users connected to the project, but it is planned to give general access to the plotting functionality for NRT data. The European Centre for Medium Range Weather Forecast (ECMWF) is the first institutional user of this service. ECMWF uses the NRT data for validating the research version of its weather forecast model that includes an aerosol module. Also with respect to NRT data collection and dissemination, EMEP / EUSAAR is collaborating with the WMO GAW programme, adding stations around the globe to the map of NRT stations (see Figure 4.4)

The synergy between EMEP and EUSAAR can be considered as a successful implementation of EMEP's strategy on collaboration between frameworks and networks. While receiving policy support for continued operation of the network from EMEP, EUSAAR provided EMEP with needed standard operating procedures for aerosol parameters observed at level 2 EMEP sites, a public web-interface for its database, an inter-UN link to the WMO GAW aerosol programme, and an infrastructure for near-real-time data collection and dissemination. This work will be continued in the EUSAAR follow-up project Aerosols, Clouds, and Trace gases Research InfraStructure Network (ACTRIS, http://www.actris.net) which started this year, funded by the EU 7th framework programme.

5 Atmospheric mineral dust in regional background sites

*By Xavier Querol, Fulvio Amato, Andrés Alastuey, Michael Cusack,
Cristina Reche, Angeliki Karanasiou, Mar Viana, Teresa Moreno, Jorge Pey,
Noemí Pérez*

5.1 Introduction

On a global planetary scale, after sea salt with 10 000 Gt of aerosols continuously in suspension in the atmosphere, mineral dust, with 1500 Gt, is the second major contributor to the Earth’s atmospheric aerosol load (Andreae and Rosenfeld, 2008). Most of this global mineral dust is released to the atmosphere from arid or semiarid areas. The major dust source areas are located in subtropical latitudes of the North Hemisphere, and extend from the West coast of North Africa, the Middle East, Central and South Asia to China (Prospero et al., 2002).

Crustal or mineral aerosols influence the atmospheric radiative balance through scattering and absorption processes (IPCC, 2007), and by acting as cloud condensation nuclei when sulphation and nitration occur (Levin et al., 1996). Dust outbreaks may also greatly increase the ambient air levels of PM recorded in air quality monitoring networks. This is especially relevant in Southern Europe (Bergametti, et al., 1989; Dayan et al., 1991; Querol et al., 1998a; Rodriguez et al., 2001; Escudero et al., 2005, 2007; Kallos et al., 2007; Mitsakou et al., 2008; Gerasopoulos et al., 2006; Kocak et al., 2007), Eastern Asia (Zhang and Gao, 2007) and in some Atlantic islands (Prospero and Nees, 1986; Coudé-Gaussen et al., 1987; Chiapello et al., 1995; Arimoto et al., 1997; Viana et al., 2002). Dust particles frequently act as reaction surfaces for reactive gaseous species (Dentener et al., 1996; Alastuey et al., 2005), and the content of secondary PM may greatly increase when dust particles are present in the atmosphere. Moreover, atmospheric deposition fluxes of specific nutrients in Southern Europe are also enhanced by dust outbreaks from Northern Africa (Àvila and Rodà, 2002). Oceanic or marine regions may be also highly influenced by crustal dust deposition, when dust iron and phosphate deposition may act as fertilizing agents for phytoplankton (Arimoto, 2001). Furthermore, chemical compounds emitted from deserts may represent a source of alkalinity that neutralizes atmospheric acidity (Àvila and Rodà, 2002). Finally, dust transport episodes may also cause health impacts (Pérez et al., 2008a; Middleton et al., 2008) due to the high levels of PM and to the transport of anthropogenic pollution (Erel et al., 2006) and also to the possible transport of micro-organisms (Koulouri et al., 2008).

Other sources of mineral matter, such as natural regional resuspension, and a number of anthropogenic sources, including agricultural, industrial, construction and road dust, may greatly exceed African dust in terms of their source contribution to ambient PM_{10} levels in Europe, especially in urban and industrial areas.

5.2 The chemical composition of mineral dust

A large fraction of mineral aerosols arise from soil particles that have been mobilized by strong wind currents and entrained into the atmosphere. Since these particles are eroded soils, their chemical composition will be similar to that of crustal rocks (Usher et al., 2003), even though some minerals are preferentially fractionated when soil particles are resuspended to the atmosphere as PM_{10} or $PM_{2.5}$ (Moreno et al., 2008).

The abundance of the major elements and oxides found in the continental crust is displayed in Table 5.1. Therefore the most abundant elements of the Earth's crust after oxygen (Si, Al, Fe, Ca, K and Ti, and Mg when levels of mineral dust are relatively high) are typically used as tracers of mineral dust, excepting Na and Mg, more suitable tracers for sea-salt particles when levels of dust are reduced (Taylor and McLennan, 1995; Wedepohl, 1995).

Table 5.1: Abundance of Major Elements in the Upper Continental Crust and Major Elements as Oxides in the Continental Crust (modified from Usher et al. 2003, based on Wedepohl, 1995).

Element	**%**	**Oxide**	**%**
Oxygen	47		
Silicon	30.348	SiO_2	61.5
Aluminum	7.744	Al_2O_3	15.1
Iron	3.089	Fe_2O_3	6.28
Calcium	2.945	CaO	5.5
Sodium	2.567	Na_2O	3.2
Magnesium	1.351	MgO	3.7
Potassium	2.865	K_2O	2.4
Titanium	0.3117	TiO_2	0.68
Barium	0.00668	BaO	0.0584
Manganese	0.0527	MnO	0.1

The aforementioned atoms are combined in form of minerals. In general the most common minerals in atmospheric mineral dust are quartz, feldspars, micas, clay minerals (chlorite, kaolinite, illite, smectite, palygorskite), carbonate minerals (calcite, dolomite) and gypsum (formulas are shown in Table 5.2), even though their percentages can vary largely depending on the source location. Indeed, mineralogy varies from one region to another depending on the local bedrock geology. In fact, bedrock geology provides the primary raw material from which, modified over time by climate, topography, sedimentary transport and biogenic activity, soils and dusts will be generated. In addition, the atmospheric mineral "cocktail" found in a certain location, can be influenced by air mass transport: long-range transported desert dust is enriched in clay minerals due to their finer size and laminar shape both favouring longer residence-time and transport (Pósfai and Molnár, 2000).

Table 5.2: Chemical formula for common minerals in atmospheric dust.

Mineral	**Formula**
Calcite	$CaCO_3$
Corundum	α-Al_2O_3
Chlorite	$A_{5\text{-}6}Z_4O_{10}(OH)_8$ †
Dolomite	$CaMg(CO_3)_2$
Feldspars	WZ_4O_8 ‡
Gypsum	$CaSO_4{\cdot}2H_2O$
Hematite	Fe_2O_3
Illite	$(K,H_3O)(Al,Mg,Fe)_2(Si,Al)_4O_{10}[(OH)_2,H_2O]$
Kaolinite	$Al_4Si_4O_{10}(OH)_8$
Magnesite	$MgCO_3$
Montmorillonite (smectite)	$(Na,Ca)_{0.33}(Al,Mg)_2Si_4O_{10}(OH)_2{\cdot}nH_2O$
Mica	$W(X,Y)_{2\text{-}3}Z_4O_{10}(OH,F)_2$ ∫
Opal	$SiO_2{\cdot}nH_2O$
Palygorskite	$(Mg,Al)_2Si_4O_{10}(OH)\ {\cdot}4H_2O$
Quartz	SiO_2

† Typically A) Al, Fe, Li, Mg, Mn, and/or Ni; Z) Al, B, Si, and/or Fe.
‡ Typically W) Na, K, Ca, and/or Ba; Z) Si and/or Al.
∫ Typically W) K or Na; X and Y) Al, Mg, Fe^{2+}, Fe^{3+}, and Li; Z) Si and Al.

There are also more subtle effects that produce geochemical variations in mineral dusts, particularly those involving the relative susceptibilities of trace elements and their host minerals to surface weathering and transport processes. Trace elements-hosting minerals are typically accessory (in low concentration) minerals such as rutile (TiO_2), monazite [$(Ce,La,Nd,Th,Y)\ PO_4$], xenotime (YPO_4), apatite [$Ca_5(PO_4)_3\ (F,OH,Cl)$], zircon ($ZrSiO_4$) and thorite ($ThSiO_4$) among others. However, ion exchange and differential adsorption mechanisms tend to favour the retention of some trace elements over major constituents of clay minerals. As examples, in clay minerals Rb can substitute K, while Al is frequently substituted by V, Ba and Sr can easily replace K and Ca in feldspars and Ca-rich micas. Lanthanoids, especially Heavy Rare Earth Elements, can be also adsorbed in clay minerals (illlite and montmorillonite). Nb can be present within various rock-forming silicates such as biotite, titanate, and zircon.

Only few laboratories in Europe include trace elements when analyzing the chemical composition of mineral dust. Pey et al. (2009) reviewed the reported concentrations in Mediterranean, Central European and US rural sites of all trace elements (mineral and anthropogenic). The most analyzed elements were V, Mn, Ni, Cu, As, Zn, Se, Pb and Cd (Puxbaum et al., 2004; Hueglin et al., 2005; Marenco et al., 2006; Lall and Thrurston, 2006; Salvador et al., 2007; Viana et al., 2008; Rodríguez et al., 2004). Other elements, more of mineral origin, such as Li, Be, Sc, Co, Ga, Ge, Sr, Ba, Rb, La and Ce were analyzed only in a few cases (Salvador et al., 2007; Viana et al., 2008; Rodríguez et al., 2004; Hueglin et al., 2005; Pey et al., 2009).

In addition to this complex chemical composition, various heterogeneous reactions on mineral dust or mineral dust proxies may change the original composition. Weathering or aging processes, such as exposure to reactive inorganic or organic chemical species or exposure to varying amounts of water vapour in the atmosphere, may influence the chemical nature of mineral dust (Usher et al., 2003). As already mentioned above, a mineral dust particle may have a coating of a chemical species due to the transport of that particle through an atmospheric region containing that species. Consequently, the outermost layer of a dust surface may be different from the mineralogy of the original dust. Mineral dust particles collected in different regions of the world are often found associated with nitrate. Wu and Okada (1994) concluded that heterogeneous reaction with dust particles could account for the accumulation of nitrate during high dust events. Lee et al. (2002) found that the nitrate ion peak intensity was at a maximum in the late afternoon when the gas-phase nitric acid peak was highest. The association between calcium ions and nitrate has been observed in several studies (Pakkanen, 1996; Querol et al., 1998b).

The content of mineral dust in ambient air PM can be quantified by means of different techniques, being the most common X-Ray Fluorescence (XRF), Inductively Coupled Plasma Spectrometric techniques (ICP-MS, ICP-AES or ICP-OES) and Proton-Induced X-ray Emission (PIXE). Furthermore, aerosol time-of-flight mass spectrometry (ATOFMS) and electron microscopy, both transmission (TEM) and scanning (SEM) methods, have also been used to characterize individual mineral dust particles. Table 5.3 summarizes the methods used by European laboratories to analyze the typically crustal elements in rural monitoring sites and therefore estimating the percentage of mineral dust to PM_{10}.

Despite that the chemical composition of mineral dust varies depending on its origin, is it possible to give a prioritized list of elements associated with mineral dust which ought to be measured regardless of location. These include: Si, Al, Ca, Fe and Ti. Furthermore, levels of Si, Al, Fe, Ca, K and Ti in ambient PM correlate generally very well suggesting that they originate from the same source and can be easily used to calculate the mineral dust in PM. However the elemental weight alone is not enough, but requires a correction for the oxidised form (e.g., Si is mostly present as SiO_2). Although Si typically is the most important constituent of mineral dust, it is probably the element for which the threshold is the highest when it comes to initiating measurements, as most labs use quartz microfiber filters for sampling. However SiO_2 can be easily estimated form the Al_2O_3 content (Querol et al., 2001) since aluminium-silicates are the most common mineral phases present in mineral dust and their relative abundances are generally constant. Experimental data show that SiO_2/Al_2O_3 ratio in PM_{10} in most places range from 2.5 to 3.5 (Putaud et al., 2004). All kinds of other minerals may be present, but contribute much less to mineral dust, with the exception of areas dominated by calcareous soils where carbonate minerals, such as $CaCO_3$, may be important. A detailed chemical analysis can easily provide all relevant elements, thus being possible to account for all mineral dust mass after correction for the oxidation status.

Table 5.3: Crustal elements analyzed in PM samples collected at rural sites by European laboratories.

Location		PM Fraction	Crustal elements analyzed	Reference	Method
SWE	Aspvreten	PM_{10} and $PM_{2.5}$	Si, Al, Fe, Ca, Mg and K	*Sjödin et al., 2010*	PIXE and ICP-MS
IRL	Ahascaragh/ County Galway	PM_{10} and $PM_{2.5}$	K+, Mg2+ and Ca2+	*Yin et al., 2005*	IC
	Wicklow	PM_{10} and $PM_{2.5}$	K+, Mg2+ and Ca2+	*Yin et al., 2005*	IC
NL	Vredepeel	PM_{10} and $PM_{2.5}$	Si, Al, Fe, Ca, K, Ti Rb and Sr.	*Visser et al., 2001*	ED-XRF
	De Zilk	PM_{10} and $PM_{2.5}$	Si, Al, Fe, Ca, K, Ti Rb and Sr.	*Visser et al., 2001*	ED-XRF
BEL	Waasmunster	PM_{10} and $PM_{2.5}$	Mg, Al, Si, P, S, K, Ca, Ti, Mn, Fe, Ga, Rb, Sr, Zr	*Maenhaut and Cafmeyer, 1998*	PIXE and INAA
CH	Chaumont	PM_{10} and $PM_{2.5}$	Mg, Al, K, Ca, Fe, La, Ce,	*Hueglin et al., 2005*	ICP-MS
	Payerne	PM_{10}	Mg, Al, K,Ca, Fe, La, Ce,	*Hueglin et al., 2005*	ICP-MS
AUT	Illmitz	PM_{10} and $PM_{2.5}$	nss-Ca^{2+}	*Schneider and Lorbeer, 2002*	IC
GER	Melpitz	PM_{10} and $PM_{2.5}$	nss-Ca^{2+}	*cited by Putaud et al., 2004*	IC
	Neuglobsow	PM_{10}	NA	*Lenschow et al. (2001)*	Not reported
FRA	Plan d'Aups	$PM_{2.5}$	Si, Al, K, Ca, Mg	*Marinoni et al., 2005*	PIXE
ITA	Monte Cimone	PM_{10}	Mg, Al, Si, P, K, Ca, Ti, Fe	*Marenco et al., 2006*	ED-XRF
	Montelibretti	PM_{10} and $PM_{2.5}$	Al, Si, Fe, K, Mg, Ca, Ti	*Perrino et al., 2008*	XRF
	Fontechiari	PM_{10} and $PM_{2.5}$	Al, Si, Fe, K, Mg, Ca, Ti	*Perrino et al., 2008*	XRF
ESP	Monagrega	PM_{10}	Al, Ca, Fe, Mg, K, Ti, Rb, Li and Sr.	*Rodriguezet al., 2003*	ICP-AES and ICP-MS
	Montseny	PM_{10} and $PM_{2.5}$	Al, Ca, Fe, Mg, K, Ti, Rb, Li and Sr.	*Querol et al., 2008*	ICP-AES and ICP-MS
	Bemantes	PM_{10} and $PM_{2.5}$	Al, Ca, Fe, Mg, K, Ti, Rb, Li and Sr.	*Querol et al., 2008*	ICP-AES and ICP-MS
	M. Perdón (Pamplona)	PM_{10}	Al, Ca, Fe, Mg, K, Ti, Rb, Li and Sr.	*Zabalza et al., 2006*	ICP-AES and ICP-MS
FIN	Sevettjarvi	PM_{10} and $PM_{2.5}$	NA	*Virkkula et al., 1999*	PIXE & INAA
NOR	Skreådalen	PM_{10} and $PM_{2.5}$	Al, Si, Ca, Sc, Ti, Fe, La, and Sm	*Maenhaut et al., 2000*	PIXE & INAA
	Birkenes	PM_{10} and $PM_{2.5}$	Al, Si, Ca, Sc, Ti, Fe, La, and Sm	*Maenhaut et al., 2000*	PIXE & INAA

INAA: instrumental neutron activation analysis; NA: not available

Querol et al. (2001) and Van Loy et al. (2000) proposed the following formula to estimate the total mineral dust mass by using some of the abovementioned crustal elements:

Mineral Mass = 5.67*[Al] + 1.5*[Ca] + 2.5*[Mg]
Mineral Mass = 2.14* [Si] + 1.89*[Al] + 1.43*[Fe] + 1.4*[Ca] + 1.2*[K]

However, caution must be paid to Ca, Fe and K since they may also (partly) originate from other sources, for example, Fe from brake wear and steel industry, K from biomass burning, Ca from lubricants in motor engines, mostly where the potential impact of these sources is high and assigning all their mass to mineral dust could thus result in overestimation. This inconvenient can be solved by estimating the "mineral" fraction of elements other than Si and Al (hardly present in PM from other sources) from the ratio to Si or Al in top-soil material or average crust composition. Also the carbonate (CO_3^{2-}) content might be overestimated given that some Ca can be associated with nitrate and sulphate.

Si and Al can also be used alone to estimate the total mineral dust mass. Several algorithms are available in literature and are based on the Si and Al content in the Earth's crust (Visser et al., 2001; Denier van der Gon et al., 2010):

Mineral Mass = 0.49*[Si] + (2.36*[Si]+2.70*[Al])
Mineral Mass = 1.80* [Si] + 6.15*[Al]

These formulas include the average mass from other non-Al and non-Si minerals, nevertheless their use in areas dominated by calcareous soils can be effected by large errors.

Denier van der Gon et al. (2010) investigated the suitability of other elements in well-representing mineral dust concentrations by cross-correlation analysis. Titanium was strongly correlated with Al and Si and seemed to have the same crustal origin. Ca and Fe resulted to be less reliable tracers due to contributions from other sources than natural. They also concluded that calcium is not a suitable tracer for natural dust: although it would correlate with the mineral dust content, it does not have a fixed correlation with Al and Si in soils. Hence, estimating mineral dust content in PM_{10} by using Ca data can be done, only when using empirically derived relationship between atmospheric mineral dust and Ca concentrations in PM_{10} and not by using the average Ca content in soils.

5.3 Levels of mineral matter

Reports from countries around the Mediterranean Basin and Eastern Europe show especially high levels of atmospheric PM compared to Northern and some Central European regions (ETC, 2010; Putaud et al., 2010). Both anthropogenic (transport, industrial processes, power generation, biomass burning, among others) and natural (African dust, resuspension, sea spray, forest fires, biogenic compounds (primary and secondary) emissions, as well as geographic and climatic factors contribute to those enhanced PM levels.

In Europe the contribution of mineral dust to PM_{10} concentrations varies from 10% to more than 30% depending on location and season (Putaud et al., 2004).

Table 5.4 provides the average annual levels (µg m^{-3}) of PM_{10}, $PM_{2.5}$, mineral elements, and the equivalent contributions to bulk mass concentrations (% wt), recorded at regional background locations in Europe during 1998-2002. The lowest levels of mineral dust are reported for Central European countries. For the period 1998-2002 the mean regional mineral contribution to PM_{10} (mainly of a natural origin) ranged from 5.5 µg m^{-3} in Spain to around 2 µg m^{-3} for Germany, UK, Netherlands, Switzerland, Austria, Sweden), with the exception of the Canary Islands (8 µg m^{-3}). In $PM_{2.5}$ the marine and natural mineral regional contributions decrease significantly with respect to PM_{10}, but these are still present in around 3 µg/m^3 in Spain and about 1.5 µg m^{-3} in Central Europe.

Table 5.4: Average annual levels (µg m^{-3}) of PM_{10}, $PM_{2.5}$, mineral elements, and the equivalent contributions to bulk mass concentrations (% wt), recorded at regional background locations in central Europe (examples from Austria, Germany, Switzerland, the Netherlands, the United Kingdom), northern Europe (13 locations in Sweden) and southern Europe (10 locations in Spain).

Sampling period 1998-2002	Central Europe	Northern Europe	Southern Europe
PM_{10} (µg m^{-3})	14–24	8–16	14–21
Mineral matter (µg m^{-3})	1–2	2–4	4–8
% Mineral matter in PM_{10}	5–10	20–30	12–40
$PM_{2.5}$ (µg m^{-3})	12–20	7–13	12–16
Mineral matter (µg m^{-3})	0.5–2	1–3	1–3
% Mineral matter in $PM_{2.5}$	2–8	15–25	8–20

Source: Denier van der Gon et al., 2010; Querol et al., 2004

Table 5.5: Average contributions (%) of mineral dust to PM_{10}, $PM_{2.5}$ and PM_{coarse} ($PM_{coarse} = PM_{10} - PM_{2.5}$), recorded at rural locations in Central Europe, N-Westhern Europe and Southern Europe. na: not available.

Sampling period 1996-2007	Central Europe	N-Western Europe	Southern Europe
% Mineral matter in PM_{10}	9	4	15
% Mineral matter in $PM_{2.5}$	5	5	11
% Mineral matter in PM_{coarse}	na	na	22

Source: Putuad et al., 2010

Putaud et al. (2010) report the average contribution of mineral dust to PM_{10}, $PM_{2.5}$ and PM_{coarse} ($PM_{coarse} = PM_{10} - PM_{2.5}$) mass levels for European regions (North-western, Southern and Central Europe) during the period 1996-2007, Table 5.5. The highest contribution of mineral dust in both PM_{10} and $PM_{2.5}$ size fractions is observed in rural sites in Southern Europe. Figure 5.1 shows the average chemical composition of PM_{10} at rural sites in the three European regions (Putaud et al., 2010). Results evidence a clear increasing gradient in the mineral matter content from North-Western to Southern Europe in PM_{10} (4 to 15% of the PM_{10} mass).

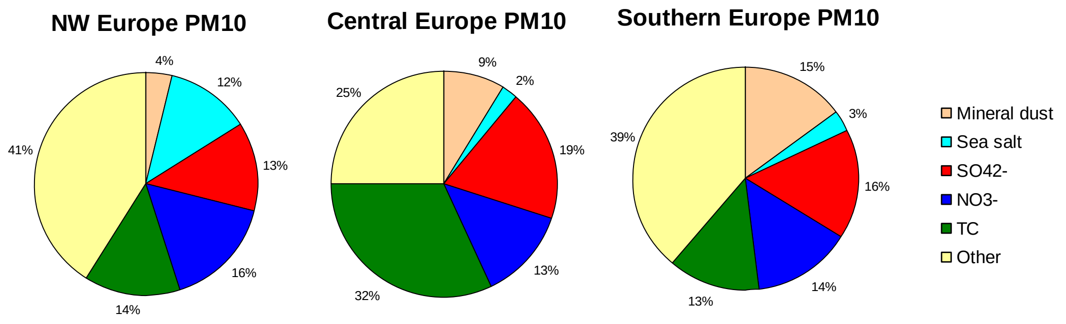

Figure 5.1: Figure 1. Average chemical composition of PM_{10} *at rural sites in three European regions: North-western, Southern and Central Europe (from Putaud et al., 2010).*

5.4 The Mediterranean region

According to Querol et al. (2009a), the mean annual PM_{10} levels across the Mediterranean Basin revealed clear W-E and N-S increasing trends, Figure 5.2. Thus, the mean PM_{10} levels range from 15 $\mu g/m^3$ in the W and NW Mediterranean, to near 35 $\mu g_0/m^3$ in the Eastern Mediterranean Basin (EMB). An increasing trend is also evident from the Rodope Range (Serbia and Macedonia region) and Northern Italian heights (with levels close to 10 $\mu g/m^3$) to SW, SE and central Mediterranean (22-35 $\mu g/m^3$).

One of the more distinctive features of the regional background Mediterranean PM is the relatively high load of mineral matter, when compared with central and northern European regions (Querol et al., 2004 and 2009a, Figure 5.2). More than 70 % of the exceedances of the PM_{10} daily limit value (2008/50/CE European directive) in most EMEP sites of Spain have been attributed to dust outbreaks (Escudero et al., 2007). Similar findings are mentioned in Gerasopoulos et al. (2006), Kocak et al. (2007) and Mitsakou et al. (2008) for the EMB. However, at urban environments the scenario is very different, since most mineral dust load has an anthropogenic origin (Amato et al., 2009a).

Many scientific studies on speciation of PM in central Europe have classically unconsidered mineral matter, by including it in the unaccounted matter or deduced it by applying ‘factors’ to specific mineral matter related (soluble) cations. In the last decades the influence of mineral dust on air quality in the EMEP domain has been considered as a peculiarity of Southern European countries. Nowadays the entire Air Quality community agrees in considering resuspension of road dust (containing anthropogenic mineral matter) as one of main causes of non-attainment to the PM_{10} limit values in large urban environments. This is reflected by the II Position Paper on PM where the possibility of focusing PM monitoring for air quality purpose only on $PM_{2.5}$ (finishing with PM_{10} limit values and measurements) was fortunately dismissed. Several studies evidences the health effect of the coarse fraction ($PM_{2.5\text{-}10}$) (Brunekreef and Fosberg, 2005; Pérez et al., 2009). This coarse fraction is made in a significant proportion by mineral matter from anthropogenic and natural origin.

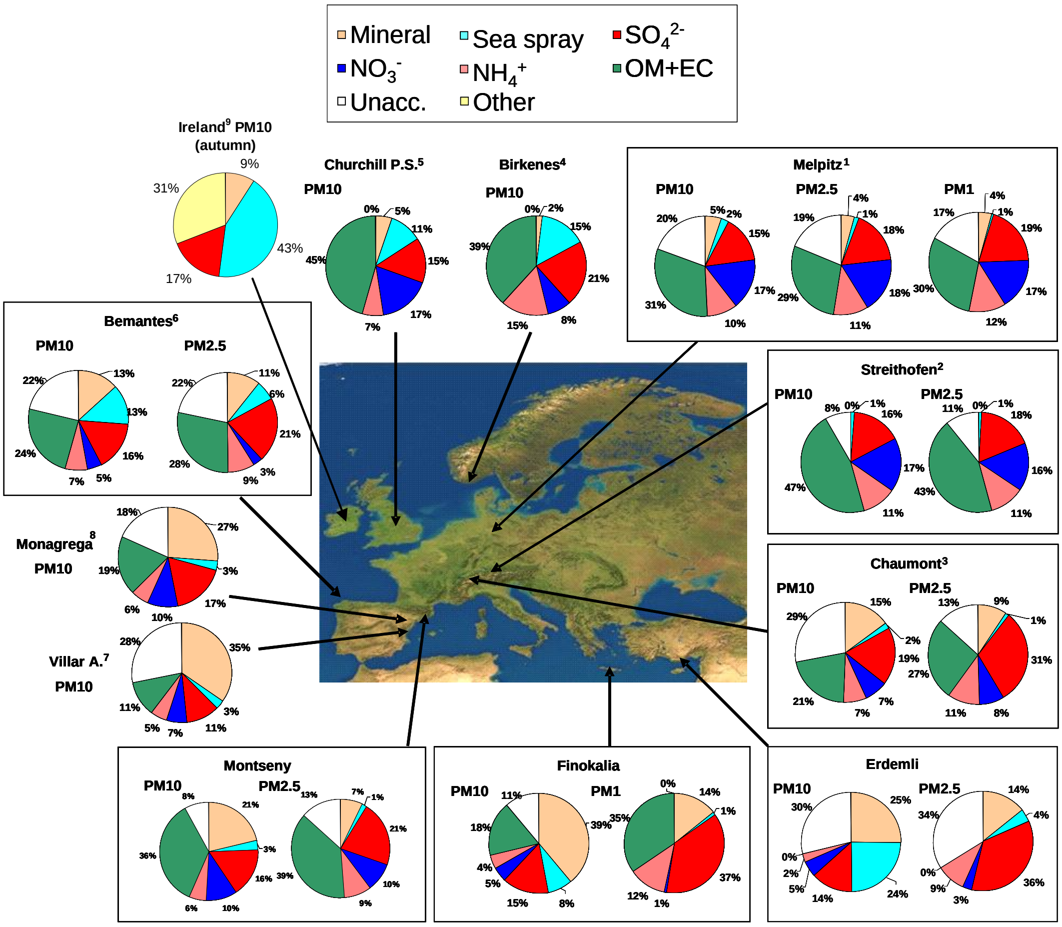

Figure 5.2: Mean annual levels of PM_{10} and $PM_{2.5}$ components measured at MSY, FKL and ERL and a selection of rural-regional background sites. 1 Spindler et al. (2007); 2 Puxbaum et al. (2004); 3 Hueglin et al. (2005); 4 Yttri (2007); 5 Yin and Harrison (2008); 6 Salvador et al. (2007); 7 Viana et al. (2008); 8 Rodriguez et al. (2004); 9 Barry et al. (2005). OM+EC: organic matter + elemental carbon. Modified from Querol et al. (2009a).

Levels of the mineral matter at regional background range from 2-4 to 12 µg/m^3 PM_{10}, 1 to 2 µg/m^3 $PM_{2.5}$ and 0.3 to 0.8 µg/m^3 PM_1 in the Western Mediterranean Basin (WMB) and EMB, respectively (Figure 5.3, Querol et al., 2009a). Mineral matter may account for around of 20-35% of the mean annual PM_{10} regional background load with the lowest values being recorded in the WMB. This proportion is much reduced for $PM_{2.5}$, with 5-7% in the WMB and around 10-15% in the EMB (Querol et al., 2009a). Thus, the levels of mineral matter in $PM_{2.5}$ usually account for less than 50% of those measured for PM_{10}, although this ratio varies throughout the year. In the WMB the lowest ratio of the $PM_{2.5}/PM_{10}$ mineral matter is measured from late spring to mid summer (20-30%), and the highest in winter (35-45%). However, this does not occur in the EMB where the ratio remains constantly low (around 15%) throughout the year, indicating the presence of coarser dust particles (Querol et al., 2004 and 2009a).

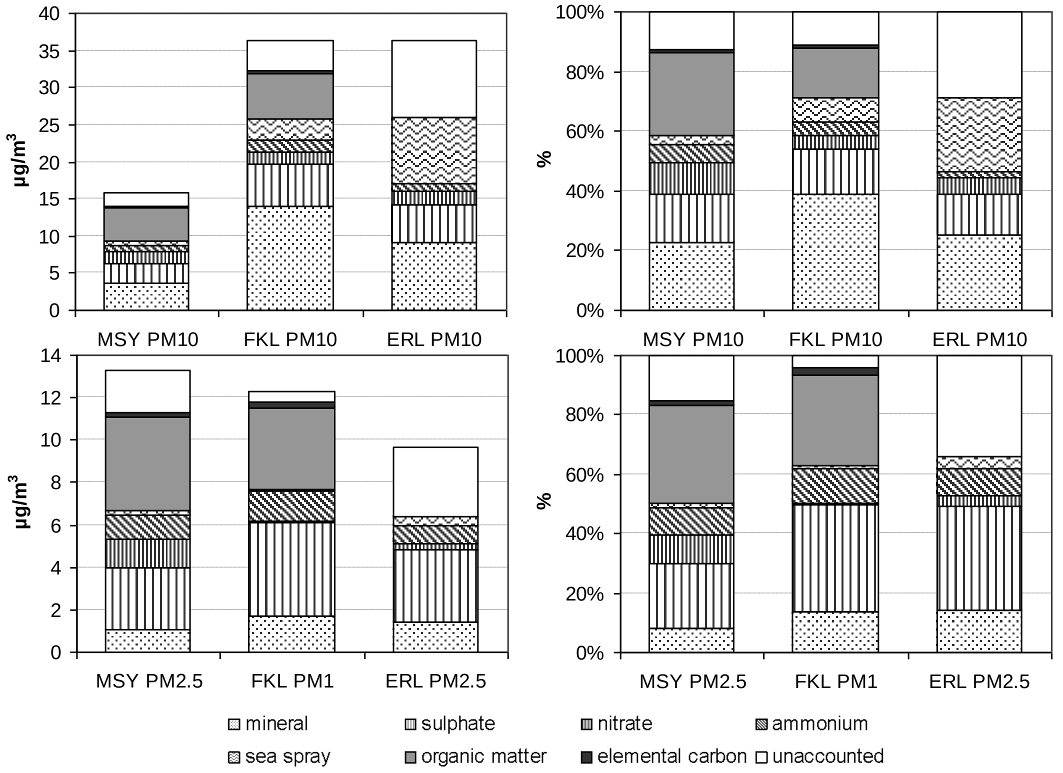

Figure 5.3: PM major composition (µg/m3 left, and % right) at Montseny (MSY) and Erdemli (ERL) in PM_{10} and $PM_{2.5}$, and Finokalia (FKL) in PM_{10} and PM_1 (From Querol et al., 2009a).

As shown by Figure 5.4, mineral matter in a regional background site of the WMB is reaching almost 16% of the mean annual PM_{10} load, near 40% of the $PM_{2.5\text{-}10}$ mass, and only 3 % of PM_1. Figure 5.4 also evidences that the relative contributions of mineral matter and other PM components to the $PM_{1\text{-}2.5}$ fraction is very similar to those of PM_{10}, in other words $PM_{2.5}$ is also importantly influenced by mineral matter, whereas PM_1 is much less influenced. Thus the combination of PM_{10} and PM_1 monitoring is a better option to separately control levels of coarse and fine PM fractions.

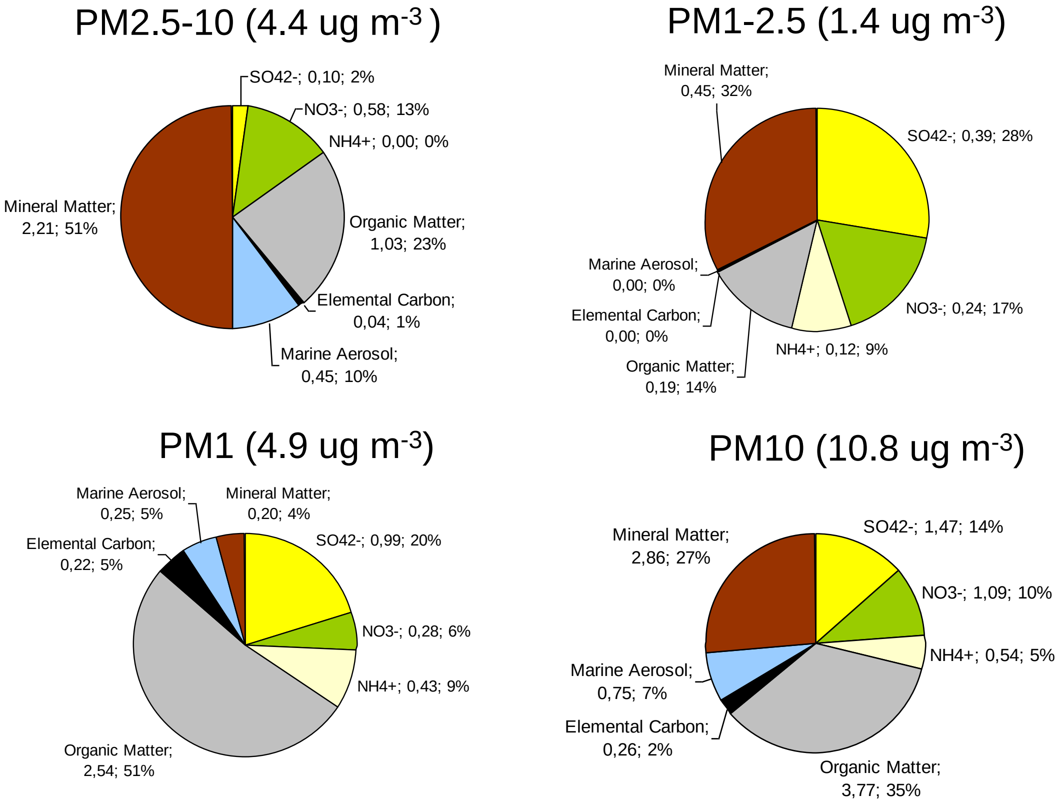

Figure 5.4: Annual average composition of PM1, $PM_{1-2.5}$, $PM_{2.5-10}$ and PM_{10} at the regional background of Montseny (NE, Spain).

5.5 Temporal trends

Along the year, mineral matter exhibits strong seasonal variability and episodic peak concentrations throughout the year at both WMB and EMB (Figure 5.5). This fact can be attributed to: a) seasonality: increased dust resuspension of local and regional origin due to high convective dynamics and low rainfall, and b) episodic peaks: the higher frequency of African dust episodes occurring with higher rate of recurrence during spring and autumn in the EMB and spring and summer in the WMB, but also sporadically in other periods of the year (Pérez et al., 2008b; Querol et al., 2009b).

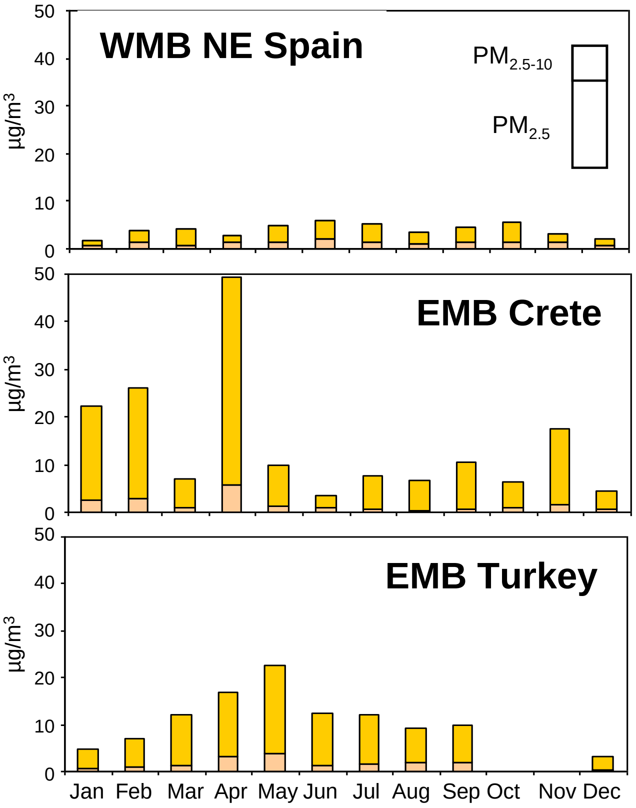

Figure 5.5: Monthly mean levels of mineral matter in PM_{10} and $PM_{2.5}$ across the Mediterranean Basin (from Querol et al., 2009a).

5.6 Origin of ambient air mineral matter

Although in urban environments of the WMB most of the mineral matter in PM has an anthropogenic origin (Amato et al., 2009a, b), the natural contribution of mineral dust to regional background levels of PM may be significant (Querol et al., 2009a). Thus, as shown in Figure 5.6, 69 out of 78 exceedances of the PM_{10} daily limit value recorded in the last 16 years in a regional background site located in a semi-arid zone in North-eastern Spain (Monagrega) are caused by African dust outbreaks, and only 5 by local dust resuspension.

According to Escudero et al. (2005), four meteorological scenarios originate the transport of African dusty air masses towards the Western Mediterranean Basin (WMB). These scenarios are characterized by the presence of (1) a North African high located at surface levels (NAH-S), (2) an Atlantic depression (AD) situated in front of Portugal, (3) a North African depression (NAD), and (4) a North African high located at upper levels (NAH-A). During spring and early summer, the development of Saharan thermal lows in the South of Atlas takes place under the influence of the strong thermal contrast between the temperature of the cold marine waters and the warm continental surfaces (Moulin et al., 1998). These cyclones (NAD scenario) travel eastward along this thermal gradient and finally cross the Mediterranean between Libya and Egypt, constituting the main atmospheric scenario responsible for the transport of desert dust over the Eastern Mediterranean Basin (EMB), where also severe episodes can be associated with the combination of a deep trough over West Mediterranean and NW Africa and relatively high pressures to the Eastern part (Kallos et al., 2007).

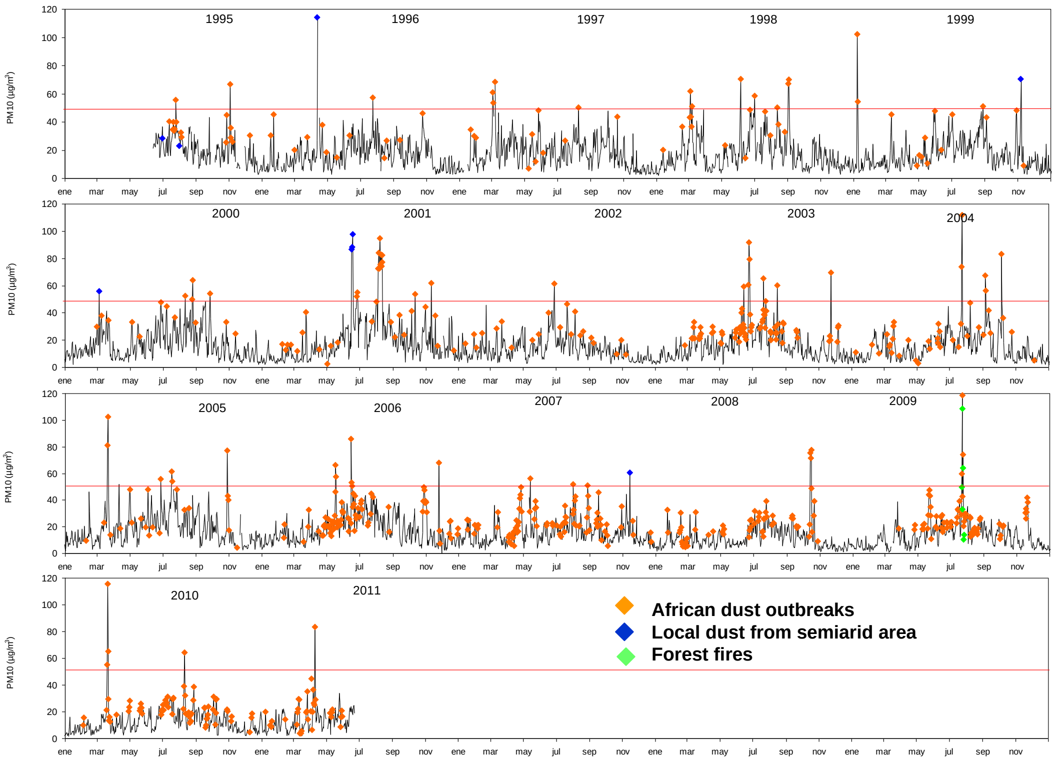

Figure 5.6: Daily 1995-2011 PM$_{10}$ levels at Monagrega regional background site in NE Spain, with identification of African dust episodes.

The above described W-E and N-S trends of regional background PM$_{10}$ levels are fully coincident with the spatial distribution of the mean annual net African dust contribution to PM$_{10}$ (Querol et al., 2009b). This reaches 9-10 µg/m^3 in the EMB, 6 µg/m^3 in the SWMB, 2-3 µg/m^3 in the WMB and <2 µg/m^3 in the NMB (Figure 5.7). In addition, the number of days with NAF episodes, with PM$_{10}$ levels exceeding 50 µg/m^3 (at regional background sites), reached mean values of 20 to 26 days/year in the EMB, 16 days/year in the SWMB, 4 days/year in the WMB and <2 days/year for the NMB. If the days without African dust outbreaks are considered, the exceedances are reduced to <3 days/year in most of the regional background of the Mediterranean. Dust episodes seem to increase easterly not only in frequency but also in intensity. Thus the mean PM$_{10}$ levels for dust days reached 51-52 µg/m^3 in the EMB, 25-36 µg/m^3 in the S, SW and WMBs, and 19-25 µg/m^3 in the NMB.

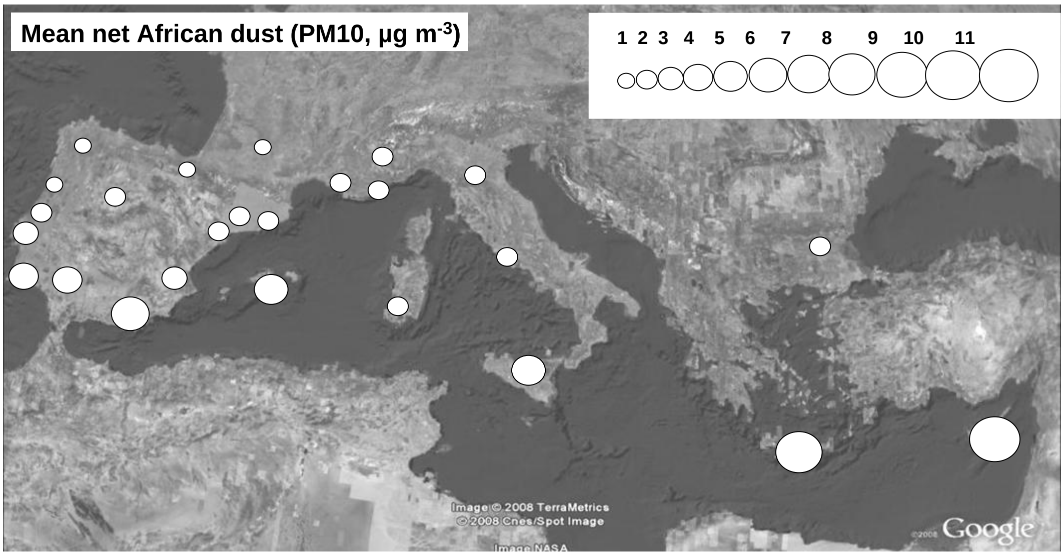

Figure 5.7: Mean annual African net dust load in PM_{10} across the Mediterranean Basin (Querol et al., 2009b).

In addition to African dust, regional resuspension may be significant in Europe that experiences significant wind erosion (Warren, 2003). According to Oldeman (1994), 42 million hectares in Europe are affected by wind erosion. Major wind erosion areas are located in Iceland and in South (Spain, Greece, South Italy) and Southeastern Europe (Romania, Ukraine and Russia). Less severe wind erosion occurs in central and northwest Europe (Czech Republic, Hungary, Slovakia, Serbia, Western France, Northeast England). López et al. (1998) and Gomez et al. (2003) studied dust emissions from agricultural land in Northeastern Spain. The observed dust concentrations during periods of active wind erosion (at 1 m height) ranged from 16 to 89 $\mu g/m^3$. No information on the particle size of the dust emitted was provided.

Apart from wind erosion other activities such as driving on paved and (especially) unpaved roads also causes resuspension of dust. Although the quantities emitted by these processes are very small compared to those produced by wind erosion and tillage operations they may substantially contribute to the dust load in and near cities (especially in dry areas). Dust inventories and dust prediction models usually include these types of emissions, showing that they cannot be neglected. In Europe, the sources that dominate mineral dust contributions are:

- Wind-blown dust
- African dust
- Agricultural activities
- Construction, demolition, handling of mineral goods
- Resuspended dust (road dust, road wear, road gritting and use of studded tyres)

At an urban scale most of the large mineral PM contribution measured in a number of Southern European cities has a major anthropogenic origin. Thus, as shown in Figure 5.8, around 50% of the regional background mineral load in

PM_{10} and $PM_{2.5}$ have an African origin in the WMB (this proportion may markedly increase in the EMB), whereas in the urban background and traffic sites, anthropogenic dust prevails over the natural one.

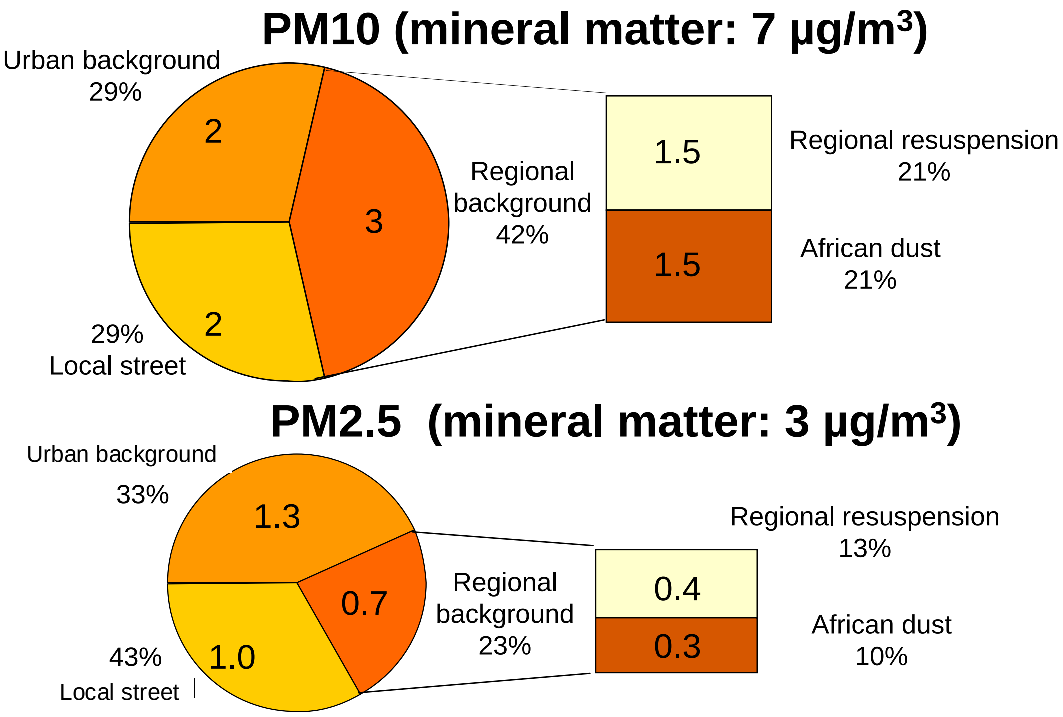

Figure 5.8: Quantification of mineral dust contributions from North African dust, regional resuspension, urban background and traffic increment.

5.7 Is it possible to address various sources of mineral dust at rural sites based upon speciation of the mineral dust?

Separating the contribution of different mineral sources to atmospheric mineral dust at rural sites is difficult given the chemical similarity of the different emission sources: local soil, long-range transported dust and possible contributions from urban dust. As a consequence, researchers proposed specific minerals, ratios between minerals and elemental ratios as tracers of source regions and therefore, potentially able to separate contributions of local mineral dust from long-range transported mineral aerosols and to trace the source area of airborne dusts detected in locations far from the source (see Schütz (1989) and references therein). Caquineau et al. (1998) proposed palygorskite as a clay signature to trace soil particles from the northern Saharan Desert. Another method relies on evaluating the ratio of various clays in order to determine fractionation patterns. The ratio of illite to kaolinite or kaolinite-tochlorite can provide insight into the regional source. Several elemental ratios have been used as fingerprints to trace the contribution of Saharan dust. Blanco et al. (2003) found that the Al/Si ratio of the transported dust varies from 0.41 to 0.50, and that the Al/Si, Ca/Al, K/Ca, and Fe/Ca ratios differ according to source regions and therefore can be also used to identify dust source regions. Marenco et al. (2006) proposed average elemental ratios for the African dust events as follows: Si/Al = 2.31, Fe/Ca = 0.94, Ca/Al = 0.90, K/Ca = 0.44, Ti/Ca = 0.11, and Ti/Fe = 0.12. Therefore, Al/Si ratios higher than 0.3 are generally considered indicative of the desert origin of the particles (Guerzoni et al., 1997). However, a clear variation of the Al/Si ratios with particle size has been found by Coude-Gaussen et al. (1987) at Fuerteventura Island. Furthermore, naturally occurring Nd, Sr and O isotopes have been used as markers to identify the source region of transported mineral dust (Usher et al., 2003 and references therein).

In addition, other methods are currently being developed to apportion the amount of mineral dust due to Saharan dust outbreaks (Escudero et al., 2007; Ganor et al., 2009; Viana et al., 2010) based on the identification of desert dust inputs (back-trajectory analysis, satellite imagery and aerosol dust maps), receptor modelling or simply statistical data treatment of bulk PM_{10} measurements.

5.8 Future research

- The construction of an emission inventory map for Europe is recommended. However this is complicated due to the difficulties to carry out mineral dust emission measurements. These are caused by equipment issues (calibration, standardization) and the fact that dust emissions are highly variable in space and in time.
- Future studies should attempt to distinguish the origin of mineral dust (natural or anthropogenic) as these categories are useful to decision makers. Routine PM_{10}, $PM_{2.5}$ measurements do not provide much information on the source of mineral dust. More information could be provided by the extension of the sampling network with respect to mineral dust source areas.
- Addressing issues such as the size distribution of dust, the improvement of models that can result in more accurate prediction of dust transport, the environmental processes that affect dust generation in the source regions and the meteorological factors that control the dust transport.

5.9 Acknowledgements

Results presented here were obtained from studies supported by the Spanish Ministry of the Environment, Rural and Marine Affairs, by the Spanish Ministry of Science and Innovation (VAMOS CGL2010-19464/CLI, GRACCIE-CSD2007-00067) and the European Union (6th framework CIRCE IP, 036961, EUSAAR RII3-CT-2006-026140).

6 Measurements of particulate matter in the EECCA countries

By Karl Espen Yttri and Wenche Aas

The number of sites which report mass concentration of particulate matter (PM) to EMEP has increased steadily since this variable was implemented to the EMEP monitoring program in 1999 (EB.AIR/GE.1/1998/3/Rev.1). Unfortunately, these sites are not equally distributed throughout the EMEP monitoring network, and particularly the Eastern Mediterranean and the Eastern Europe, the Caucasus and Central Asia (EECCA) countries appears to be poorly represented.

The EECCA countries host a number of anthropogenic and natural sources which have the potential to cause both severe local and regional PM air pollution. Some of Europe’s largest agricultural land areas can be found in the EECCA countries. Agricultural activity, e.g. emissions from ploughing and off-road vehicles, is a well known source of ambient PM. While agricultural waste burning is banned in most western European countries, it is common practice in large parts of the world including the EECCA countries, thus likely to represent a substantial source of combustion aerosol. Indeed, several studies have shown how such emissions can substantially deteriorate the air-quality in Europe ranging from the Eastern-Mediterranean (Sciare et al., 2008) to the European Arctic (Stohl et al., 2007).

Further, countries bordering the Black Sea have particularly high SO_2 emissions, accounting for more than one third of the total SO_2 emissions reported over Europe in 2004 (Vestreng et al., 2007). According to Sciare et al. (2008) it is likely that levels of carbonaceous aerosol having the same origin as SO_2 will remain high the coming years. Large areas of the EECCA countries are semi-arid land which is subject to erosion. Subsequently the eroded material, i.e. mineral and soil dust, can be entrained into the atmosphere.

To help implementing the obligations under the EMEP protocol in the EECCA region, the work plan of EMEP (ECE/EB.AIR/WG.5/2010/16) specifically urge for enhanced cooperation between the EMEP centres, Task Forces and the countries in the region to improve the emission reporting as well as establishing monitoring and modelling activities. Thus in order to improve our current understanding of PM in this region, a one year measurement program funded by the Norwegian Ministry of Foreign Affairs has been initiated to determine the mass concentration of PM_{10} from ambient aerosol filter samples collected at four sites in Armenia, Georgia, Kazakhstan and Moldova. In addition to establish the mass concentration of PM_{10} the filter samples will also be subjected to analyses of elemental (EC) and organic carbon (OC), as well as the biomass burning tracer levoglucosan.

Here we present some preliminary results for PM_{10}, EC and OC from the sites in Armenia, Georgia and Kazakhstan. These preliminary results are from the first filters analyzed, which were selected based on what was assumed to be relatively low loading filters (based on visual inspection of the filters). Consequently, the results presented in Table 6.1 are possibly biased towards the lower concentration range. Further, the filters are collected during different time periods and thus reflecting conditions characteristic for different seasons.

Table 6.1: Mean concentrations of EC, OC, TC and PM_{10}, and the EC/TC ratio, in selected (assumed low PM loading) ambient aerosol filter samples at the sites Abastamani (Georgia), Borovoe (Kazakhstan) and Leova II (Moldova).

Site/Country	**Time period**	**n**	**EC**	**OC**	**TC**	**EC/TC**	**PM_{10}**
			µg C m^{-3}	**µg C m^{-3}**	**µg C m^{-3}**	**%**	**µg m^{-3}**
Abastumani/Georgia	Sept. 2010 - Feb 2011	18	0.46 ± 0.19	2.4 ± 1.1	2.9 ± 1.2	16 ± 4.7	12 ± 8.2
Borovoe/Kazahkstan	Apr 2010 – Jul 2010	12	0.45 ± 0.24	4.1 ± 1.4	4.5 ± 1.5	9.6 ± 3.0	18 ± 5.2
Leova II/Moldova	Oct 2010 - May 2011	11	0.60 ± 0.14	3.6 ± 1.8	4.2 ± 1.8	16 ± 4.1	20 ± 8.7

6.1 **Mass** concentration **of PM_{10}**

The mean PM_{10} mass concentration ranged from 12 ± 8.2 µg m^{-3} at the Abastumani site (Georgia) to 20 ± 8.7 µg m^{-3} at Leova II (Moldova). For the Borovoe and the Leova II sites, the mean concentration is well above the annual mean PM_{10} concentration (15.3 ± 5.9 µg m^{-3}; see Figure 6.1) for all EMEP sites reporting this variable for 2009, as well as they should be considered in the upper range. The somewhat lower concentrations observed for the Abastumani site (12 ± 8.2 µg m^{-3}) might be attributed to its rather high elevation; i.e. 1650 m asl. With the remaining filters being analyzed, as well as for the Armenian site Amberd, further insight to the PM_{10} mass concentrations levels and their seasonality will be gained.

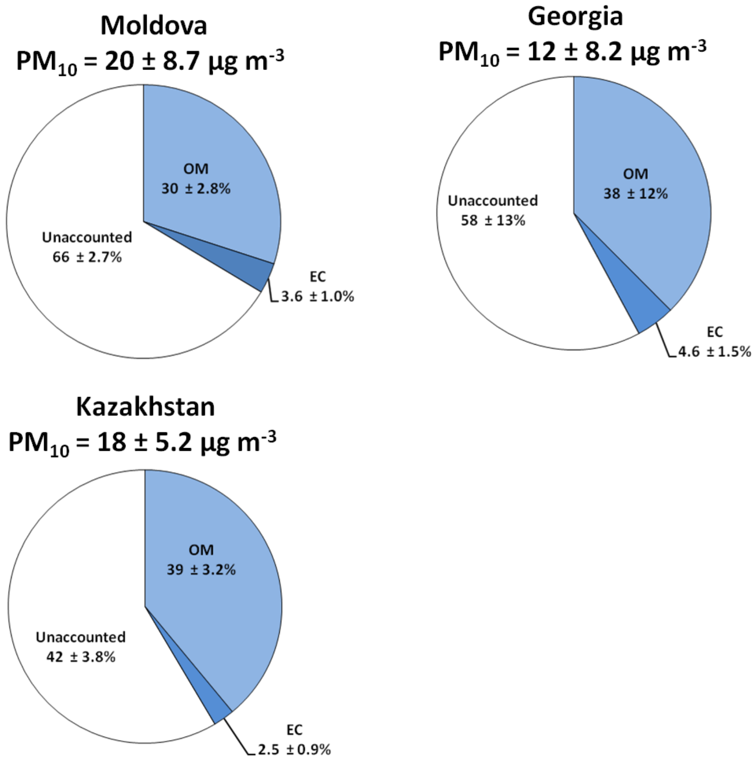

Figure 6.1: Relative contribution of OM (Organic matter = OC x 1.7) and EC (EC x 1.1) to PM_{10} for selected samples (likely low loading samples) collected at the sites Leova II (Moldova), Abastumani (Georgia), and Borovoe (Kazakhstan) during 2010 and 2011.

6.2 Concentration of EC and OC in PM_{10}

The mean EC concentrations did not differ much between the three sites, ranging from 0.45 ± 0.24 at Borovoe to 0.60 ± 0.14 at Leova II. This concentration range should be considered to be in the medium to the upper end of the annual mean EC concentrations reported for EMEP sites in 2009, ranging from 0.09 µg C m^{-3} to 1.4 µg C m^{-3} (see Table 2.6). The observed EC/TC ratios (9.6 – 16%) were comparable to that observed for the Scandinavian countries and the for high altitude sites in western/south-western Europe. The mean EC/TC ratio observed for the Borovoe site (9.6%), based on samples collected in spring/summer, was substantially less compared to the ratio observed for the two other sites (16%), which were based on filters collected during fall/winter. It is however not yet possible to draw conclusions concerning seasonal variability of the EC/TC ratio.

The variability of the mean OC concentration was wider than for EC, ranging from 2.4 ± 1.1 µg m^{-3} at Abastumani to 4.1 ± 1.4 µg m^{-3} at the Borovoe site. These levels are in the upper range of the annual mean concentrations reported for 2009 at EMEP sites (See Table 2.6), second only to the Ispra site. It should be noted that the samples were collected according to the quartz-behind-quartz set up, which makes it possible to estimate the positive sampling artifact attributed to semi-volatile OC, but that the mean concentrations reported in Table 6.1 not yet have been corrected for this.

The presence of carbonate (CO_3^{2-}) carbon is known to be detected by thermal-optical analysis (TOA) along with EC and OC, and thus has the potential to interfere with the EC/OC results. Depending on the thermal protocol used, the presence of carbonate will interfere with either OC or EC, or both. As carbonate appears to be present in low concentrations in the European rural background environment, although with some exceptions, it is not considered a major confounding factor for EC/OC analysis. However, for regions substantially influenced by mineral and soil dust, such as the EECCA countries, the potential presence of carbonate in the ambient aerosol should be addressed when performing TOA analysis.

Quantifying carbonate is important not only in order to get more correct figures for EC and OC. For mass closure exercises it is important as the conversion factor of carbonate-carbon to carbonate equals 5, which is a pretty high number, thus even low concentrations of carbonate could make a substantial contribution to the particulate mass. For source apportionment studies it is of course important that one avoid attributing carbonate-carbon to either OC or EC, but rather to the mineral dust fraction where it rightfully belongs. For the very few samples addressed with respect to the presence of carbonate, the results vary widely, from a relative contribution of carbonate-carbon to TC of 1.5% to 40%. Further, the results show that the carbonate in these samples evolves as both OC and EC. These results underpin the importance of the ongoing work concerning how to best address the presence of carbonate using the EUSAAR2 protocol.

As we currently do not know the amount of carbonate in each sample, what any likely conversion factor of OC to OM (Organic Matter) might be, calculating OM and subsequently finding the relative contribution of OM and EC to the mass concentration of PM_{10}, have to be associated with great uncertainty. Nevertheless an attempt has been made, using a conversion factor of 1.7 for OC to OM and 1.1 for EC. These calculations suggest that 2.5 – 4.6% of PM_{10} could be attributed to EC, where as the corresponding range for OM was 30 – 39%.

In addition to this one year campaign, these sites have regular EMEP level 1 measurements using filter pack samplers with a PM_{10} inlet to quantify the contribution of inorganic components in air. Data from Moldova, Kazakhstan (and Armenia) has been reported for 2009, though at Borovoe only nitrate and sulphate representing 50% of the year. These data are discussed and presented in the EMEP status report 1 (2011). The uncertainty in these inorganic measurements is relatively high, and they don’t represent the same period as the PM measurements. They are therefore hard to use to assess the contribution of inorganic components to the PM_{10} mass. Though using the annual average for 2009 from Moldova as an estimate, the SIA contribution (sulphate, nitrate and ammonium) is almost 40% of the PM_{10} mass at this site, while sea salt and base cations contribute with about 5% each.

7 Main uncertainties in the assessment of transboundary PM

By Svetlana Tsyro, Wenche Aas, Karl Espen Yttri and Martin Schultz

As in 2006 (EMEP, 2006), this report has a chapter devoted to the main uncertainties in the assessment of transboundary PM. The aim is to repeat this evaluation every five year to document the progress of the EMEP Programme.

Particulate matter (PM), which is known to cause adverse health effects including increased risk of death from cardiopulmonary diseases, and to interfere with the radiative balance, is currently not included in the Gothenburg protocol, but SO_2, NO_x, NH_3, and VOCs are all important precursors of PM formed in the atmosphere, hence the protocol has a positive effect on the ambient PM levels nevertheless. However, there is still a considerable fraction of PM (primary particles, secondary organic aerosols from both anthropogenic and biogenic sources, natural particles) that remains unaddressed. Thus, it would be an obvious step as well as a step forward to include also the regulation of anthropogenic primary particles under the Gothenburg Protocol. At present, negotiations are ongoing, with the aim to have a draft agreement ready for adoption before the end of 2011. The revised Gothenburg protocol is expected to set national emission ceilings for the already regulated species (SO_2, NO_x, NH_3, and VOCs) and to include PM (here: $PM_{2.5}$), to be achieved by 2020.

7.1 Uncertainties in PM model calculations

Three potential sources of uncertainties can be identified in model calculated PM_{10} and $PM_{2.5}$: 1. Uncertainties in emission data; 2. Imprecisions of meteorological data, and 3. Inaccuracies related to model description of dynamical and/or chemical processes due to incomplete understanding of those. The ultimate goal is that the model results reproduce the actual concentration fields of pollutants in the atmosphere, or in our case, the surface concentrations.

Typically, the correctness of model calculations is evaluated through comparison with observations and requires a good quality of observation data. Discrepancies between calculated and measured concentrations of PM and individual aerosol components can occur due to both erroneous model results as well as erroneous (poor quality) measurement data (measurement artefacts, sampling failure etc.). In addition, to ensure valid comparison between aerosol concentrations from model and observations, strictly comparable groups of components should be considered (further clarification and examples are given in the section).

1. Uncertainties in the EMEP emission data are discussed in chapter 1.1.4 though a major issue is related to incomplete reporting. Compared to the emissions of gaseous pollutants covered by the Gothenburg Protocol, fewer countries report emissions of primary PM. Further, of those countries that did report PM emission it is suspected not all Parties reported emissions from all sectors in which releases of PM are likely. Some of the sectors in which non-reporting appears common (e.g. agriculture or small combustion sources) may be significant sources with respect to national totals, In addition to the problem of incomplete national inventories, the emission factors used to develop the emission estimates are still a source of uncertainties. For the individual sectors, the largest uncertainties in the

PM emission inventories are reported to be due to fugitive emissions from industrial processes (e.g. metal production), quarrying, agriculture (agricultural soils, manure management etc.), constructions etc. Emission estimates for fuel combustion in transport, power production, industrial and commercial sectors are generally considered more reliable. However, significant uncertainties are associated with PM emissions from bio fuel combustion in the residential sector.

2. The sensitivity of EMEP model results to meteorological input data were in-depth discussed in last year's status report 1/2010 and summarised in the PM report (EMEP 2010). The effect of using three different meteorological drivers (PARLAM-PS, HIRLAM and ECMWF-IFS) on modelled concentrations was studied. One of the main findings was that the EMEP/MSC-W model calculated 20-30% lower aerosol concentrations when HIRLAM and ECMWF-IFS meteorology was used compared to calculations with PARLAM-PS. This was explained by more efficient upward transport and wet scavenging of the aerosols and precursors when using the meteorology from the first two models. The consequence of that was the greater underestimation of PM_{10} and $PM_{2.5}$ by the EMEP model, driven by HIRLAM and ECMWF-IFS meteorological data.

Clearly, our choice of meteorological driver for the EMEP/MSC-W should not solely be made based on how well the model performs. Among the criteria for meteorology selection, outlined in Report 4/2010, verification results of the meteorological model is a central one. A number of meteorological parameters, essential for a sound description of pollutants' dispersion and removal in the EMEP/MSC-W, can be quite different calculated with different meteorological models. Unfortunately, not all of the meteorological parameters can be verified with measurements, thus leaving us with inevitable uncertainties in the modelling of pollutants evolution in the atmosphere.

3. The EMEP/MSC-W model is a subject to continual development and improvement. Unfortunately, the current knowledge and understanding of many processes, controlling the evolution of pollutants in the atmosphere, is still insufficient. Furthermore, some processes are rather complex and/or happen on sub-grid scales, thus making their implementation in the regional model rather challenging. A rigorous evaluation of the model for varying meteorological and chemical conditions is needed for testing the soundness of process parameterisations. For this purpose, we analyse the performance of the EMEP/ MSC-W model for all EMEP sites for multiple years, as summarised in Table 7.1. It should be emphasised that the evaluation results in Table 7.1 do not represent a trend analysis as the number and the set of measurement stations are not exactly the same for all those years. Thus, they should be regarded as a robustness test of model results in the changing chemical and meteorological environments.

PM concentrations in Table 7.1 do not account for SOA contribution, and the effects of including SOA in PM on the model performance are discussed in Chapter 2.4. The performance of the EMEP/MSC-W model for PM_{10} and $PM_{2.5}$ compared to observations appears relatively stable for years from 2005 to 2009 as indicated by little changes in the Index of Agreement (IOA).

However, some variability is seen in the statistical parameters. The model underestimation varies between the lowest 32% for PM_{10} and 42% for $PM_{2.5}$ in 2006 and 41% for PM_{10} and 52% for $PM_{2.5}$ in 2009. In the same period, the spatial correlation is in the range of 0.44 to 0.72 for PM_{10} and 0.51 to 0.81 for $PM_{2.5}$. Unlike bias, the years with the best and worst correlation do not coincide for PM_{10} and $PM_{2.5}$.

A closer look at the scatter plots shows that the changes in correlation are often caused by model results for just a few sites. For example, a relatively low correlation for PM_{10} in 2006 is due to model underestimation for Czech CZ03 in combination with overestimation for Spanish ES17. The latter is likely due to overestimation of windblown dust as the same is not seen for $PM_{2.5}$. Somewhat larger negative biases for 2009 are partly due to two Latvian sites, which are thought to be frequently affected by some strong local sources, unaccounted for in the EMEP emission database (see Chapter 2.1.9).

Table 7.1: Summary of model performance for the years from 2005 to 2009.

		2005	2006	2007	2008	2009
PM_{10} excl. SOA	Bias (%)	-35	-32	-37	-39	-41
	R	0.65	0.44	0.72	0.59	0.62
	IOA	0.64	0.60	0.63	0.65	0.59
$PM_{2.5}$ excl. SOA	Bias (%)	-43	-42	-45	-49	-52
	R	0.81	0.64	0.78	0.51	0.78
	IOA	0.55	0.55	0.54	0.55	0.57
SO_4^{2-}	Bias (%)	-31	-31	-37	-41	-43
	R	0.76	0.77	0.64	0.63	0.74
	IOA	0.77	0.78	0.67	0.65	0.68
NO_3^-	Bias (%)	-2	-3	-1	1	-27
	R	0.83	0.87	0.77	0.65	0.85
	IOA	0.91	0.93	0.86	0.78	0.77
NH_4^+	Bias (%)	-25	-30	-30	-33	-39
	R	0.81	0.80	0.76	0.76	0.66
	IOA	0.84	0.81	0.78	0.76	0.63
Na^+	Bias (%)	18	2	7	3	-2
	R	0.92	0.83	0.85	0.89	0.83
	IOA	0.93	0.92	0.92	0.94	0.91

Being complex pollutants, PM_{10} and $PM_{2.5}$ in model results inherit the uncertainties from calculations of all their components (in addition to inaccuracies related to unaccounted components). Accurate calculations of all of the individual aerosol components is essential for ensuring reliable results for PM concentrations, chemical composition and the effect of different emission reduction policies. A short discussion concerning uncertainties in model calculations of individual PM components is given below.

7.2 SIA

Given a considerable contribution of secondary inorganic aerosols to PM_{10}, and particularly to $PM_{2.5}$ mass, it would be impossible to properly reproduce PM concentrations without accurately calculating SIA. Some ideas around uncertainties in SIA results are outlined below. Relevant to all SIA components, one important change as regards observations in 2009 should be flagged, namely the change of sampling instrumentation from filter-packs to low-volume samplers from 2008 to 2009 at Dutch sites. The consequences are quite higher SIA concentrations at the DUTCH sites in 2009 compared to 2008.

7.2.1 Sulphate aerosol SO_4^{2-}

Though the set of sites is not exactly the same, there is an increase in model underestimation for SO_4^{2-} from 2005 to 2009 (Table 7.1). The trend-series show that in some areas (for example at Polish, British, Finnish sites, and the Dutch ones because of the changes in sampling technique), the model calculated a larger than observed decrease in SO_4^{2-} concentrations. This might indicate that the rate of SO_2 oxidation has been increasing in some areas, whereas the model has not captured this process.

SO_4^{2-} is underestimated by 43% compared to observations in 2009. Several processes have been identified as potential reasons for SO_4^{2-} underestimation by the model. Among those are:

- Inadequate (out-of-dated) temporal profile of SO_x emissions with too large winter maximum (the winter to summer variation of SO_x emissions have flattened out during last decades).
- Decrease in cloud water acidity as a result of SO_x emissions reduction, which would enhance SO_2 to SO_4^{2-} heterogeneous oxidation. The pH=4.3 has been used in the model, whereas EMEP precipitation data give mean pH=5.55 in 2009 (though this value is not strictly representative for cloud water due to possible local contamination by base minerals). First model tests increasing pH from 4.3 to 5 reduced SO_4^{2-} bias from -43% to 19%.
- The contribution of SO_4^{2-} from sea spray can be considerable at coastal sites. Figure 7.1 shows scatterplots for model versus observed SO_4^{2-}, with and without accounting for sea spray contribution to calculated SO_4^{2-} concentrations (taken as 7.7% of calculated sea salt concentration). Accounting for sea spray SO_4^{2-} improves comparison of model result with observations with respect to both bias and correlation.

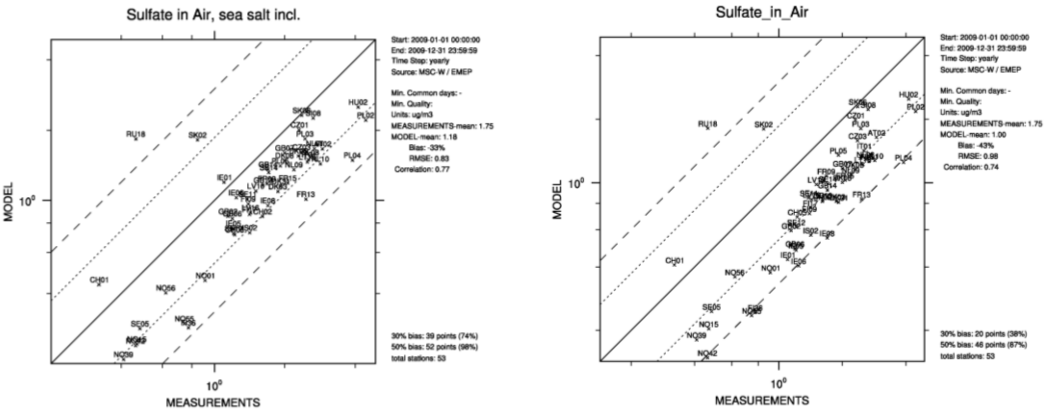

Figure 7.1: Scatterplots for model versus observed SO_4^{2-}, with (left) and without (right) accounting for SO_4^{2-} from sea spray.

7.2.2 Nitrate aerosol NO_3^-

Calculated NO_3^- concentrations agree quite well with observations for 2005-2008, but they are underestimated by 27% in 2009. This large negative model bias is largely the effect of very large (close to doubling) increase in measured NO_3^- at the Netherlands' sites, whereas the model calculates some NO_3^- decrease from 2008 to 2009. The reason for the large change in observed NO_3^- could be due to the sampling instrumentation change from filter-packs to low-volume samplers from 2008 to 2009 at the Dutch sites. The underestimation of NO_3^- is just 11-12% in the autumn and winter, increases to 35% in the summer and to 44% in the spring of 2009.

NO_3^- aerosol consists of fine and coarse particles, which are formed by different mechanisms. Most of fine NO_3^- is typically ammonium nitrate, whereas coarse NO_3^- is formed on sea salt and mineral particles. In the EMEP/MSC-W model, formation of ammonium nitrate in an equilibrium gas/aerosol partitioning between HNO_3 and NH_3 is calculated with the EQSAM model (Metzger et al., 2002). A rather simple parameterisation of coarse nitrate formation (on sea salt and dust particles) is presently implemented in the model, i.e. coarse NO_3^- is formed from remaining HNO_3 using a constant reaction rate and accounting for enhanced formation at a higher relative humidity. In order to identify inaccuracies in the modelling of specific processes, calculated concentrations of fine and coarse NO_3 should be individually evaluated against observations. Standard EMEP measurements with filter packs do not allow such individual evaluation, however EMEP intensive measurements in 2006-2007 provided data for NO_3^- in PM_{10} and $PM_{2.5}$ at several sites.

Comparison of calculated fine NO_3^- with measured NO_3^- in $PM_{2.5}$ ($NO_3^-\_PM_{2.5}$) indicates that the equilibrium parameterisation of ammonium nitrate formation tends to produce too unstable aerosols as ambient temperature rises, particularly in summer and daytime. Another uncertainty when comparing calculated fine NO_3^- with measured $NO_3^-\_PM_{2.5}$ could be due to that some of non-volatile $NaNO_3$ and $Ca(NO_3)_2$ may reside in $PM_{2.5}$ (Pakkanen, 1996). This can crudely be accounted for by assigning some of calculated coarse NO_3^- to $NO_3^-\_PM_{2.5}$, however the volume of this fraction is uncertain. Figure 7.2 shows time-series examples of observed NO_3^-_$PM_{2.5}$ and calculated fine NO_3^- and total (fine + coarse) NO_3^-. We anticipate that calculated NO_3^-_$PM_{2.5}$ lies somewhere between those fine and total NO_3^-, and show a time-series for calculated sum of the fine NO_3^- and 30% of the coarse NO_3^-. Calculated NO_3^-_$PM_{2.5}$ shows often a better than fine NO_3^- agreement with measured NO_3^-_$PM_{2.5}$, especially when EQSAM fails to form any ammonium nitrate (red curves) at all, as at IT04 after 12 June and at NO01 in June 2006 (Figure 7.2). However, there are also a number of cases when calculated NO_3^-_$PM_{2.5}$ overestimates observations, especially in colder conditions (January 2007).

Furthermore, underestimations of NO_3^- in the fine fraction can also be related to insufficiency of ammonia in NO_x rich areas. Partly this can be due to the uncertainties in NH_3 emissions or/and its insufficient long-range transport from the source areas. Also, a number of works have been showing that accounting for NH_3 compensation point increases NH_3 air concentrations due to its release by vegetation. This would consequently facilitate the formation of ammonium nitrate.

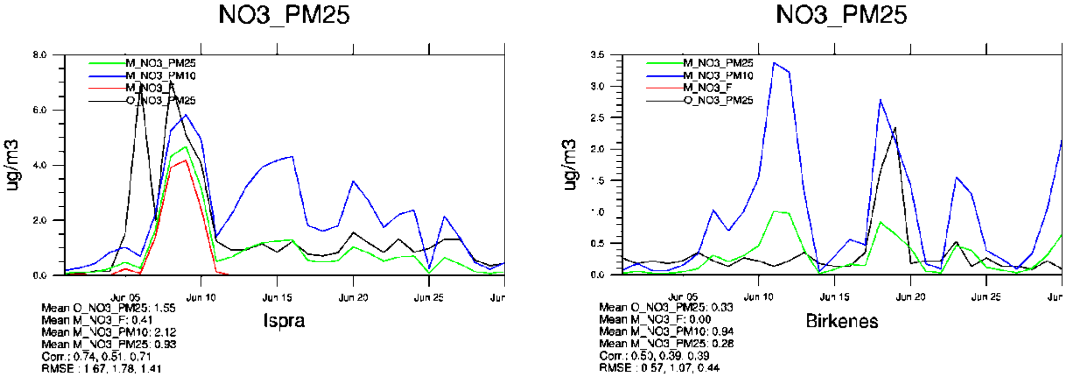

Figure 7.2: Time-series of observed NO_3^-_$PM_{2.5}$ (black) and calculated fine NO_3^- (red), NO_3^-_PM_{10} (blue), and NO_3^-_$PM_{2.5}$ derived as fine NO_3^- plus 30% of the coarse NO_3^- (green) for June 2006 at Ispra (IT04) and Birkenes (NO01).

One more possible source of discrepancies between calculated and observed NO_3^- can be mentioned. In ammonia emission areas, strong local ammonia gradients may occur close to the ground, enhancing ammonium nitrate formation. This ammonium nitrate will be measured (if the sites is located in such areas), but hardly captured by the model due to a sub-grid character of this process.

Among future developments of the model with respect to NO_3^- is the improvement of the description of NO_3^- formation on sea salt and mineral dust particles. This would also help to improve description of the size distribution of

7.2.3 Ammonium aerosol NH_4^+

Dependent on sulphate-to-ammonium ratio, NH_4^+ aerosol can be present as ammonium sulphate or/and ammonium nitrate. Thus, the main features of model performance for SO_4^{2-} and NO_3^- would also be reflected in its performance for NH_4^+.

Compared to observations, the model bias for NH_4^+ varies between -25 and -33% in 2005-2008, increasing similar to SO_4^{2-} and NO_3^- in 2009 to -39% (see above). The main reason for that is the underestimation of SO_4^{2-}, but also ammonium nitrate is underestimated, especially in the spring and summer.

7.3 Primary PM

Calculated with the EMEP/MSC-W model concentrations of primary PM are by far and large determined by the quality of emission data. It is practically infeasible to quantify the accuracy of primary PM concentrations from the model. However, one component of primary PM, namely elemental carbon (EC) can be compared with available (though rather scarce) measurements. Using EC and OC emission estimates from IIASA (Kupiainen and Klimont, 2007 and in EMEP Status Report 4/2010), the emissions of primary $PM_{2.5}$ and coarse PM (PM_{10} - $PM_{2.5}$) provided by CEIP are split to EC, primary organic carbon (POC) and remaining mineral dust. Model calculated EC are compared to EMEP observations available at six sites in 2009 (Figure 7.3).

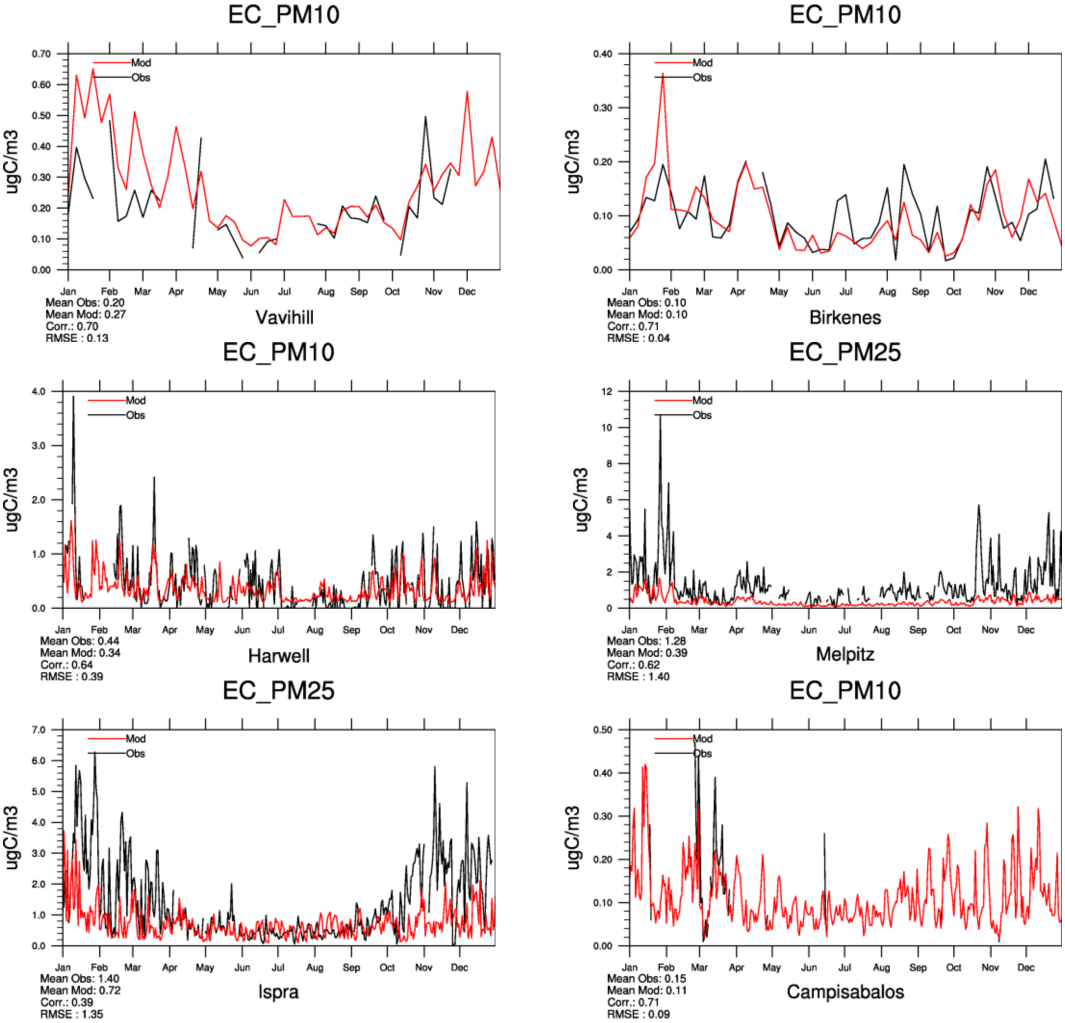

Figure 7.3: Time-series of calculated and measured EC in PM_{10} and $PM_{2.5}$ in 2009.

The results are in line with the findings reported earlier in Tsyro et al. (2007) and EMEP Reports 4/2006 and 4/2010. The model reproduces observed EC quite well in Northern Europe, shows some underestimation in the UK and the underestimation increases in Central and Southern Europe (note that only a rather short period with EC data is available for Campisábalos). At Melpitz (DE0044) and Ispra (IT0004), the large EC underestimations are seen in cold periods, which are thought to be due to underestimation of EC emissions from residential combustion (likely wood burning for heating of private houses). Actually, EC is underestimated at Mepitz during the whole year of 2009 which can also be related to uncertainties in road traffic emissions (at least in the spring-summer months).

One of the major uncertainties in modelling EC is associated with description of its life time. In this respect, the model do account for the ageing of EC from hydrophobic to hydrophilic. In the model, the freshly emitted hydrophobic EC does not get rained out from the clouds, which increases EC's lifetime and thus EC air concentrations.

7.4 Anthropogenic and Biogenic SOA

Recent advances in measurements techniques have made it possible to distinguish between formation of biogenic or anthropogenic SOA. For example, Szidat et al. (2006) used ^{14}C analysis to attribute the sources of aerosol to either 'fossil' carbon (from coal, oil) or 'modern' carbon (from recent vegetation, either by combustion or emissions). They found that fossil-fuel combustion accounted for only 30% of OC throughout the year, even in the city center of Zürich (Switzerland). Biomass burning in wintertime and SOA in summertime seemed to account for the majority of the remaining OC. Follow-up studies in Switzerland using a variety of techniques have confirmed the basic source patterns (Szidat et al., 2007; Lanz et al., 2007, 2008). Similar results from the EU CARBOSOL project (CARBOnaceous AeroSOLs over Europe, Legrand and Puxbaum, 2007). Wintertime residential-wood burning was found to be a significant contributor to measured particulate carbonaceous matter levels at all the sites, whereas in summertime, biogenic SOA (BSOA) was the dominant contributor. These data enabled for the first time an evaluation of the components (primary, secondary, anthropogenic, biogenic) of chemical transport model simulations (Simpson et al., 2007).

The modelling of SOA is however still very uncertain, for the simple reason that the mechanisms behind SOA formation are still speculative. Though there has been large development of this modelling activity the last years (Chapter 2.4). The new scheme includes secondary organic aerosol (SOA) formation, from biogenic and anthropogenic VOCs, and gas/particle partitioning of semi-volatile organic compounds, using the volatility basis set (VBS) approach (Simpson et al., 2009; Andersson-Sköld & Simpson, 2001; Simpson et al., 2007). Further examples of EMEP-VBS approaches were presented in Bergström and Simpson (2010) and Kulmala et al. (2011).

Summertime levels are quite well captured by some versions of the VBS scheme. It is hard however to know if the BVOC emissions which are the major summertime precursor to SOA are correct – there are significant uncertainties in European BVOC estimates (e.g. Rinne et al., 2009). There are problems matching wintertime OA levels, with the model in general underestimating. Some of these problems may stem from dispersion issues (in stable boundary layers), but there are signs that there are also problems with the emission inventories.

7.5 Natural sources of primary PM

7.5.1 Sea salt

In general, sea salt contribution to PM_{10} and especially to $PM_{2.5}$ is quite little at in-land locations, but it can significantly affect the air quality in coastal areas. Being of a natural origin itself, sea salt can act as a sink for anthropogenic and natural gases and thus alter the regional distribution of other inorganic aerosols. In particular, formation of coarse nitrate on sea salt particles is an important nitrate source.

Modelling of sea salt aerosol relies on the accuracy of sea spray production calculated with so-called source function. There are a number of source functions available from scientific literature; however their calculations of sea spray fluxes differ by orders of magnitude. Sea spray generation is to a large degree driven by wind velocity at 10m height. Therefore the resulting emissions are very sensitive to the wind speed values and thus strongly rely on the meteorological data used. Calculation of sea salt production in the EMEP/MSC-W model is based on parameterisations from Monahan et al. (1987) and Mårtensson et al. (2003). In-depth evaluation and sensitivity tests of sea salt calculations with the EMEP/MSC-W model can be found in Tsyro et al. (2011).

The present version of the EMEP/MSC-W model shows a good ability of reproducing observed sodium (Na^+) concentrations, derived as 30.6% of the calculated sea salt mass. The model calculated Na^+ is practically unbiased and quite well correlated with measured concentration for the years 2005-2009 (Table 7.1). This provides a good starting point for calculations of NO_3^- formation on sea salt particles.

One of the uncertainty sources in model calculated sea salt is a rather crude representation of its size distribution, which affects the accuracy of dry deposition calculations. The earlier model versions only distinguished between fine and coarse aerosols. This has been extended in the present version, so that three size fractions (i.e. fine, coarse and 'giant') are used now. This allowed improving of modelling of the lifetime of sea salt particles, which is also seen in a large improvement of Na^+ concentrations in precipitation (which was very under-estimated by the earlier model versions).

7.5.2 Windblown dust

Windblown dust is probably one of the most uncertain components in model calculations. This is not too surprising, as existing parameterisations of dust production, including the one in the EMEP/MSC-W model, strongly rely on several rather uncertain empirical parameters, whereas appropriate measurements to constrain model results are still lacking.

In the model, natural dust includes windblown dust produced within the calculation domain (based on works of Marticorena and Bergametti, 1995; Gomes et al., 2003; Zender et al., 2003) and Saharan dust described as boundary conditions (based on monthly dust concentrations in 2000 calculated with the global CTM2 model of the University of Oslo). The uncertainties in modelled concentrations of natural dust are both with respect to the time and location of dust emissions and to the magnitude of erosion dust produced. Calculated production of erosion dust is very sensitive to the input meteorological parameters and the information on soil properties. In particular, the threshold of dust generation onset is sensitive to soil moisture, which is taken from the meteorological model and is usually a very uncertain (and usually unverified) parameter.

The evaluation of model calculated mineral dust is presently hampered due to the lack of measurements. The only appropriate data were obtained in the course of EMEP intensive measurement periods in June 2006 and January 2007 at Montelibretti (IT01). The time-series in Figure 7.4 shows that the model manages to reproduce the main features of observed variations of dust concentrations. Calculated dust both in PM_{10} and $PM_{2.5}$ is overestimated by the model in June 2006, whereas it is underestimated in January 2007.

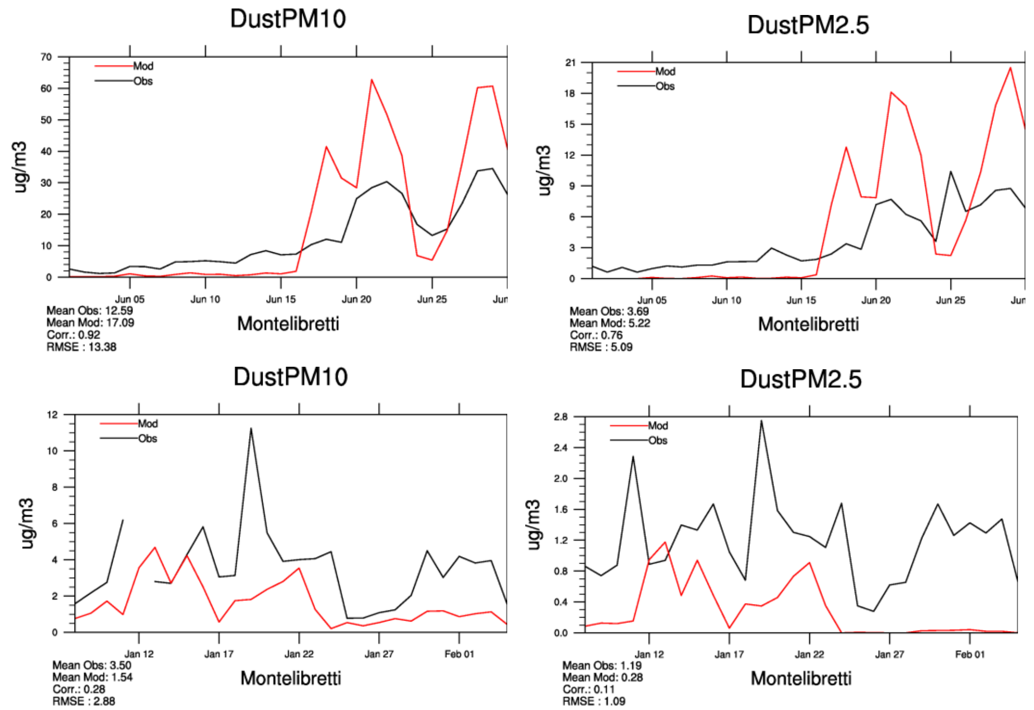

Figure 7.4: Timeseries of calculated and measured concetrations of mineral dust in PM_{10} and $PM_{2.5}$ at Montelibretti in June 2006 (upper panels) and January 2007 (lower panels).

To illustrate the improvement in PM calculations due to accounting for natural dust, 2009 time-series for PM_{10} and $PM_{2.5}$, with and without windblown dust in the model, at the Cypriot site Ayia Marina (Figure 7.5). The PM concentrations calculated including for windblown dust agree much better with observations. The model reproduces several of the high PM episodes due to dust intrusion which significantly improves correlation.

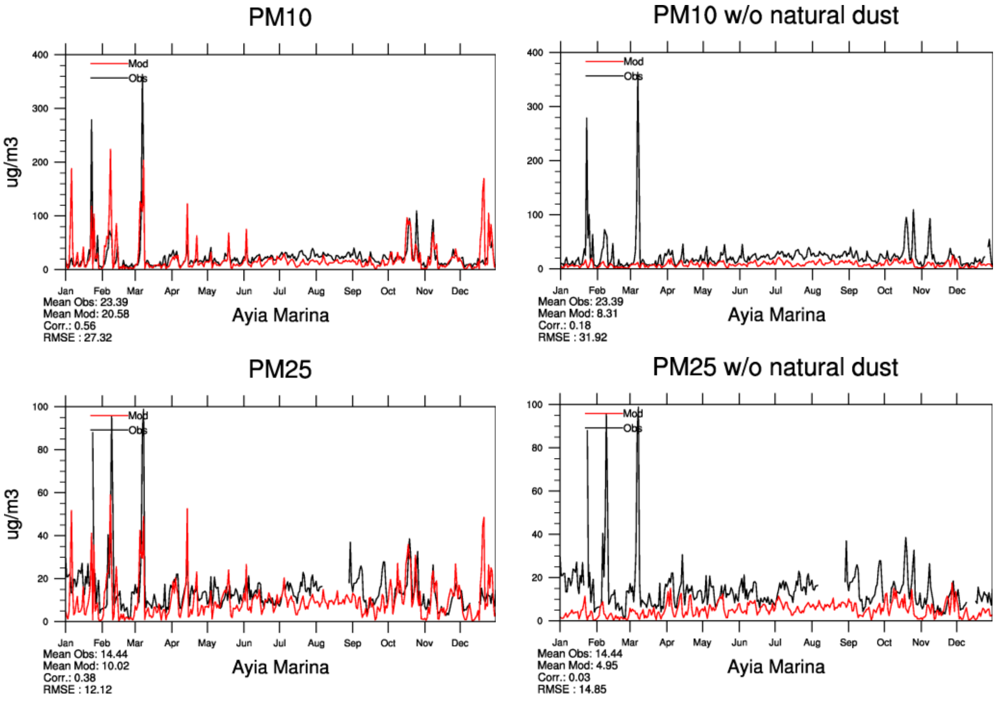

Figure 7.5: Time-series of calculated and observed PM_{10} and $PM_{2.5}$, with (left) and without (right) windblown dust in the model, at the Ayia Marina (CY02) for 2009.

7.5.3 Provisional evaluation of model with base cations

For the first time, we have compared model results with measurements of base cations in air, notably calcium (Ca^{2+}), magnesium (Mg^{2+}) and potassium (K^{+}). The EMEP/MSC-W model does not calculate the base cations in an explicit way; therefore their concentrations have been estimated from calculated concentrations of anthropogenic and natural dust and sea salt. Calculating the marine contribution to base cations, the composition sea salt aerosols are assumed to be the same as a typical composition of sea water. The coefficients for mineral dust are taken from a broad range of reported values and the same coefficients are applied to both natural and anthropogenic dust from all types of sources, which is a rather crude approach.

The scatterplots for modelled versus observed air concentrations of Ca^{2+}, Mg^{2+} and K^{+} for 2009 are shown in Figure 7.6 . The results of this first comparison appear quite promising. The scatterplots show that the model reproduces quite well the spatial distribution of Ca^{2+} and Mg^{2+}, but also K^{+} with the exception of a few outlying sites. This indicates that the location and the strength of the main emission sources (anthropogenic and windblown dust and sea salt), as well as their long-range transport, are described reasonably well. Using the coefficients given in the Figure 7.6 caption, we obtain a 40% underestimation for Ca^{2+}, 6% overestimation for Mg^{2+}, and 42% underestimation for K^{+}. In addition to a large uncertainty with respect to the content of these compounds in dust, the underestimation of K^{+} is probably also due to underestimations in biomass (wood) burning emissions.

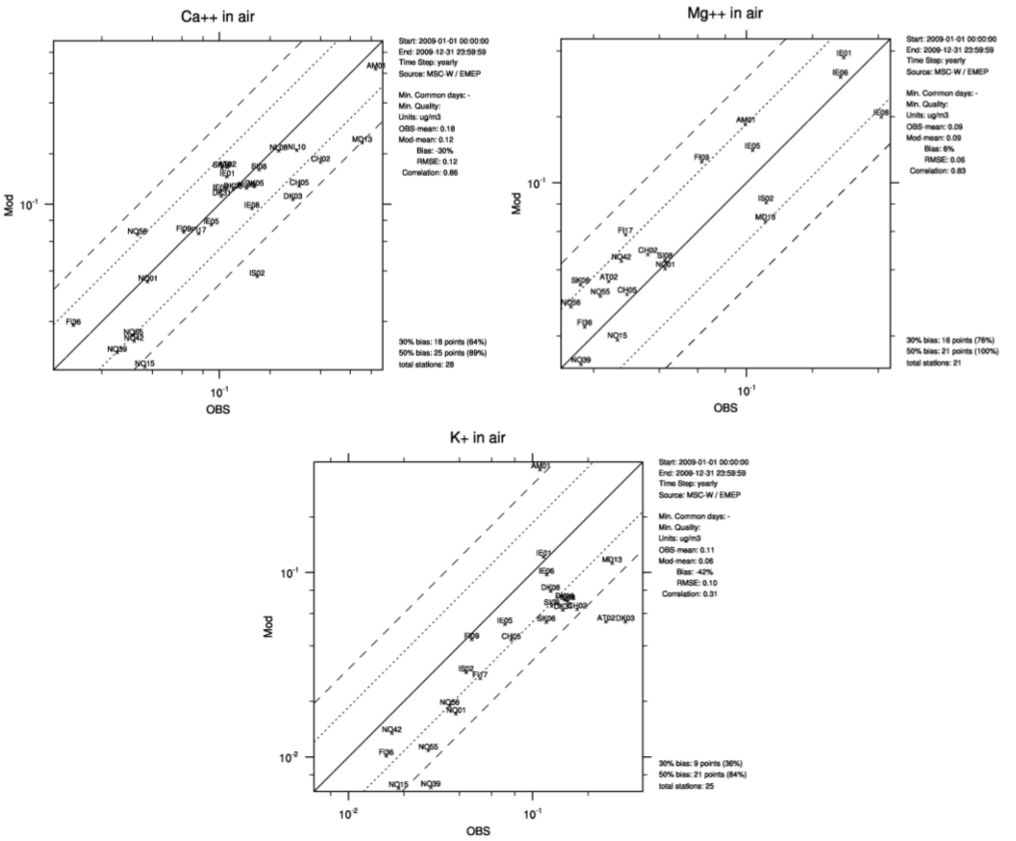

Figure 7.6: Scatterplots of calculated versus observed air concentrations of Ca^{2+}, Mg^{2+} and K^{+} for 2009. Calculated concentrations are derived from the EMEP/MSC_W model as the sums of: 5% of Natural dust, 8% of anthropogenic dust and 1.2% of sea salt for Ca^{2+}, 2 % of Natural dust, 0.8% of anthropogenic dust and 3.7% of sea salt for Mg^{2+}, and 4% of Natural dust, 1.8% of anthropogenic dust and 1.1% of sea salt for K^{+} (van Loon et al., 2005; Formenti et al., 2011).

7.5.4 Natural primary sources of OC

Natural sources of primary organic carbon contributing to ambient particulate matter can be divided into primary biological aerosol particles (PBAP) and carbonaceous aerosol originating from wildfires.

Despite advances over the last few years, our knowledge about the relative contribution from these sources to the ambient aerosol loading remains limited. There is currently no easy and efficient way of recognising and quantifying such aerosol in ambient air. This shortcoming, amongst others, has also excluded the possibility to validate model performance.

Primary biological aerosol particles (PBAP)

Definition:
Primary biological aerosol particles (PBAP) are defined as airborne solid particles (dead or alive) that are or were derived from living organisms, including micro-organisms and fragments of all varieties of living thing (e.g. viruses, bacteria,

algae, spores, pollen, plant debris, parts of insects, human and animal epithelial cells etc.) (Matthias-Maser, 1998).

Why of interest:

Certain PBAP are causes of allergenic reactions of humans, animals and plants and thus of interest. Another aspect for investigating PBAP is the part they play in cloud physics; While most particles need temperatures < –10ºC, certain PBAP have ice-nucleating (IN) capacity at temperatures about –4ºC, making it possible to initiate cloud forming processes even though the surroundings are super cooled (Matthias-Maser, 1998). A recent study by Hoose et al. (2010) shows that the simulated contribution of PBAPs to the global average ice nucleation rate has an uppermost estimate of no more than 0.6%.

Quantification:

There is no common or standardized way to quantify the level of PBAP in aerosol samples. Thus, knowledge about PBAP sources and their source strength has been limited, as well as knowledge concerning their seasonal and temporal variations.

Matthias-Maser (1998) used a combination of electron microscopy techniques (typically SEM) and certain staining schemes to quantify ambient air PBAP. This is a very time consuming approach and suitable only for a very limited number of samples. Within the past ten years a number of studies (e.g. Bauer et al., 2002; Graham et al., 2003; Puxbaum and Tenze-Kunit, 2003) have demonstrated that the aerosols content of sugars, sugar alcohols and cellulose can be used to trace, and quantify, certain types of PBAP [e.g. fungal spores and plant debris (primarily decaying leaf litter)]. Consequently, an increasing number of studies have reported the ambient air concentration of such molecules in the European rural background environment, but only a few studies (e.g. Gelencser et al., 2007; Gilardoni et al., 2011; Yttri et al., 2011a, b) have attempted to *quantify* the ambient air level of PBAP based on such tracers, and for a limited part of the EMEP domain only (findings are summarized in the following paragraph). PBAP are included in the Background-OC (BGND-OC) fraction of the EMEP model, which is supposed to account for the numerous sources of OC, which are not covered by the emissions. The BGND-OC concentrations are currently treated as reservoir species, with a constant concentration of 0.5 $\mu g\ m^{-3}$ all year around, regardless of the geographical situation of the site.

Emissions:

PBAP has typically been considered a minor source of primary particles, and for the year 2000 bioaerosols (> 1 micron in size) were thought to account for only 56 Tg/year compared to 3300 Tg/year for sea-salt and 2000 Tg/year for mineral dust (IPCC). Elbert et al. (2007) estimated that the global emission of fungal spores was 50 Tg yr^{-1} based on ambient concentrations of the fungal spore tracer mannitol. As fungal spores are only one category of PBAP (although likely a major one), the total PBAP concentration is likely substantially higher than the 50 Tg yr^{-1} estimated by Elbert et al. (2007.)

Levels:

Based on light and scanning microscopy, and staining of the samples content of PBAP, it has been reported that approximately 22% of the total aerosol volume of aerosols with a radius 0.2 to 50 micron was attributed to PBAP at a rural influenced urban site (Matthias-Maser, 1998), 10% for a marine environment (Matthias-Maser et al., 1999), and 30% for a remote continental environment (Matthias-Maser et al., 2000).

In the study by Gelencser et al. (2007) (CARBOSOL), plant debris accounted for 2-10% of OM (Organic Matter) in $PM_{2.5}$ at five European rural background sites on an annual basis. The estimates were based on the samples content of cellulose, thus an abundant fraction of PBAP such as fungal spores were not accounted for. Gilardoni et al. (2011) found that the contribution of fungal spores to TC in $PM_{2.5}$ was no more than approximately 1% at the rural background site Ispra in Northern Italy; plant debris was not accounted for. The sum of fungal spores and plant debris were found to account for 20-32% of TC in PM_{10} at five rural background sites in the Nordic rural background environment (Yttri et al., 2011a, b) during a one month sampling period in late summer.

The higher relative contribution of PBAB in the Nordic countries compared to continental Europe, which can be observed from the three abovementioned studies, can be attributed to the PM size fraction studied (i.e. $PM_{2.5}$ in continental Europe versus PM_{10} in the Nordic countries) as PBAP typically is larger than $PM_{2.5}$; that the study conducted in the Nordic rural environment took place during the vegetative season, whereas the studies for Continental Europe included all four seasons; and that the carbonaceous aerosol loading originating from other sources than PBAP (i.e. SOA and primary carbonaceous aerosol emissions of anthropogenic origin) is larger in continental Europe than in the Nordic countries.

Seasonal variation:
There appears to be a pronounced seasonal variation of PBAP with increased summer time levels, which also is reflected with respect to the relative contribution of PBAB to TC (Yttri et al., 2011 b). At Ispra however, an increased fungal spore concentration is observed in winter, however, the relative contribution to TC appears to be levelled out by increased levels of TC.

Size distribution:
Most studies report PBAP to reside in the coarse fraction, however PBAP range in size from a few tens of nanometres to millimetres, hence this can vary considerably depending on the source of PBAP. Studies reporting size distributions of sugars, sugar alcohols and cellulose, which are tracers of various types of PBAP, tend to show that they are associated primarily with the coarse fraction (Carvalho et al., 2003; Yttri et al., 2007), although occasions of the opposite have been reported (Carvalho et al., 2003); Puxbaum and Tenze-Kunit, 2003).

PBAP from the marine environment:
O’Dowd et al. (2004) showed that 65% of the mass of submicron marine aerosols at Mace Head could be accounted for by TOC (Total Organic Carbon) during the period of the year with high biological activity (high concentration of chlorophyll) in the North-Atlantic (spring-autumn). The corresponding percentage for the period with low biological activity (low concentration of chlorophyll) (winter-spring) in the North Atlantic was 15%. This TOC material was suggested to be of

primary origin, originating from biological material enriched in the oceanic surface layer, and transferred into the atmosphere by bubble bursting processes. They also found that the relative contribution of TOC was enriched with respect to decreasing particle size. In a recent study, Ceburnis et al. (2011) reported a predominant (80%) marine biogenic source for submicron carbonaceous aerosol in clean marine air over the North-East Atlantic. Analysis of model simulations performed by Gantt et al. (2011) showed that global annual submicron marine organic emission associated with sea spray was estimated to range from 2.8 to 5.6 Tg C yr^{-1}, providing additional evidence that the marine primary organic aerosol are a globally significant source of organics in the atmosphere.

7.6 Biomass burning/forest fires

Vegetation fires are a major source of carbonaceous aerosol in many world regions including Europe. On the global or hemispheric scale, European fire emissions are relatively low, but European air quality can be influenced by smoke plumes advected from large forest fires in North America or Siberia. There is less influence on particle concentrations over Europe from subtropical and tropical fires, although smoke plumes from fires in Northern Africa and Southern Asia can be advected into the Mediterranean region. Quantitative estimates of primary and secondary aerosol formation from fires is still very uncertain even though some progress was made recently by linking fire emission estimates that are derived from satellite observations to data assimilation of aerosol optical depth (see http://www.gmes-atmosphere.eu). Yet model studies are still inconclusive as to how much aerosol is produced from fires in Europe or advected into the region from fires outside Europe.

On the global scale, source estimates for average black carbon (BC) emissions vary by a factor of 5, while organic carbon (OC) emission estimates fall somewhat closer together (factor of 3). One of the major uncertainties is the emission factor, determining how much BC or OC is emitted per unit of dry fuel matter burned. There are indications that the commonly used BC emission factors from the tabulation of Andreae and Merlet (2001) are low by a factor of 2-3 (see Kaiser et al., 2011). While burned area statistics are rather complete for (Western) Europe, there is also considerable uncertainty (factor of 2 at least) about the area burned annually in boreal forest and tundra regions, particularly in Siberia. Existing estimates based on satellite data are often inconsistent, and aerial surveillance is far from complete. Further complications for accurately estimating aerosol emissions from fires in the northern hemisphere arise from the large inter-annual variability of these fires (about a factor of 10 variation of burned area from one year to the next), and from difficulties in estimating the fuel load and combustion efficiency correctly. A major factor in this respect is understory fires consuming large amounts of organic soil carbon. This has become prominent during the extreme fire situation around Moscow in July/August 2010. Assessing the impact of fire emissions with modelling tools faces other challenge besides obtaining accurate emission estimates: for example, the injection height of a fire plume is a critical parameter determining the subsequent spread and transport of the plume, and this parameter is poorly known at present. Considering the impact of fire emissions in the future, one must be aware of the fact that many fires are of human origin (on purpose, by arson, or accidentally), and fire severity can also be largely influenced by human behaviour (i.e. the increase in fuel load in North

American forests after 1960 due to strict fire prevention programs). Climate change is expected to play a role, in particular for boreal forests, where recent studies indicate a significant increase in future burned areas due to less rainfall and additional warming in higher latitudes.

7.7 Conclusions and recommendations

The amount and quality of the compiled information on emissions and measurements of PM has steadily increased in the last five years since the similar evaluation in 2006, and especially after such information began to be regularly compiled within EMEP in year 2000. Also the Unified EMEP model has undergone an extensive development with respect to PM representation in the last few years.

All this has increased the confidence in the assessment of transboundary PM. However, this field is especially challenging and considerable uncertainties remain. Continued developments in the basic scientific understanding are needed, as well as continued model development and evaluation against data are required in order to significantly improve the accuracy of transboundary PM estimates.

8 References

Alastuey, A., Querol, X., Castillo, S., Escudero, M., Avila, A., Cuevas, E., Torres, C., Romero, P.M., Exposito, F., Garcia, O., Diaz, J.P., Dingenen, R.V., Putaud, J.P. (2005) Characterisation of TSP and PM2.5 at Izaña and Sta. Cruz de Tenerife (Canary Islands, Spain) during a Saharan dust episode (July 2002). *Atmos. Environ., 39*, 4715-4728.

Amato, F., Pandolfi, M., Escrig, A., Querol, X., Alastuey, A., Pey, J., Perez, N., Hopke, P.K. (2009a) Quantifying road dust resuspension in urban environment by Multilinear Engine: A comparison with PMF2. *Atmos. Environ., 43*, 2770-2780.

Amato, F., Pandolfi, M., Viana, M., Querol, X., Alastuey, A., Moreno, T. (2009b) Spatial and chemical patterns of PM10 in road dust deposited in urban environment. *Atmos. Environ., 43,* 1650-1659.

Anderson, T.L., Covert, D.S., Marshall, S.F., Laucks, M.L., Charlson, R.J., Waggoner, A.P., Ogren, J.A., Caldow, R., Holm, R.L., Quant, F.R., Sem, G.J., Wiedensohler, A., Ahlquist, N.A., Bates, T.S. (1996) Performance characteristics of a high-sensitivity, three-wavelength, total scatter/backscatter nephelometer. *J. Atmos. Ocean. Technol., 13*, 967-986.

Anderson, T.L., Ogren, J.A. (1998) Determining aerosol radiative properties using the TSI 3563 integrating nephelometer. *Aerosol. Sci. Technol., 29*, 57-69.

Andersson-Sköld, Y., Simpson, D. (2001) Secondary organic aerosol formation in Northern Europe: a model study. *J. Geophys. Res., 106D*, 7357-7374.

Andreae, M.O., Merlet, P. (2001) Emission of trace gases and aerosols from biomass burning. *Global Biogeochem. Cycles*, *15*, 955-966.

Andreae, M.O., Rosenfeld, D. (2008) Aerosol-cloud-precipitation interactions. Part 1. The nature and sources of cloud-active aerosols. *Earth-Sci. Rev., 89*, 13-41.

Arimoto, R. (2001) Eolian dust and climate: relationships to sources, tropospheric chemistry, transport and deposition. *Earth-Sci. Rev., 54,* 29–42.

Arimoto, R., Ray, B.J., Lewis, N.F., Tomza, U., Duce, R.A. (1997) Mass-particle size distributions of atmospheric dust and the dry deposition of dust to the remote ocean. *J. Geophys. Res., 102D,* 15867-15874.

Àvila, A., Rodà, F. (2002) Assessing decadal changes in rainwater alkalinity at a rural Mediterranean site in the Montseny mountains (NE Spain). *Atmos. Environ., 36*, 2881-2890.

Barry, E., Ceburnis, D., McCusker, D. (2005) Major component composition of urban PM_{10} and $PM_{2.5}$ in Ireland. *Atmos. Res., 78,* 149-165.

Bauer, H., Kasper-Giebl, A., Loflund, M., Giebl, H., Hitzenberger, R., Zibuschka, F., Puxbaum, H. (2002) The contribution of bacteria and fungal spores to the organic carbon content of cloud water, precipitation and aerosols. *Atmos. Res., 64,* 109–119.

Bergametti, G., Dutot, A.L., Buat-Menard, P., Losno, R., Remoudaki, E. (1989) Seasonal variability of the elemental composition of atmospheric aerosol particles over the NW Mediterranean. *Tellus, 41B,* 353-361.

Bergström, R., Simpson, D. (2010) Organic aerosol modelling in EMEP: Recent developments. In: *Transboundary particulate matter in Europe. Status report 2010.* Kjeller, Norwegian Institute for Air Research (EMEP status report, 4/2010), pp. 54-58.

Blanco, A., De Tomasi, F., Filippo, E., Manno, D., Perrone, M.R., Serra, A., Tafuro, A.M., Tepore, A. (2003) Characterization of African dust over southern Italy. *Atmos. Chem. Phys., 3*, 2147-2159.

Bohren, C.F., Huffman, D.R. (1983) Absorption and scattering of light by small particles. New York, John Wiley & Sons, Inc.

Bond, T.C., Anderson, T.L., Campbell, D. (1999) Calibration and intercomparison of filter-based measurements of visible light absorption by aerosols. *Aerosol Sci. Tech., 30,* 582-600.

Brunekreef, B., Forsberg, B. (2005) Epidemiological evidence of effects of coarse airborne particles on health. *Eur. Respir. J., 26*, 309-318.

Caquineau, S., Gaudichet, A., Gomes, L., Magonthier, M.-C., Chatenet, B. (1998) Saharan dust: Clay ratio as a relevant tracer to assess the origin of soil-derived aerosols. *Geophys. Res. Lett., 25,* 983-986.

Carvalho, A., Pio, C., Santos, C. (2003) Water-soluble hydroxylated organic compounds in German and Finnish aerosols. *Atmos. Environ., 37,* 1775–1783.

Cavalli,F., Viana, M., Yttri, K.E., Genberg, J., Putaud, J.-P. (2010) Toward a standardised thermal-optical protocol for measuring atmospheric organic and elemental carbon: the EUSAAR protocol. *Atmos. Meas. Tech., 3,* 79–89.

Ceburnis, D., Garbaras, A., Szidat, S., Rinaldi, M., Fahrni, S., Perron, N., Wacker, L., Leinert, S., Remeikis, V., Facchini, M.C., Prevot, A.S.H., Jennings, S. G., O'Dowd, C.D. (2011) Quantification of the carbonaceous matter origin in submicron marine aerosol particles by dual carbon isotope analysis. *Atmos. Chem. Phys. Discuss., 11*, 2749–2772.

Chiapello, I., Bergametti, G., Gomes, L., Chatenet, B., Dulac, F., Pimenta, J., Suares, E.S. (1995) An additional low layer transport of Sahelian and Saharan dust over the North-Eastern Tropical Atlantic. *Geophys. Res. Lett., 22*, 3191-3194.

Coude-Gaussen, G., Rognon, P., Bergametti, G., Gomes, L., Strauss, B., Gros, J.M., Le Coustumer, M.N. (1987) Saharan dust on Fuerteventura Island (Canaries): chemical and mineralogical characteristics, air mass trajectories, and probable sources. *J. Geophys. Res., 92D,* 9753-9771.

Dayan, U., Heffter, J., Miller, J., Gutman, G. (1991) Dust intrusion events into the Mediterranean Basin. *J. Appl. Meteorol., 30,* 1185-1199.

Denier van der Gon, H., Jozwicka, M., Hendriks, E, Gondwe, M, Schaap M. (2010) Mineral dust as a component of particulate matter. Report of the Netherlands Research Program on Particulate Matter (BOP). Bilthoven, PBL Netherlands Environmental Assessment Agency (Report 500099003).

Dentener, F.J., Carmichael, G.R., Zhang, Y., Leleieveld, J., Crutzen, P.J. (1996) Role of mineral aerosols as a reactive surface in the global troposphere. *J. Geophys. Res., 101D,* 22869-22889.

Donahue, N., Robinson, A., Stanier, C., Pandis, S. (2006) Coupled partitioning, dilution, and chemical aging of semivolatile organics. *Environ. Sci. Technol., 40*, 2635-2643.

Dusek, U., Frank, G.P., Hildebrandt, L., Curtius, J., Schneider, J., Walter, S., Chand, D., Drewnick, F., Hings, S., Jung, D., Borrmann, S., Andreae, M.O. (2006) Size matters more than chemistry for cloud nucleating ability of aerosol particles. *Science, 312,* 1375-1378.

EEA (2009) Proposed gap-filling procedure for the European Community LRTAP Convention emission inventory. Technical paper for the meeting of the Air and Fuels Committee under Directive 96/62/EC, concerning 'Information on the Member States' reporting under the National Emission Ceilings Directive 2001/81/EC'. 28 September 2009, Brussels. European Environment Agency. Available upon request.

EEA/CEIP (2011) Inventory review 2011 stage 1 and 2 and review of gridded data. By Mareckova, K., Wankmueller, R., Tista M. Vienna, EEA/CEIP (in prep.).

Elbir, T. (2003) Comparison of model predictions with the data of an urban air quality monitoring network in Izmir, Turkey. *Atmos. Environ., 37,* 2149-2157.

EMEP (2006) Transboundary particulate matter in Europe. Kjeller, Norwegian Institute for Air Research (EMEP CCC & MSC-W Status Report 4/2006).

EMEP (2011) Transboundary acidification, eutrophication and ground level ozone in Europe in 2009. Oslo, Norwegian Meteorological Institute (EMEP MSC-W & CCC & CEIP Status Report 1/2011).

Elbert, W., Taylor, P.E., Andreae, M.O., Pöschl, U. (2007) Contribution of fungi to primary biogenic aerosols in the atmosphere: wet and dry discharged spores, carbohydrates, and inorganic ions. *Atmos. Chem. Phys., 7,* 4569–4588.

Erel, Y., Dayan, U., Rabi, R., Rudich, Y., Stein, M. (2006) Trans boundary transport of pollutants by atmospheric mineral dust. *Environ. Sci. Technol., 40,* 2996-3005.

Escudero, M., Castillo, S., Querol, X., Avila, A., Alarcón, M., Viana, M.M., Alastuey, A., Cuevas, E., Rodríguez, S. (2005) Wet and dry African dust episodes over Eastern Spain. *J. Geophys. Res., 110,* D18S08, doi:10.1029/2004JD004731.

Escudero, M., Querol, X., Pey, J., Alastuey, A., Perez, N., Ferreira, F., Alonso, S., Rodriguez, S., Cuevas, E. (2007) A methodology for the quantification of the net African dust load in air quality monitoring networks. *Atmos. Environ., 41,* 5516-5524.

ETC (2010) Reporting on ambient air quality assessment in the EU Member States, 2008. Bilthoven, European Topic Centre for Climate and Air Quality. (ETC/ACC Technical Paper 2010/11).

Fagerli, H., Simpson, D., Tsyro, S. (2004) Unified EMEP model: Updates. In: *Transboundary acidification, eutrophication and ground level ozone in Europe.* Oslo, Norwegian Meteorological Institute (EMEP Status Report 1/2004). pp. 11-18.

Formenti, P., Schütz, L., Balkanski, Y., Desboeufs, K., Ebert, M., Kandler, K., Petzold, A., Scheuvens, D., Weinbruch, S., Zhang D. (2011) Recent progress in understanding physical and chemical properties of African and Asian mineral dust. *Atmos. Chem. Phys.*, *11*, 8231-8256.

Gantt, B., Meskhidze, N., Facchini, M.C., Rinaldi, M., Ceburnis, D., O'Dowd, C. (2011) Wind speed dependent size-resolved parameterization for the organic enrichment of sea spray. *Atmos. Chem. Phys. Discuss*., *11*, 10525-10555.

Ganor, E., Stupp, A., Alpert, P. (2009) A method to determine the effect of mineral dust aerosols on air quality. *Atmos. Environ., 43*, 5463-5468.

Gelencser, A., May, B., Simpson, D., Sánchez-Ochoa, A., Kasper-Giebl, A., Puxbaum, H., Caseiro, A., Pio, C., Legrand, M. (2007) Source apportionment of $PM_{2.5}$ organic aerosol over Europe: primary/secondary, natural/anthropogenic, fossil/biogenic origin. *J. Geophys. Res., 112,* D23S04, doi:10.1029/2006JD008094.

Genberg, J., Hyder, M., Stenström, K., Bergström, R., Simpson, D., Fors, E., Jönsson, J.Å., Swietlicki, E. (2011) Source apportionment of carbonaceous aerosol in southern Sweden. *Atmos. Chem. Phys. Discuss., 11*, 13575-13616.

Gerasopoulos, E., Kouvarakis, G., Babasakalis, P., Vrekoussis, M., Putaud, J.-P., Mihalopoulos, N. (2006) Origin and variability of particulate matter (PM10) mass concentrations over the Eastern Mediterranean. *Atmos. Environ., 40*, 4679-4690.

Gilardoni, S., Vignati, E., Cavalli, F., Putaud, J.P., Larsen, B.R., Karl, M., Stenström, K., Genberg, J., Henne, S., Dentener, F. (2011) Better constraints on sources of carbonaceous aerosols using a combined 14C -- macro tracer analysis in a European rural background site. *Atmos. Chem. Physics, 11,* 5685-5700.

Gomes, L., Arrue, J.L., Lopez, M.V., Sterk, G., Richard, D., Gracia, R., Sabre, M., Gaudichet, A., Frangi, J.P. (2003) Wind erosion in a semiarid agricultural area of Spain: the WELSONS project. *Catena, 52,* 235-256.

Graham, B., Guyon, P., Maenhaut, W., Taylor, P., Ebert, M., Matthias-Maser, S., Mayol- Bracero, O., Godoi, R., Artaxo, P., Meixner, F., Moura, M., Rocha, C., Van Grieken, R., Glovsky, M., Flagan, R., Andreae, M.(2003) Composition and diurnal variability of the natural Amazonian aerosol. *J. Geophys. Res*., *108,* D24, doi:10.1029/2003JD004049.

Guerzoni, S., Molinaroli, E., Chester, R. (1997) Saharan dust inputs to the western Mediterranean Sea: depositional patterns, geochemistry and sedimentological implications. *Deep-Sea Res. II, 44,* 631-654.

Hjellbrekke, A.-G., Fjæraa, A.M. (2011) Data Report 2009 Acidifying and eutrophying compounds and particulate matter. Kjeller (EMEP/CCC-Report 1/2011).

Hoose, C., Kristjánsson., J. E., Burrows, S.M. (2010) How important is biological ice nucleation in clouds on a global scale? *Environ. Res. Lett*., *5,* 024009, doi: 10.1088/1748-9326/5/2/024009.

Hueglin, C., Gehrig, R., Baltensperger, U., Gysel, M., Monn, C., Vonmont, H. (2005) Chemical characterisation of $PM_{2.5}$, PM_{10} and coarse particles at urban, near-city and rural sites in Switzerland. *Atmos. Environ., 39,* 637-651.

IPCC (2007) Climate Change 2007: The physical science basis, Contribution of Working Group I to the fourth assessment report of the IPCC. Ed. by S. Salomon et al. Cambridge, Cambridge Univ. Press.

Kaiser, J.W., Heil, A., Andreae, M.O., Benedetti, A., Chubarova, N., Jones, L., Morcrette, J.-J., Razinger, M., Schultz, M.G., Suttie, M., van der Werf, G.R. (2011) Biomass burning emissions estimated with a global fire assimilation system based on observed fire radiative power. *Biogeosciences Discuss*., *8,* 7339-7398.

Kallos, G., Astitha, M., Katsafados, P., Spyrou, C. (2007) Long-Range Transport of Anthropogenically and Naturally Produced particulate matter in the Mediterranean and North Atlantic: Current State of Knowledge. *J. Appl. Meteorol. Climatol., 46,* 1230-1251.

Kocak, M., Mihalopoulos, N., Kubilay, N. (2007) Contributions of natural sources to high PM_{10} and $PM_{2.5}$ events in the eastern Mediterranean. *Atmos. Environ., 41*(18), 3806-3818.

Koulouri, E., Saarikoski, S., Theodosi, C., Markaki, Z., Gerasopoulos, E., Kouvarakis, G., Mäkelä, T., Hillamo, R., Mihalopoulos, N. (2008) Chemical composition and sources of fine and coarse aerosol particles in the Eastern Mediterranean. *Atmos. Environ., 42*, 6542-6550.

Kulmala, M., Asmi, A., Lappalainen, H.K., Baltensperger, U., Brenguier, J.-L., Facchini, M.C., Hansson, H.-C., Hov, Ø., O'Dowd, C.D., Pöschl, U., Wiedensohler, A., Boers, R., Boucher, O., de Leeuw, G., Denier van den Gon, H., Feichter, J., Krejci, R., Laj, P., Lihavainen, H., Lohmann, U., McFiggans, G., Mentel, T., Pilinis, C., Riipinen, I., Schulz, M., Stohl, A., Swietlicki, E., Vignati, E., Amann, M., Amann, M., Alves, C., Arabas, S., Artaxo, P., Beddows, D.C.S., Bergström, R., Beukes, J.P., Bilde, M., Burkhart, J.F., Canonaco, F., Clegg, S., Coe, H., Crumeyrolle, S., D'Anna, B., Decesari, S., Gilardoni, S., Fischer, M., Fjæraa, A.M., Fountoukis, C., George, C., Gomes, L., Halloran, P., Hamburger, T., Harrison, R.M., Herrmann, H., Hoffmann, T., Hoose, C., Hu, M., Hõrrak, U., Iinuma, Y., Iversen, T., Josipovic, M., Kanakidou, M., Kiendler-Scharr, A., Kirkevåg, A., Kiss, G., Klimont, Z., Kolmonen, P., Komppula, M., Kristjánsson, J.-E., Laakso, L., Laaksonen, L., Labonnote, A., Lanz, V.A., Lehtinen, K.E.J., Makkonen, R., McMeeking, G., Merikanto, J., Minikin, A., Mirme, S., Morgan, W.T., Nemitz, E., O'Donnell, D., Panwar, T.S., Pawlowska, H., Petzold, A., Pienaar, J.J., Pio, C., Plass-Duelmer, C., Prévôt, A.S.H., Pryor, S., Reddington, C.L., Roberts, G., Rosenfeld, D., Schwarz, J., Seland, Ø., Sellegri, K., Shen, X.J., Shiraiwa, M., Siebert, H., Sierau, B., Simpson, D., Sun, J.Y., Topping, D., Tunved, P., Vaattovaara, P., Vakkari, V., Veefkind, J.P., Visschedijk, A., Vuollekoski, H., Vuolo, R., Wehner, B., Wildt, J., Woodward, S., Worsnop, D.R, Zadelhoff, G.-J. van, Zardini, A.A., Zhang, K., Zyl, P.G. van, Kerminen, V.-M., Carslaw, K.S., Pandis, S.N. (2011) General overview: European Integrated project on Aerosol Cloud Climate and Air Quality interactions (EUCAARI) – integrating aerosol research from nano to global scales. *Atmos. Chem. Phys. Discuss., 11,* 17941-18160.

Kupiainen, K., Klimont, Z. (2007) Primary emissions of fine carbonaceous particles in Europe. *Atmos. Environ., 41*, 2156-2170.

Lall, R., Thrurston, G.D. (2006) Identifying and quantifying transported vs. local sources of New York City $PM_{2.5}$ fine particulate matter air pollution. *Atmos. Environ., 40,* S333-S346.

Lane, T.E., Donahue, N.M., Pandis, S.N. (2008) Simulating secondary organic aerosol formation using the volatility basis-set approach in a chemical transport model. *Atmos. Environ., 42,* 7439-7451.

Lanz, V.A., Alfarra, M.R., Baltensperger, U., Buchmann, B., Hueglin, C., Szidat, S., Wehrli, M.N., Wacker, L., Weimer, S., Caseiro, A., Puxbaum, H., Prevot, A.S.H. (2008) Source attribution of submicron organic aerosols during wintertime inversions by advanced factor analysis of aerosol mass spectra. *Environ. Sci. Technol., 42*, 214–220, 5 doi:10.1021/es0707207.

Legrand, M., Puxbaum, H. (2007) Summary of the CARBOSOL project: present and retrospective state of organic versus inorganic aerosol over Europe. *J. Geophys. Res., 112,* D23S01, doi:10.1029/2006JD008271.

Lee, S.-H., Murphy, D.M., Thomson, D.S., Middlebrook, A.M. (2002) Chemical components of single particles measured with Particle Analysis by Laser Mass Spectrometry (PALMS) during the Atlanta SuperSite Project: Focus on organic/sulfate, lead, soot, and mineral particles. *J. Geophys. Res., 107,* D4003, doi:10.1029/2000JD000011.

Lenschow, P., Abraham, H.J., Kutzner, K., Lutz, M., Preu, J.D., Reichenbacher, W. (2001) Some ideas about the sources of PM_{10}. *Atmos. Environ., 35,* suppl.1, S23-S33.

Levin, Z., Ganor, E., Gladstein, V. (1996) The effects of desert particles coated with sulfate on rain formation in the Eastern Mediterranean. *J. Appl. Meteorol., 35,* 1511-1523.

López, M.V., Sabre, M., Gracia, R., Arrue, J.L., Gomes, L. (1998) Tillage effects on soil surface conditions and dust emission by wind erosion in semiarid Aragon (NE Spain). *Soil Tillage Res., 45*, 91-105.

Maenhaut, W., Cafmeyer, J. (1998) Long-term atmospheric aerosol study at urban and rural sites in Belgium using multi-elemental analysis by particle-induced X-ray emission spectrometry and short-irradiation instrumental neutron activation analysis. *X-ray Spectrom., 27*, 236-246.

Maenhaut, W., Francois, F., Ptasinski, J., Mertens, S.F., Hanssen, J.E. (2000) Five-year study of the atmospheric aerosol composition, sources and chemical mass closure at two sites in southern Norway. *J. Aerosol Sci., 31,* S180-S181.

Marenco, F., Bonasoni, P., Calzolari, F., Ceriani, M., Chiari, M., Cristofanelli, P., D'Alessandro, A., Fermo, P., Lucarelli, F., Mazzei, F., Nava, S., Piazzalunga, A., Prati, P., Valli, G., Vecchi, R. (2006) Characterization of atmospheric aerosols at Monte Cimone, Italy during summer 2004: Source apportionment and transport mechanisms. *J. Geophys. Res., 111*, D24202, doi:10.1029/2006JD007145.

Marinoni, A., Laj, P., Deveau, P.A., Marino, F., Ghermandi, G., Aulagnier, F., Cachier, H. (2005) Physicochemical properties of fine aerosols at Plan d'Aups during ESCOMPTE. *Atmos. Res., 74,* 565-580.

Marticorena, B., Bergametti, G. (1995) Modeling the atmospheric dust cycle: 1. design of a soil-derived dust emission scheme. *J. Geophys. Res*., *100*, 16415–16430.

Matthias-Maser, S. (1998) Primary biological aerosol particles: their significance, sources, sampling methods and size distribution in the atmosphere. In: *Atmospheric Particles*. Ed. by R.M. Harrison, and R. van Grieken. Chichester, John Wiley & Sons. pp. 349–368.

Matthias-Maser, S., Brinkmann, J., Schneider, W., (1999) The size distribution of marine atmospheric aerosol with regard to primary biological aerosol particles over the South Atlantic Ocean. *Atmos. Environ*., *33*, 3569-3575.

Matthias-Maser, S., Reichert, K., Jaenicke, R. (2000) Primary biological aerosol particles at the high alpine site of Jungfraujoch/Switzerland. *J. Aerosol Sci., 31*, S955–S956.

McArthur, L.J.B., Halliwell, D.H., Niebergall, O.J., O'Neill, N.T., Slusser, J.R., Wehrli, C. (2003) Field comparison of network sunphotometers. *J. Geophys. Res., 108D,* 4596, doi:10.1029/2002JD002964.

Metzger, S.M., Dentener, F.J., Lelieveld, J., Pandis, S.N. (2002) Gas/aerosol partitioning: I. A computationally efficient model, *J. Geophys. Res*., *107*, No. D16, doi:10.1029/2001JD001102.

Middleton, N., Yiallouros, P., Kleanthous, S., Kolokotroni, O., Schwartz, J., Dockery, D.W., Demokritou, P., Koutrakis, P. (2008) A 10-year time-series analysis of respiratory and cardiovascular morbidity in Nicosia, Cyprus: The effect of short-term changes in air pollution and dust storms. *Environ. Health, 7,* art. no. 39.

Mitsakou, C., Kallos, G., Papantoniou, N., Spyrou, C., Solomos, S., Astitha, M., Housiadas, C. (2008) Saharan dust levels in Greece and received inhalation doses. *Atmos. Chem. Phys., 8,* 7181-7192.

Monahan, E.C., Spiel, D.E., Davidson, K.L. (1986) A model of marine aerosol generation via whitecaps and wave disruption. In: *Oceanic whitecaps*. Ed. by E.C. Monahan and G. MacNiochaill. Norwell, Mass, Reidel. pp.167-174.

Moreno, T., Amato, F., Querol, X., Alastuey, A., Gibbons, W. (2008) Trace element fractionation processes in resuspended mineral aerosols extracted from Australian continental surface materials. *Australian J. Soil Res., 46,* 128-140.

Moulin, C., Lambert, E., Dayan, U., Masson, V., Ramonet, M., Bousquet, P., Legrand, M., Balkanski, Y.J., Guelle, W., Marticorena, B., Bergametti, G., Dulac, F. (1998) Satellite climatology of African dust transport in the Mediterranean atmosphere. *J. Geophys. Res., 103D,* 13137-13144.

Müller, T., Nowak, A., Wiedensohler, A., Sheridan, P., Laborde, M., Covert, D.S., Marinoni, A., Imre, K., Henzing, B., Roger, J.-C., Martins dos Santos, S., Wilhelm, R., Wang, Y.-Q., de Leeuw, G. (2009) Angular illumination and truncation of three different integrating nephelometers: implications for empirical, size-based corrections. *Aerosol Sci. Tech., 43*, 581-586.

Mårtensson, E.M., Nilsson, E.D., de Leeuw, G., Cohen, L.H., Hansson, H.-C. (2003) Laboratory simulations and parameterisation of the primary marine aerosol production. *J. Geophys. Res., 108D*, 4297, doi:10.1029/2002JD00226.

O'Dowd, C.D., Facchini, M.C., Cavalli, F., Ceburnis, D., Mircea, M., Decesari, S., Fuzzi, S., Yoon, Y.J., Putaud, J.-P. (2004) Biogenically-driven organic contribution to marine aerosol. *Nature, 431*, 676–680.

Oldeman, L.R. (1994) Global extent of soil degradation. In: *Soil resilience and sustainable land use.* Ed. by D.J. Greenland and I. Szabolcs. Wallingford, CAB International, pp. 99-118.

Pakkanen, T.A. (1996) Study of formation of coarse particle nitrate aerosol. *Atmos. Environ., 30*, 2475-2482.

Pérez, L., Medina-Ramón, M., Künzli, N., Alastuey, A., Pey, J., Perez, N., Garcia, R., Tobias, A., Querol, X., Sunyer, J. (2009) Size fractionated particulate matter, vehicle traffic, and case-specific daily mortality in Barcelona (Spain). *Environ. Sci. Technol., 43*, 4707-4714.

Pérez, L., Tobias, A., Künzli, N., Pey, J., Querol, X., Alastuey, A., Viana, M., Valero, N., González-Cabré, M., Sunyer, J. (2008a) Coarse particles from Saharan dust and daily mortality. *Epidemiology, 19,* 800-807.

Pérez, N., Castillo, S., Pey, J., Alastuey, A., Viana, M., Querol, X. (2008b) Interpretation of the variability of regional background aerosols in the Western Mediterranean. *Sci. Total Environ., 407,* 527-540.

Perrino, C., Canepari, S., Catrambone, M., Dalla Torre, S., Rantica, E., Sargolini, T. (2008) Influence of natural events on the concentration and composition of atmospheric particulate matter. *Atmos. Environ., 43,* 4754-4765.

Petzold, A., Schönlinner, M. (2004) Multi-angle absorption photometry—a new method for the measurement of aerosol light absorption and atmospheric black carbon. *J. Aerosol Sci., 35*, 421-441.

Pey, J., Perez, N., Castillo, S., Viana, M., Moreno, T., Pandolfi, M., Lopez-Sebastian, J.M., Alastuey, A., Querol, X. (2009) Geochemistry of regional background aerosols in the Western Mediterranean. *Atmos. Res., 94*, 422-435.

Pio, C.A., Legrand, M., Oliveira, T., Afonso, J., Santos, C., Caseiro, A., Fialho, P., Barata, F., Puxbaum, H., Sanchez-Ochoa, A., Kasper-Giebl, A., Gelencsér A., Preunkert, S., Schock. M. (2007) Climatology of aerosol composition (organic versus inorganic) at non-urban areas on a west-east transect across Europe. *J. Geophys. Res., 112,* D23S02, doi:10.1029/2006JD008038.

Pósfai, M., Molnár, A. (2000) Aerosol particles in the troposphere: a mineralogical introduction. In: *Environmental Mineralogy*. Ed. By David J. Vaughan & Roy A. Wogelius. Budapest, University Press, pp. 197-252.

Prospero, J.M., Ginoux, P., Torres, O., Nicholson, S.E., Gill, T.E. (2002) Environmental characterization of global sources of atmospheric soil dust identified with the Nimbus 7 Total Ozone Mapping Spectrometer (TOMS) absorbing aerosol product. *Rev. Geophys., 40*, 1002, doi:10.1029/2000RG000095.

Prospero, J.M., Nees, R.T. (1986) Impact of the North African drought and El Niño on mineral dust in the Barbados trade winds. *Nature*, *320*, 735-738.

Putaud, J.-P., Raes, F., Van Dingenen, R., Brueggemann, E., Facchini, M.C., Decesari, S., Fuzzi, S., Gehrig, R., Hueglin, C., Laj, P., Lorbeer, G., Maenhaut, W., Mihalopoulos, N., Mueller, K., Querol, X., Rodriguez, S., Schneider, J., Spindler, G., ten Brink, H., Tørseth, K., Wiedensohler, A. (2004) European aerosol phenomenology-2: chemical characteristics of particulate matter at kerbside, urban rural and background sites in Europe. *Atmos. Environ., 38,* 2579–2595.

Putaud, J.-P., Van Dingenen, R., Alastuey, A., Bauer, H., Birmili, W., Cyrys, J., Flentje, H., Fuzzi, S., Gehrig, R., Hansson, H.C., Harrison, R.M., Herrmann, H., Hitzenberger, R., Hüglin, C., Jones, A.M., Kasper-Giebl, A., Kiss, G., Kousa, A., Kuhlbusch, T.A.J., Löschau, G., Maenhaut, W., Molnar, A., Moreno, T., Pekkanen, J., Perrino, C., Pitz, M., Puxbaum, H., Querol, X., Rodriguez, S., Salma, I., Schwarz, J., Smolik, J., Schneider, J., Spindler, G., ten Brink, H., Tursic, J., Viana, M., Wiedensohler, A., Raes, F. (2010) A European aerosol phenomenology - 3: Physical and chemical characteristics of particulate matter from 60 rural, urban, and kerbside sites across Europe. *Atmos. Environ., 44*, 1308-1320.

Puxbaum, H., Gomiscek, B., Kalina, M., Bauer, H., Salam, A., Stopper, S., Preining, O., Hauck, H. (2004) A dual site study of $PM_{2.5}$ and PM_{10} aerosol chemistry in the larger region of Vienna, Austria. *Atmos. Environ., 38*, 3949-3958.

Puxbaum, H., Tenze-Kunit, M. (2003) Size distribution and seasonal variation of atmospheric cellulose. *Atmos. Environ., 37*, 3693–3699.

Querol, X., Alastuey, A., Moreno, T., Viana, M.M., Castillo, S., Pey, J., Rodríguez, S., Artiñano, B., Salvador, P., Sánchez, M., Garcia Dos Santos, S., Herce Garraleta, M.D., Fernandez-Patier, R., Moreno-Grau, S., Negral, L., Minguillón, M.C., Monfort, E., Sanz, M.J., Palomo-Marín, R., Pinilla-Gil, E., Cuevas, E., de la Rosa, J., Sánchez de la Campa, A. (2008) Spatial and temporal variations in airborne particulate matter (PM_{10} and $PM_{2.5}$) across Spain 1999-2005. *Atmos. Environ., 42*, 3964-3979.

Querol, X., Alastuey, A., Pey, J., Cusack, M., Pérez, N., Mihalopoulos, N., Theodosi, C., Gerasopoulos, E., Kubilay, N., Kocak, M. (2009a) Variability in regional background aerosols within the Mediterranean. *Atmos. Chem. Phys., 9*, 4575-4591.

Querol, X., Pey, J., Pandolfi, M., Alastuey, A., Cusack, M., Pérez, N., Moreno, T., Viana, M., Mihalopoulos, N., Kallos, G., Kleanthous, S. (2009b) African dust contributions to mean ambient PM_{10} mass-levels across the Mediterranean Basin. *Atmos. Environ., 43*, 4266-4277.

Querol, X., Alastuey, A., Puicercus, J. A., Mantilla, E., Miro, J. V., Lopez-Soler, A., Plana, F., Artiñano, B. (1998a) Seasonal evolution of suspended particles around a large coal-fired power station: particulate levels and sources. *Atmos. Environ., 32*, 1963–1978.

Querol, X., Alastuey, A., Lopez-Soler, A., Plana, F. Puicercus, J.A., Ruiz, C.R., Mantilla, E., Juan, R. (1998b) Seasonal evolution of atmospheric suspended particles around a coal-fired power station: chemical characterization. *Atmos. Environ., 32,* 719-731.

Querol, X., Alastuey, A., Rodríguez, S., Plana, F., Ruiz, C.R., Cots, N., Massagué, G., Puig, O. (2001) PM_{10} and $PM_{2.5}$ source apportionment in the Barcelona Metropolitan Area, Catalonia, Spain. *Atmos. Environ., 35/36,* 6407-6419.

Querol, X., Alastuey, A., Ruiz, C.R., Artinano, B., Hansson, H.C., Harrison, R.M., Buringh, E., Ten Brink, H.M., Lutz, M., Bruckmann, P., Straehl, P., Schneider, J. (2004) Speciation and origin of PM_{10} and $PM_{2.5}$ in selected European cities. *Atmos. Environ., 38,* 6547-6555.

Rinne, J., Back, J., Hakola, H. (2009) Biogenic volatile organic compound emissions from the Eurasian taiga: current knowledge and future directions. *Boreal Environ. Res., 14,* 807-826.

Rodrıguez, S., Querol, X., Alastuey, A., Kallos, G., Kakaliagou, O. (2001) Saharan dust contributions to PM_{10} and TSP levels in Southern and Eastern Spain. *Atmos. Environ., 35,* 2433-2447.

Rodriguez, S., Querol, X., Alastuey, A., Viana, M. M., Mantilla, E. (2003) Events affecting levels and seasonal evolution of airborne particulate matter concentrations in the Western Mediterranean. *Environ. Sci. Technol., 37,* 216-222.

Rodriguez, S., Querol, X., Alastuey, A., Viana, M.M., Alarcón, M., Mantilla, E., Ruiz, C.R. (2004) Comparative PM10–PM2.5 source contribution study at rural, urban and industrial sites during PM episodes in Eastern Spain. *Sci. Total Environ., 328,* 95-113.

Salvador, P., Artíñano, B., Querol, X., Alastuey, A., Costoya, M. (2007) Characterisation of local and external contributions of atmospheric particulate matter at a background coastal site. *Atmos. Environ., 41,* 1-17.

Schneider, J., Lorbeer, G. (2002) Inhaltstoffe von PM_{10}- und $PM_{2,5}$ an zwei Mess-Stationen. Wien, Umweltbundesamt (Berichte BE-208). **URL:** http://www.umweltbundesamt.at/fileadmin/site/publikationen/BE208.pdf. [2011-07-28]

Schütz, L. (1989) Atmospheric mineral dust. Properties and source markers. In: *Paleoclimatology and Paleometeorology*. *Modern and past patterns of global atmospheric transport.* Ed. by M. Leinen and M. Sarnthein. Dordrecht, The Netherlands, Kluwer, pp 359–384.

Sciare, J., Oikonomou, K., Favez, O., Liakakou, E., Markaki, Z., Cachier, H., Mihalopoulos, N. (2008) Long-term measurements of carbonaceous aerosols in the Eastern Mediterranean: evidence of long-range transport of biomass burning. *Atmos. Chem. Phys., 8,* 5551-5563.

Seaton, A., MacNee, W., Donaldson, K., Godden, D. (1995) Particulate air pollution and acute health effects. *Lancet, 345,* 176-178.

Shrivastava, M.K., Lane, T.E., Donahue, N.M., Pandis, S.N., Robinson, A.L. (2008) Effects of gas particle partitioning and aging of primary emissions on urban and regional organic aerosol concentrations. *J. Geophys. Res., 113,* D18301, doi:10.1029/2007JD009735.

Simpson, D., Yttri, K.E., Bergström, R., Denier van der Gon, H., Tørseth, K. *(ed.)* (2009) Modelling SOA in EMEP: Experiments with the VBS Approach. In: *Transboundary Particulate Matter in Europe.* Kjeller, Norwegian Institute for Air Research (EMEP Status Report 4/2009). pp. 58-63.

Simpson et al. (2011) The EMEP MSC-W Chemical Transport Model I: Model Description. *In prep.*

Simpson, D., Fagerli, H., Jonson, J. E., Tsyro, S., Wind, P., Tuovinen, J.-P. (2003) Transboundary acidification, eutrophication and ground level ozone in Europe. Part I. Unified EMEP model description. Oslo, Norwegian Meteorological Institute (EMEP/MSC-W Status report 1/2003 Part I). **URL:** http://www.emep.int. [2011-07-28].

Simpson, D., Yttri, K., Bergström, R., Denier van der Gon, H., Tørseth, K. (ed.) (2004) Modelling SOA in EMEP: experiments with the VBS approach. In: *Transboundary particulate matter in Europe.* Kjeller, Norwegian Institute for Air Research (EMEP Status Report 4/2004), pp. 58-63.

Simpson, D., Yttri, K., Klimont, Z., Kupiainen, K., Caseiro, A., Gelencsér, A., Pio, C., Legrand, M. (2007) Modeling carbonaceous aerosol over Europe. Analysis of the CARBOSOL and EMEP EC/OC campaigns. *J. Geophys. Res., 112,* D23S14, doi:10.1029/2006JD008158.

Sjödin, Å., Ferm, M., Björk, A., Rahmberg, M., Gudmundsson, A., Swietlicki, E., Johansson, C., Gustafsson, M., Blomqvist, G. (2010) WEAREM Wear particles from road traffic - a field, laboratory and modelling study. Göteborg, IVL Swedish Environmental Research Institute (IVL report B1830).

Spindler, G., Brüggemann, E., Gnauk, T., Grüner, A., Müller, K., Tuch, Th.M., Wallasch, M.B., Wehner, A., Herrmann, H. (2007) Size-segregated physical and chemical long-time characterization of particles depending from air mass origin at German lowlands (Saxony, Melpitz site). In: *EMEP Particulate Matter Assessment Report, Part B, Annex A.* Kjeller, Norwegian Institute for Air Research (EMEP/CCC-Report 8/2007), pp. 178-221.

Stohl, A., Berg, T., Burkhart, J.F., Fjǽraa, A.M., Forster, C., Herber, A., Hov, Ø., Lunder, C., McMillan, W.W., Oltmans, S., Shiobara, M., Simpson, D., Solberg, S., Stebel, K., Ström, J., Tørseth, K., Treffeisen, R., Virkkunen, K., Yttri, K.E. (2007) Arctic smoke – record high air pollution levels in the European Arctic due to agricultural fires in Eastern Europe in spring 2006. *Atmos. Chem. Phys., 7,* 511-534.

Szidat, S., Jenk, T. M., Synal, H.-A., Kalberer, M., Wacker, L., Hajdas, I., Kasper-Giebl, A., Baltensperger, U. (2006) Contributions of fossil fuel, biomass burning, and biogenic emissions to carbonaceous aerosols in Zurich as traced by 14C. *J. Geophys. Res., 111,* D07206, doi:10.1029/2005JD006590.

Szidat, S., Prevot, A.S.H., Sandradewi, J., Alfarra, M.R., Synal, H.-A., Wacker, L., Baltensperger, U. (2007) Dominant impact of residential wood burning on particulate matter in Alpine valleys during winter. *Geophys. Res. Lett., 34,* L05820, doi:10.1029/2006GL028325.

Taylor, S.R., McLennan, S.M. (1995) The geochemical evolution of the continental crust. *Rev. Geophys., 33*, 241-265.

Tsyro, S. (2008) Regional model for formation, dynamics, and long-range transport of atmospheric aerosol. *Russ. Meteorol. Hydrol., 33*, 82-90.

Tsyro, S., Simpson, D., Tarrasón, L., Klimont, Z., Kupiainen, K., Pio, C., Yttri, K.E. (2007) Modelling of elemental carbon over Europe. *J. Geophys. Res., 112*, D23S19, doi:10.1029/2006JD008164.

Tsyro, S., Aas, W., Soares, J,. Sofiev, M., Berge, H., Spindler, G. (2011) Modelling of sea salt pollution over Europe: key uncertainties and comparison with observations. *Atmos. Chem. Phys. Discuss.*, *11*, 11143-11204.

UNECE (2007) Methods and procedures for the technical review of air pollutant emission inventories reported under the convention and its protocols. Geneva (EB.AIR/GE.1/2007/16). **URL:** http://live.unece.org/fileadmin/DAM/env/documents/2007/eb/ge1/ece.eb.air.ge.1.2007.16.e.pdf. [2011-07-28]

UNECE (2009) Guidelines for reporting emission data under the Convention on Long-Range Transboundary Air Pollution. Geneva (ECE/EB.AIR/97). **URL:** http://www.ceip.at/fileadmin/inhalte/emep/reporting_2009/Rep_Guidelines_ECE_EB_AIR_97_e.pdf. [2011-07-28]

Usher, C.R., Michel, A.E., Grassian, V.H. (2003) Reactions on mineral dust. *Chem. Rev.*, *103*, 4883-4939.

van Loon, M., Tarrason, L., Posch, M. (2005) Modelling base cations in Europe. Oslo, Norwegian Meteorological Institute (EMEP/MSC-W Technical Report 2).

Van Loy, M., Bahadori, T., Wyzga, R., Hartsell, B., Edgerton, E. (2000) The aerosol research and inhalation epidemiology study (ARIES): $PM_{2.5}$ mass and aerosol component concentrations and sampler intercomparisons. *J. Air Waste Manag. Assoc., 50*, 1446-1458.

Vestreng, V. Myhre, G. Fagerli, H., Reis, S., Tarrasón, L. (2007) Twenty-five years of continuous sulphur dioxide emission reduction in Europe. *Atmos. Chem. Phys., 7*, 3663-3681.

Viana, M., Querol, X., Alastuey, A., Cuevas, E., Rodríguez, S. (2002) Influence of African dust on the levels of atmospheric particulates in the Canary Islands air quality network. *Atmos. Environ.*, *36*, 5861-5875.

Viana, M., Querol, X., Alastuey, A., Ballester, F., Llop, S., Esplugues, A., Fernández-Patier, R., García Dos Santos, S., Herce, M.D. (2008) Characterising exposure to PM aerosols for an epidemiological study. *Atmos. Environ.*, *42*, 1552-1568.

Viana, M., Salvador, P., Artíñano, B., Querol, X., Alastuey, A., Pey, J., Latz, A.J., Cabanas, M., Moreno, T., Santos, S.G.D., Herce, M.D., Hernandez, P.D., Garcia, D.R., Fernández-Patier, R. (2010) Assessing the performance of methods to detect and quantify African dust in airborne particulates. *Environ. Sci. Technol., 44*, 8814-8820.

Virkkula, A., Aurela, M., Hillamo, R., Makela, T., Pakkanen, T., Kerminen, V.-M., Maenhaut, W., François, F., Cafmeyer, J. (1999) Chemical composition of atmospheric aerosol in the European subarctic: Contribution of the Kola Peninsula smelter areas, Central Europe, and the Arctic Ocean. *J. Geophys. Res., 104D*, 23681-23696.

Visser, H., Buringh, E., van Breugel, P.B. (2001) Composition and origin of airborne particulate matter in the Netherlands. Bilthoven, National Institute for Public Health and the Environment (RIVM report 650010029).

Warren, A. (2003) Wind erosion on agricultural land in Europe. Brussels, European Commission, Directorate-General for Research.

Wedepohl, H.K. (1995) The composition of the continental crust. *Geochim. Cosmochim. Acta, 59*, 1217-1232.

WHO (2005) Air quality guidelines for particulate matter, ozone, nitrogen dioxide and sulfur dioxide - Global update 2005. Copenhagen, World Health Organization. **URL:** http://www.who.int/phe/health_topics/outdoorair_aqg/en/ [2011-08-16].

Wiedensohler, A., Birmili, W., Nowak, A., Sonntag, A., Weinhold, K., Merkel, M., Wehner, B., Tuch, T., Pfeifer, S., Fiebig, M., Fjæraa, A.M., Asmi, E., Sellegri, K., Depuy, R., Venzac, H., Villani, P., Laj, P., Aalto, P., Ogren, J.A., Swietlicki, E., Roldin, P., Williams, P., Quincey, P., Hüglin, C., Fierz-Schmidhauser, R., Gysel, M., Weingartner, E., Riccobono, F., Santos, S., Grüning, C., Faloon, K., Beddows, D., Harrison, R.M., Monahan, C., Jennings, S.G., O'Dowd, C.D., Marinoni, A., Horn, H.-G., Keck, L., Jiang, J., Scheckman, J., McMurry, P.H., Deng, Z., Zhao, C.S., Moerman, M., Henzing, B., de Leeuw, G. (2010) Particle mobility size spectrometers: harmonization of technical standards and data structure to facilitate high quality long-term observations of atmospheric particle number size distributions. *Atmos. Meas. Tech. Discuss., 3*, 5521-5587.

Winther, M., Nielsen, O.-K. (2011) Technology dependent BC and OC emissions for Denmark, Greenland and the Faroe Islands calculated for the time period 1990-2030. *Atmos. Environ.*, doi:10.1016/j.atmosenv.2011.06.066 (accepted for publication).

Wu, P.-M., Okada, K. (1994) Nature of coarse nitrate particles in the atmosphere - A single particle approach. Atmos. Environ., 28, 2053-2060.

Yin, J., Allen, A.G., Harrison, R.M., Jennings, S.G., Wright, E., Fitzpatrick, M., Healy, T., Barry, E., Ceburnis, D., McCusker, D. (2005) Major component composition of urban PM_{10} and $PM_{2.5}$ in Ireland. *Atmos. Res., 78*, 149-165.

Yin, J., Harrison, R.M. (2008) Pragmatic mass closure study for PM1.0, PM2.5 and PM10 at roadside, urban background and rural sites. *Atmos. Environ., 42*, 980–988.

Yttri, K.E. (2007) Concentrations of particulate matter (PM_{10}, $PM_{2.5}$) in Norway. Annual and seasonal trends and spatial variability. In: *EMEP Particulate Matter Assessment Report, Part B, Annex A.* Kjeller, Norwegian Institute for Air Research (EMEP/CCC-Report 8/2007), pp. 292-307.

Yttri, K.E., Aas, W., Bjerke, A., Ceburnis, D., Dye, C., Emblico, L., Facchini, M.C., Forster, C., Hanssen, J.E., Hansson, H.C., Jennings, S.G., Maenhaut, W., Putaud, J. P., Tørseth, K. (2007) Elemental and organic carbon in PM_{10}: a one year measurement campaign within the European Monitoring and Evaluation Programme EMEP. *Atmos. Chem. Phys., 7,* 5711-5725.

Yttri, K.E., Simpson, D., Nøjgaard, J.K., Kristensen, K., Genberg, J., Stenström, K., Swietlicki, E., Hillamo, R., Aurela, M., Bauer, H., Offenberg, J.H., Jaoui, M., Dye, C., Eckhardt, S., Burkhart, J.F., Stohl, A., Glasius, M. (2011a) Source apportionment of the summer time carbonaceous aerosol at Nordic rural background sites. *Atmos. Chem. Phys. Discuss., 11,* 16369-16416.

Yttri, K.E., Simpson, D., Stenström, K., Puxbaum, H. Svendby, T. (2011b**)** Source apportionment of the carbonaceous aerosol in Norway – quantitative estimates based on ^{14}C, thermal-optical and organic tracer analysis. *Atmos. Chem. Phys. Discuss., 11,* 7375-7422.

Yttri, K.E., Simpson, D., Prevot, A., Szidat, S., Ceburnis D., Hueglin, C,. Kiss, G., Noeygaard, J.K., Putaud, J.P. Spindler, G., Vana, M., Perrini, C., Aas, W. (2011 in progress) Source apportionment of the carbonaceous aerosol at European rural background sites.

Zabalza, J., Ogulei, D., Hopke, P.K., Lee, J.H., Hwang, I., Querol, X., Alastuey, A., Santamaría, J.M. (2006) Concentration and sources of PM_{10} and its constituents in Alsasua, Spain. *Water, Air, Soil Pollut., 174,* 385-404.

Zender, C., Bian, H., Newman, D. (2003) Mineral Dust Entrainment and Deposition (DEAD) model: Description and 1990s dust climatology. *J. Geophys. Res*., *108*, 4416-4437.

Zhang, K., Gao, H. (2007) The characteristics of Asian-dust storms during 2000–2002: From the source to the sea. *Atmos. Environ., 41,* 9136-9145.

APPENDIX A

Table A.1: Statistic analysis of model calculated $PM_{2.5}$ against observations in $PM_{2.5}$ in 2009.

Here, Obs – the measured mean, Mod – the calculated mean, Bias is calculated as Σ(Mod-Obs)/Obs x 100%, R– the temporal correlation coefficient and RMSE – the Root mean Square Error= $1/Ns \times \Sigma(\text{Mod-Obs})^2]^{1/2}$.

Code	Station name	Obs	Mod	Rel. bias	R	RMSE
AT02	Illmitz	17.25	7.38	-57	0.73	14.02
CH02	Payerne	12.16	5.58	-54	0.65	9.50
CH05	Rigi	7.10	4.79	-33	0.67	5.12
CY02	Ayia Marina	14.43	9.77	-32	0.39	12.18
CZ03	Košetice	15.64	6.01	-62	0.69	11.49
DE02	Langenbrügge/Waldhof	11.76	5.34	-55	0.71	8.51
DE03	Schauinsland	6.98	4.64	-34	0.62	5.00
DE44	Melpitz	16.50	6.79	-59	0.70	12.14
ES01	Toledo	6.04	3.29	-46	0.67	3.73
ES07	Viznar	9.52	5.45	-43	0.64	5.98
ES08	Niembro	9.98	4.22	-58	0.63	7.69
ES09	Campisábalos	5.58	2.74	-51	0.53	3.91
ES10	Cabo de Creus	8.03	5.51	-31	0.61	4.43
ES11	Barcarrota	6.91	4.22	-39	0.68	3.91
ES12	Zarra	6.43	4.47	-30	0.74	3.24
ES13	Penausende	5.17	2.86	-45	0.75	3.27
ES14	Els Torms	8.01	5.20	-35	0.65	4.98
ES16	O Saviñao	6.91	4.02	-42	0.62	5.24
FI50	Hyytiaelae	3.86	1.92	-50	0.44	3.13
GB36	Harwell	8.69	4.15	-52	0.74	7.06
GB48	Auchencorth Moss	4.48	2.76	-38	0.80	3.17
IT04	Ispra	19.01	6.48	-66	0.41	19.72
LV10	Rucava	16.80	4.11	-76	0.51	17.16
LV16	Zoseni	11.51	4.09	-64	0.46	10.70
NL09	Kollumerwaard	11.50	4.81	-58	0.73	8.81
NL10	Vreedepeel	19.25	7.77	-60	0.73	14.98
NL11	Cabauw	16.35	8.25	-50	0.78	11.35
NL91	De Zilk	14.45	7.00	-52	0.63	12.75
PL05	Diabla Gora	13.15	5.08	-61	0.76	11.64
SE14	Råö	6.27	4.33	-31	0.49	4.02
SI08	Iskrba	12.42	6.98	-44	0.67	9.36
Hourly						
GB36	Harwell	9.39	4.32	-54	0.68	6.07
GB48	Auchencorth Moss	3.39	2.71	-20	0.83	2.58
IE31	Mace Head	8.64	2.63	-70	0.60	6.70
SE11	Vavihill	7.54	3.98	-47	0.64	5.02
SE12	Aspvreten	6.15	2.34	-62	0.62	5.20
Weekly						
NO01	Birkenes	3.53	1.62	-54	0.56	2.87
Mean		**10.02**	**4.80**	**-49**	**0.64**	**7.75**

Table A.2: Statistic analysis of model calculated daily PM_{10} *against observations in 2009.*

Code	Station name	Obs	Mod	Rel. bias	R	RMSE
AT02	Illmitz	21.82	10.04	-54	0.62	16.91
AT05	Vorhegg	8.70	5.71	-34	0.37	7.74
AT48	Zoebelboden	8.80	7.75	-12	0.57	6.18
CH01	Jungfraujoch	2.69	3.66	36	0.29	5.15
CH02	Payerne	17.70	8.41	-53	0.63	12.26
CH03	Tänikon	17.09	8.36	-51	0.56	12.65
CH04	Chaumont	8.92	8.34	-7	0.58	6.52
CH05	Rigi	10.02	6.86	-32	0.63	6.86
CY02	Ayia Marina	23.43	21.05	-10	0.55	27.32
CZ01	Svratouch	15.10	8.49	-44	0.34	10.26
CZ03	Košetice	16.47	8.16	-51	0.71	10.99
DE01	Westerland/Wenningsted	17.22	10.70	-38	0.63	9.02
DE02	Langenbrügge/Waldhof	15.63	8.22	-47	0.64	9.99
DE03	Schauinsland	9.20	6.91	-25	0.65	6.14
DE07	Neuglobsow	13.37	7.77	-42	0.64	8.19
DE08	Schmücke	10.29	7.87	-24	0.64	6.85
DE09	Zingst	14.54	8.34	-43	0.66	8.85
DE44	Melpitz	20.90	9.04	-57	0.70	14.28
DK05	Keldsnor	18.98	11.44	-40	0.33	16.01
DK41	Lille Valby	18.28	8.99	-51	0.47	12.88
ES01	Toledo	11.23	7.59	-32	0.58	7.46
ES07	Viznar	17.13	15.94	-7	0.63	13.00
ES08	Niembro	17.54	9.09	-48	0.31	15.62
ES09	Campisábalos	10.78	6.02	-44	0.60	7.68
ES10	Cabo de Creus	16.82	12.93	-23	0.64	7.42
ES11	Barcarrota	14.05	10.83	-23	0.51	9.50
ES12	Zarra	14.28	9.63	-33	0.70	8.23
ES13	Penausende	9.04	5.78	-36	0.60	5.47
ES14	Els Torms	13.67	9.35	-32	0.70	7.51
ES16	O Saviñao	10.35	6.58	-37	0.62	6.27
ES17	Doñana	16.18	15.94	-2	0.39	10.62
FI50	Hyytiaelae	4.53	3.24	-29	0.36	3.47
GB36	Harwell	13.81	8.24	-40	0.66	8.45
GB48	Auchencorth Moss	7.00	6.02	-14	0.70	4.04
IT01	Montelibretti	29.82	11.22	-62	0.58	22.33
LV10	Rucava	18.83	6.91	-63	0.34	17.17
LV16	Zoseni	16.75	4.85	-71	0.15	17.68
MD13	*Leova II*	*15.59*	*11.31*	*-28*	*-0.06*	*21.69*
PL05	Diabla Gora	16.31	7.39	-55	0.68	13.05
SE14	Råö	14.60	9.43	-35	0.53	8.79
SI08	Iskrba	15.86	10.01	-37	0.56	11.44
Hourly						
CZ03	Košetice	18.12	8.01	-56	0.74	12.72
FR09	Revin	22.62	9.55	-58	0.75	14.78
FR13	Peyrusse Vieille	17.91	8.11	-55	0.52	11.56
FR15	La Tardière	18.41	10.17	-45	0.78	10.55
FR18	La Coulonche	13.35	8.37	-37	0.73	6.83
GB06	Lough Navar	10.22	5.93	-42	0.72	6.29
GB36	Harwell	16.24	8.05	-50	0.71	9.87
GB43	Narberth	11.27	8.89	-21	0.60	8.13
GB48	Auchencorth Moss	6.56	6.49	-1	0.75	4.04
GR02	Finokalia	17.48	37.70	116	0.52	62.17
HU02	K-puszta	27.84	11.20	-60	0.57	21.80
MK07	Lazaropole	17.45	13.53	-23	0.31	19.34
NL07	Eibergen	24.90	11.10	-55	0.69	19.04
NL09	Kollumerwaard	21.10	10.46	-50	0.74	13.18
NL10	Vreedepeel	24.45	11.74	-52	0.75	17.10
NL91	De Zilk	23.28	13.14	-44	0.62	14.19
SE11	Vavihill	14.59	6.93	-53	0.67	9.16
SE12	Aspvreten	6.59	5.59	-15	0.67	3.79
Weekly						
EE09	Lahemaa	6.84	4.42	-35	0.26	3.66
NO01	Birkenes	5.93	2.90	-51	0.54	4.22
SK04	Stará Lesná	13.38	8.64	-35	0.44	7.15
SK06	Starina	15.36	9.18	-40	0.24	9.28
SK07	Topolniky	22.75	11.36	-50	0.58	13.28
Mean		**15.16**	**9.31**	**-35**	**0.56**	**11.63**

At MD13 (Leova II) measured PM_{10} concentrations are at the detection limit every other day.

emep

Chemical Co-ordinating Centre of EMEP
Norwegian Institute for Air Research
P.O. Box 100, N-2027 Kjeller, Norway

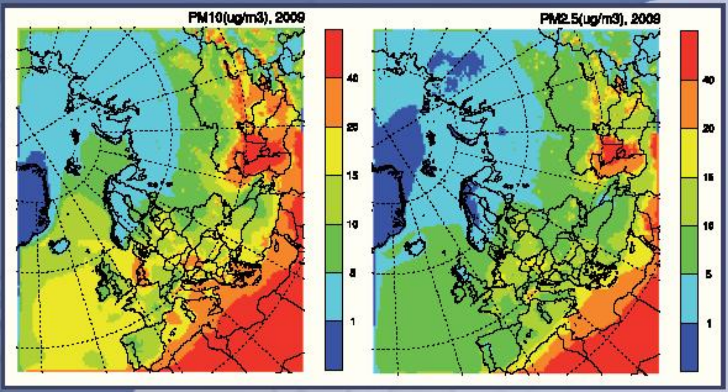

ccc
NILU
Norwegian Institute for Air Research
P.O. Box 100
NO-2027 Kjeller
Norway
Phone: +47 63 89 80 00
Fax: +47 63 89 80 50
E-mail: kjetil.torseth@nilu.no
Internet: www.nilu.no

ciam
International Institute for Applied Systems Analysis (IIASA)
A-2361 Laxenburg
Austria
Phone: +43 2236 80 70
Fax: +43 2236 71 31
E-mail: amann@iiasa.ac.at
Internet: www.iiasa.ac.at

ceip
Umweltbundesamt GmbH
Spittelauer Lände 5
1090 Vienna
Austria
Phone: +43-(0)1-313 04
Fax: +43-(0)1-313 04/5400
E-mail:
emep.emissions@umweltbundesamt.at
Internet:
http://www.umweltbundesamt.at/

msc-e
Meteorological Synthesizing Centre-East
Krasina pereulok, 16/1
123056 Moscow
Russia
Phone +7 495 981 15 66
Fax: +7 495 981 15 67
E-mail: msce@msceast.org
Internet: www.msceast.org

msc-w
Norwegian Meteorological Institute (met.no)
P.O. Box 43 Blindern
NO-0313 OSLO
Norway
Phone: +47 22 96 30 00
Fax: +47 22 96 30 50
E-mail: emep.mscw@met.no
Internet: www.emep.int